University of Tunis El Manar
National Engineering School of Tunis
Doctoral School "Sciences et Techniques de l'Ingénieurs"
Laboratory of Mathematical Modelling and Numeric in
Engineering Sciences

PhD Thesis

Presented by

Emna JAÏEM

to fulfill the requirements for the grade of

Doctor

Specialty

Applied Mathematics

ENERGY GAP-COST FUNCTIONALS AND IDENTIFICATIONS: LINEAR ELASTICITY

Defended on July 18th, 2016
In front of the jury

Hend BEN AMEUR	University of Tunis El Manar	President
Amel BEN ABDA	University of Tunis El Manar	Supervisor
Abdelmalek ZINE	Institut Camille Jordan	Co-supervisor
Kaïs AMMARI	University of Monastir	Reviewer
Bernard TROCLET	École Normale Supérieure de Cachan	Reviewer

La confiance en soi est le premier secret du succès.

Ralph Waldo Emerson

... se io avessi a ricominciare i miei studii,
vorrei seguire il consiglio di Platone
e cominciarmi dalle matematiche ...

Galileo Galilei

Most people, if you describe a train of events to them, will tell you what the result would be. They can put those events together in their minds, and argue from them that something will come to pass. There are few people, however, who, if you told them a result, would be able to evolve from their own inner consciousness what the steps were which led up to that result. This power is what I mean when I talk of reasoning backwards.

Sherlock Holmes to Dr. Watson in: A Study in Scarlet,
Sir Arthur Conan Doyle, 1887.

Dédicace

Je dédie ce travail, en témoignage de reconnaissance

À mes parents; vous êtes le soleil qui illumine ma journée et la lune qui éclaircit ma nuit. Vous êtes la lumière dans l'obscurité.

À mes frères et mes belles soeurs pour leurs amours, leurs encouragements et tous les moments agréables qu'on a passés ensemble que ce soit en Suède ou en Tunisie.

Je souhaite un très bon courage pour mon frère Anouar pour sa thèse de doctorat.

À mes nièces Souleyma et Lina et mes neveux Yosef et Elyes; vous me procurez la joie de vivre.

Ainsi qu'à tous ceux qui me sont chers.

Remerciements

Cette thèse en Mathématiques Appliquées marque pour moi une étape importante dans mon parcours universitaire et dans le domaine de recherche et ce n'est en fait qu'un commencement.

Mes premières pensées vont à ma directrice de thèse Professeur Amel Ben Abda et à mon co-directeur Professeur Abdelmalek Zine pour leur expertise et les bons moments passés ensemble et sans qui je n'aurais développer tous ces outils.

Je tiens à signifier mon respect et ma gratitude à Professeur Kaïs Ammari et à Professeur Bernard Troclet pour leur rapport d'évaluation ainsi qu'à Professeur Hend Ben Ameur qui a accepté d'être présidente du Jury.

J'ai beaucoup appris auprès du Professeur Amel Ben Abda qui a su m'initier au monde de la recherche depuis mon mastère et qui m'a aidée à développer mon désir pour les problèmes inverses. Le dialogue permanent qui s'est instauré entre nous a été un atout majeur dans l'aboutissement de cette thèse. Je remercie aussi Amel Ben Abda pour la confiance qu'elle m'a accordée depuis le mastère, pour sa disponibilité, pour ses qualités pédagogiques et scientifiques sans oublier son amitié.

Grâce aux bourses d'alternance offertes par le Ministère de l'Enseignement Supérieur en Tunisie et à la subvention obtenue par LABEX MILYON (ANR-10-LABX-0070) de l'Université de Lyon, j'ai pu profiter de deux séjours au sein du laboratoire de Mathématiques et Informatique à l'École Centrale de Lyon. Je remercie de nouveau mon co-directeur Professeur Abdelmalek Zine pour l'accueil chaleureux, sa gentillesse, toutes les échanges mathématiques très instructifs et pour m'avoir intégré dans le groupe de travail au sein du Laboratoire de Tribologie et Dynamique des Systèmes à l'École Centrale de

Lyon où c'était l'occasion de confronter mes idées au jugement de différents participants et d'être attentif aux conceptions d'autrui.
A ce passage, je remercie particulièrement Professeur Mohamed Ichouchoun, Professeur Manuel Collet et notamment mes amis Christophe, Jean Loup, Rita et Alexa pour le partage de leur savoir faire.

Je voudrais aussi remercier Sinda Khalfallah et Badreddine Rjaibi qui m'ont accompagnée tout au long de ces années de thèse et avec qui j'ai collaboré une partie de mes travaux de recherche.

Il m'est aussi agréable de remercier mon ami et collègue Mohamed Sayeh pour les discussions enthousiastes que j'ai pu avoir avec lui.

Je tiens à remercier chaleureusement Professeur Bernard Troclet pour l'intérêt qu'il porte à mon travail et pour les échanges qui n'ont pu qu'enrichir mes connaissances sur la théorie des matériaux composites. Je le remercie également de m'avoir accordé l'opportunité de participer à la conférence industrielle Dyncomp'2015 qui a été une expérience tout à fait enrichissante.

Il m'est parfois arrivé au cours de ma thèse d'être démotivée et c'est grâce au soutien et à l'encouragement des membres de l'association T3SM, plus particulièrement Dr. Fethi Ben Belgacem, Anis Khalfi, Mohamed Jebalia, Moncef Mahjoub et Ibtihel Ben Gharbia, que j'étais de nouveau confiante et prête à attaquer avec le sourire les questions passionnates que j'avais à répondre.

Il me vient naturellement une pensée pour toute l'équipe du Laboratoire LAMSIN-ENIT où la bonne ambiance a toujours régné et régne encore. Je ne saurais oublier de remercier tous les membres qui m'ont aidée chacun de leur manière, dans un cadre mathématique ou non avec une pensée particulière à Raoudha.

Au Laboratoire de Mathématiques et Informatiques, j'ai eu la chance de partager le bureau avec mon ami et collègue Vincent Runge; je le remercie pour les discussions enrichissantes et pour les agréables moments passés ensemble sans oublier aussi Loïc, Mona et notamment Isabelle pour sa grande patience concernant les papiers administratifs.

Il me vient naturellement une pensée pour mes anciens amis matheux notamment Marianne Chartard et Mohamed Lasmer qui m'ont soutenu de près ou de loin depuis mon mastère.

Je ne peux m'empêcher enfin de remercier mes amies non matheuses particulièrement Amal et Ahlem. Leur amitié a été déterminante pendant ces années de thése.

Je remercie également mon cousin Souheil pour m'avoir toujours encouragée à faire une thèse de doctorat en Mathématiques Appliquées.

À mon Professeur du collège Monji Abid, le premier qui a su naître en moi l'amour pour les Mathématiques.

Fonctionnelles d'erreur de type écart à la loi de comportement et identifications : Élasticité linéaire

Résumé

Les travaux regroupés dans ce manuscrit apportent une contribution au problème inverse géométrique relatif à l'identification de défauts (cavités) dans les structures mécaniques.
En effet, l'ambition de cette thèse était d'approfondir l'étude à la fois sur les aspects théoriques et numériques de ce problème inverse géométrique et de construire des méthodes adaptées à des applications relatives aux systèmes d'élasticité linéaire.
Notre contribution se situe au niveau de la mise en place d'une procédure numérique originale qui s'appuie sur la transformation de notre problème inverse en un problème d'optimisation de forme par le biais de la minimisation d'une fonctionnelle d'erreur de type écart à la loi de comportement, à savoir la fonctionnelle Kohn-Vogelius dont une étude bibliographique fouillée est présentée dans le deuxième chapitre.
Les outils développés concernent ainsi l'optimisation de forme et se regroupent en deux catégories : la méthode du gradient de forme combinée avec la méthode Level Set et la méthode du gradient topologique.
Nous détaillons la résolution théorique et numérique de ce problème inverse tout d'abord dans le cadre du champ scalaire, celui régi par l'équation de Laplace en troisième chapitre et ensuite dans le cadre du champ vectoriel relatif à l'élasticité linéaire avec des données surdéterminées dans un premier lieu en quatrième chapitre et avec des données partiellement surdéterminées dans un second lieu en cinquième chapitre.
L'originalité dans ce cinquième chapitre réside dans le traitement de données partiellement surdéterminées sur le bord. Plus précisément, nous sommes dans ce cas face à un sous-problème de Cauchy dans la mesure où (en élasticité bidimensionnelle) seuls le champ de déplacement et une composante de la contrainte normale sont accessibles à la mesure.
Pour ce nouveau cadre de problème inverse géométrique, l'accent est mis sur la question d'identifiabilité de cavités. Un résultat d'unicité est démontré en cinquième chapitre pour le cas de cavités monotones.

Pour mener à bien cette étude, nous mettons en oeuvre tout le long du troisième et quatrième chapitres théoriquement la méthode de dérivation par rapport au domaine et numériquement la méthode Level Set. Un algorithme de descente est mis en oeuvre avec succès et permet de maîtriser les changements de topologie au cours du processus.
Dans le cinquième chapitre, nous avons visé à enrichir notre étude en mettant l'accent sur un outil d'optimisation de forme, différent de celui exploité dans les deux derniers chapitres, qui est le gradient topologique, nécessitant le calcul d'un développement asymptotique de la fonctionnelle Kohn-Vogelius. Cette méthode mise en place dans le cadre des données partiellement surabondantes n'est pas itérative dans la mesure où les cavités sont identifiées par les zones où le gradient est le plus négatif.
Sur le plan de la fiabilité et la validation des outils évoqués ci-dessus, notre approche a été appliquée avec succès à différents cas tests pour ces problèmes d'identification de cavités.
De notre étude, sont issues quelques perspectives approfondies dans le sixième chapitre. Notre manuscrit est couronné par une synthèse des conclusions les plus marquantes tout en proposant quelques axes de recherche qu'il serait intéressant de développer.

Mots-clés: Problèmes inverses géométriques, identification de cavités, optimisation de forme, fonctionnelle Kohn-Vogelius, méthode de gradient de forme, méthode de gradient topologique, méthode Level Set, sous-problème de Cauchy, données partiellement surdéterminées, identifiabilité.

Energy gap-cost functionals and identifications: Linear Elasticity

Abstract

The geometrical inverse problem related to the identification of defects (cavities) in mechanical structures has been an important area of research for engineers. Such a question arises from the need to improve damage resistance of mechanical components.

This thesis aims to develop mathematical tools to solve such a problem.

To this end, throughout this work, we transform our inverse problem into a shape optimization one by the means of the minimization of an energy gap-cost functional, the so-called Kohn-Vogelius error functional. A detailed literature review of this functional is reported in the second chapter.

Since classical optimization fails to solve such an inverse probelm as it doesn't allow the change of topology, computational tools based on optimization theory have been developed in the last three decades. These include the shape gradient method combined with the level set method and the topological gradient method.

In this work, we focus our attention on these powerful and promising tools. On one hand, we consider the scalar case governed by Laplace operator in the third chapter and on the other hand, the vectorial case related to linear elasticity framework from overdetermined boundary data as a first case in the fourth chapter and from partially overdetermined boundary data as a second case in the fifth chapter.

This new framework investigated in the fifth chapter arises when the displacement field and the normal component of the normal stress are available for the reconstruction of cavities. While, no information is given on the shear stress. The contribution herein lies on these non-standards overdetermined boundary data. Special focus is put on the question of the identification of cavities and an identifiability result is demonstrated in the case of monotonous cavities.

The third and fourth chapters bring together the shape gradient method, as a theoretical approach and the level set method, as a numerical tool.

However, the approach proposed in the fifth chapter is concerned with the topological gradient method.

Numerical validations are presented in each chapters to demonstrate the power of the methodologies investigated.

The last part draws some conclusions and perspectives.

Keywords : Geometrical inverse problem, cavities identification problem, shape optimization problem, Kohn-Vogelius error functional, shape gradient method, Level Set method, topological gradient method, partially overdetermined boundary data, identifiability.

Contents

List of Figures

Chapter 1

Introduction

Contents

1.1 Motivation

Industrial process such as the mould filling used in the fabrication of the metal pieces involves complex phenomena. Indeed, gas bubbles may be trapped by the fluid and cannot escape. These small bubbles are considered as flaws as they weaken the solidity of casted pieces. One seeks, therefore to the localization of these cavities, namely micro-voids in order to minimize the probability of failure during the mechanical process.
As a consequence, in recent years, it has become apparent that solving cavities problems is of high interest to the scientific and especially engineering community.

Motivated by the need to improve damage resistance of mechanical structures, we shall focus, in this thesis, our attention on the problem related to cavities identification which falls within the scope of geometrical inverse problems associated with mathematical models governed by partial differential equations (PDE).

Solving inverse problems is an important and necessary key step in a broad spectrum of fields application in science, industry and engineering such as heat conduction, diffusion, geophysics, medical imaging and non-destructive testing.
Since the last three decades, the rapid and tremendous evolution of computer capabilities settled the engineers and mathematicians to develop and adopt techniques for a variety of difficult problems they faced.
As a consequence, further progress become possible in the field of inverse problems that makes it one of the fastest growing areas in applied mathematics.

In contrast to forward problems, the inverse ones are often ill-posed (Hadamard 1923) that is, they may suffer from non existence and non uniqueness of the solution as well as ill-conditioning of the inverse process, namely numerical instability. To overcome this important question of ill-posedness and to find solution to our geometrical inverse problem related to cavities identification, we resort to the shape optimization theory by transforming the inverse problem into a minimization one.

However, one can remark that the classical shape optimization present some drawbacks. On the one hand, it doesn't allow a change of topology which makes it less effective. On the other hand, the huge computational cost related to remeshing makes the classical method expansive. As a result, in order to treat such shape reconstruction problems, various tools have been emerged and developed. Some of the most popular ones are the shape gradient

method combined with level set method and topological gradient method.
This manuscript presents a treatment of cavities identification problems based on these last methods.
In the next section, we give a brief introduction to shape optimization and recall some important concepts such as shape sensitivity analysis, level set method and topological gradient method.

1.2 Shape optimization tools

The typical aim of shape optimization problems is to reconstruct an unknown shape satisfying a certain criterion which is usually related to the minimization of a certain cost functional, expressed in terms of state variables. Usually, partial differential equations describe these state variables.
In our case, it is about the minimization of an energy gap-cost functional J over some admissible subset. The shape optimization problem can be stated as follows

$$\inf_{\Omega \in U_{ad}} J(\Omega), \tag{1.1}$$

where $\Omega \subset \mathbb{R}^n$ is the domain occupied by the mechanical structure and U_{ad} is a set of admissible shapes. J depends usually on a partial differential equation or other constraints.
The main technical problem which one has to be faced when solving a shape optimization problem stems from the computation of the gradient of the cost functional chosen. Indeed, shape optimization problems are usually solved numerically by some method requiring some gradient information.
There are two fundamental approaches which can provide such information : the shape sensitivity analysis and the topological sensitivity analysis. A short description of these methods is delivered in the sequel.
The next subsection deals with the first approach while in the second subsection, we focus our attention to the level set method usually connected to shape sensitivity analysis. An overview of the second approach also-called the topological gradient method follows in the third subsection.

1.2.1 Shape sensitivity analysis

This part regards the shape sensitivity analysis also-called the shape gradient method which is a fundamental tool in shape optimization. Its goal is to evaluate the sensitivity of the cost functional with respect to small perturbation

in the object shape. Indeed, it can be interpreted as a derivative of J with respect to the domain Ω. We present here the approach of Murat and Simon [79]. Let us review the basic idea of this method.
For a bounded, open reference domain $\Omega \subset U \subset \mathbb{R}^n$ (U is a fixed set) with sufficient smooth boundary $\Gamma = \partial\Omega$, one needs to change its geometry and to determine a new configuration Ω_t. This will be able by the means of a suitable family of transformations $F_t : \overline{U} \longrightarrow \overline{U}$, $t \geqslant 0$ as follows

$$F_t = id + t\,h, \tag{1.2}$$

with $F_0 = id$. Being the perturbation of identity operator, F_t is a diffeomorphism from Ω onto its image for t sufficiently small and h is a deformation field, namely a vector field on $\mathbb{R}^n$ with $h = 0$ on ∂U and id denotes the identity mapping on $\mathbb{R}^n$. t is taken as the implicit control parameter. The perturbation of Ω leads to a family of domains $\{\Omega_t\}$ defined by

$$\Omega_t = F_t(\Omega). \tag{1.3}$$

Let us now introduce the so-called Eulerian derivative (namely the directional derivative) and define the shape derivative.

Definition 1. *Let $\Omega \subset \mathbb{R}^n$ be a bounded Lipschitz domain and let J be a functional defined on Ω : $J : \Omega \longmapsto \mathbb{R}$. Then, the Eulerian derivative (if it exists) of the functional J at Ω in the direction of a vector field h is given by*

$$J'(\Omega, h) = \lim_{t \mapsto 0} \frac{J(\Omega_t) - J(\Omega)}{t},$$

with $\Omega_t = F_t(\Omega)$. The Eulerian derivative is called shape derivative if $J'(\Omega, h)$ exists for all h and the mapping $h \mapsto J'(\Omega, h)$ is linear and continuous with respect to the topology of $\mathcal{C}^{1,1}(\overline{\Omega})^2$.

This shape derivative of the cost functional provides the most important quantity of interest in shape optimization, namely the descent direction that we need to deform the shape boundaries towards the optimum shape.
Historically, the shape sensitivity analysis was firstly introduced by Hadamard [58] for the problem of elastic plates.

1.2.2 The level set method

In this subsection, we focus on the level set method which has gained an increasing attention from the numerical point of view for tracking evolving

interfaces. Indeed, over the last years, the level set method proposed by Osher and Sethian in 1988 [84] in the framework of a flame propagation model, has become an interesting tool in shape optimization and has been widely applied in a variety of research areas [82], since topology changes can naturally occur during the optimization process on a fixed cartesien grid. The level set method allows boundary motion and merging as well as the formation of new holes [47]. The key idea of the level set method is to parameterize implicitly the shape of an admissible domain Ω via the zero level of the so-called level set function φ defined as

$$\begin{cases} \varphi(x) = 0 & \text{if} \quad x \in \partial\Omega \cap U, \\ \varphi(x) < 0 & \text{if} \quad x \in \Omega, \\ \varphi(x) > 0 & \text{if} \quad x \in (U \setminus \overline{\Omega}). \end{cases}$$

Above, U is an open and bounded domain containing all admissible shapes. Furthermore, useful geometric properties related to the outward normal vectors and to the mean curvature of the interface $\Gamma := \partial\Omega$ are provided by the level set method in the case of a regular domain Ω (that is, $\nabla\varphi \neq 0 \, \forall \, x \in \Gamma$). Indeed, the unit outward normal vector ν on Γ and the mean curvature κ on Γ are easy to compute as they are expressed as [82]

$$\nu = \frac{\nabla\varphi}{|\nabla\varphi|} \qquad \text{and} \qquad \kappa = \nabla \cdot \frac{\nabla\varphi}{|\nabla\varphi|}.$$

In an optimization process, the shape is evolving in the time interval $[0, T]$ according to a certain velocity. Hence, the level set function φ will be a one dimension higher than the interface dimension as it depends on time t : $\varphi(x, t)$. Thus, for a fixed time t, the time-dependent position of the boundary $\Gamma(t)$ is defined as

$$\Gamma(t) = \{x(t) \in \Omega_t; \ \varphi(x(t), t) = 0\}, \quad \forall t \in [0, T].$$

One can derive the following so-called level set equation by differentiating the equation $\varphi(x(t), t) = 0$ with respect to time :

$$\begin{cases} \partial_t\varphi(x,t) + \dfrac{dx}{dt}\nabla\varphi(x,t) = 0 & t \in (0,T] \text{ and } \forall x \in \Gamma(t), \\ \varphi(x,0) = \varphi_0(x) & \forall x \in \Gamma(t). \end{cases} \tag{1.4}$$

Initializing φ_0 and updating the level set function is a delicate process as φ can become too flat or too steep during evolution [83, 88]. Having advantageous properties, the signed distance function, that is $d(x) := dist(x, \Gamma)$ for all $x \in \Omega$, is often used to initialize and re-intialize the level set function.
This equation (1.4) can be extanded in the whole domain U contained all

admissible shapes $\Omega(t)$, since the same reasoning can be obtained for any value c of the level set function $\varphi(x(t),t) = c$.
Structural optimization can be performed by updating this function, that is by re-initializing the level set function by the solution of the equation of (1.4). Let us denote $\dfrac{dx}{dt}$ by $V(t,x)$ and let us decompose $V(t,x)$ as the following

$$V(t,x) = V_\nu(t,x)\,\nu + V_\tau(t,x)\,\tau,$$

where $V_\nu(t,x) = V(x,t)\cdot\nu$ and $V_\tau(t,x) = V(x,t)\cdot\tau$. Then, making use of the fact that

$$\nu = \frac{\nabla\varphi}{|\nabla\varphi|},$$

the equation (1.4) leads to the so-called Hamilton-Jacobi equation

$$\begin{cases} \partial_t\varphi(x,t) + V_\nu(t,x)\,|\nabla\varphi(x,t)| &= 0, \\ \varphi(x,0) &= \varphi_0(x). \end{cases}$$

For the optimization process, the level set method is then designed to track interfaces moving along the normal direction to the boundary with respect to the "speed vector" $V_\nu(t,x)$. The quantity $V_\nu(t,x)$ is usually obtained as the steepest descent direction dirived by the shape sensitivity analysis of the cost functional which depends on a physical problem. Hence, the level set method is combined with the shape gradient method. Historically, Osher and Santosa [83] were the first to propose such incorporation in the framework of optimization of structural frequencies.
In our work, whenever we apply the level set method of the identification of cavities, we will choose $V_\nu = -G$ where G will be the shape derivative of the functional chosen. Indeed, taking into account that $x(t) = F_t(x) := x + t\,h(x)$ as explained in the last section and considering $h = -G\,\nu = -G\dfrac{\nabla\varphi}{|\nabla\varphi|}$, we get the partial differential equation given by

$$\begin{cases} \partial_t\varphi(x,t) - G\,|\nabla\varphi(x,t)| &= 0, \\ \varphi(x,0) &= \varphi_0(x), \end{cases} \tag{1.5}$$

One has to solve this level set equation (1.5) in order to get a new level set function representing the new configuration of the domain, namely Ω_t. Above, φ_0 is a signed distance function corresponding to Γ_0.
ENO (Essential Non-Oscillatory) and WENO (Weighted ENO) schemes are widely used for the spatial discretization of the level set equation. While, an upwind scheme, namely a Runge-Kutta-scheme can be chosen for the temporal

discretization of the level set equation. We adress the interested reader to [82, 92].
Although the drawback of the method caused on the one hand by being one dimension higher than the interface dimension and on the other hand by the difficulty encountered during the numerical discretization, the level set method has been widely applied in the iterature [82, 88], for exemple in computer vision, image processing, computational physics etc.
Motivated by its fruitful connection with the shape sensitivity analysis and its robustness with respect to topological changes of the interface, the level set method is employed in the present work to recover cavities in mechanical structures.

1.2.3 Topological gradient method

Usually, when solving cavities identification problems, we have to deal with multiple cavities. However, in classical shape optimization theory, the final shape has the same topology as the initial one. As a consequence, the classical shape optimization doesn't allow the recovery of multiple defects in mechanical structures, as generally no a priori knowledge of their topologies can be given.
Hence, a major development in the shape optimization theory have been achieved in the last three decades. These recent improvements include the topological gradient method precisely designed to find optimal shape without any a priori assumption about the topology of the stucture.
Historically, it was introduced in 1994 by Schumacher et al. in the context of compliance optimization for linear elasticity problem under the name of bubble method [50]. During the last two decades, this method has received much attention and has been applied to various problems among them image processing [10, 11, 12, 13] and inverse problems since no restriction of the topology of the optimal shape (that is, the number of holes) is imposed. Indeed, it can be seen as a generalization of classical shape optimization. In inverse problems, for instance, the topological gradient method stands as a sprightly domain of research since it has successfully been applied for the identification of conductivity imperfections [38], cracks identification problem [6, 31], reconstruction of the electromagnetic properties of a medium and a set of objects buried inside it [35], inclusion recovery problem [41, 51, 56] and many others.
The topological gradient method aims to assess the sensitivity of a shape functional J when an infinitesimal object is created at a prescribed location x_0

inside the solid. Depending on the application, the object may be a cavity, an inhomogeneity, a source term or even cracks.
Let us present briefly the main idea of the topological sensitivity analysis. One aims to minimize a cost functional $j(\Omega) = J(\Omega, u_\Omega)$ where Ω is a variable domain of $\mathbb{R}^2$ and u_Ω is the solution to a given partial differential equation defined over the domain Ω. Let ρ be a small positive parameter . The key idea is to create a spherical hole $\omega_\rho = x_0 + \rho\,\omega$ of radius ρ around a point x_0 in Ω, where $\omega \subset \mathbb{R}^2$ is a fixed open and bounded subset containing the origin. We denote by $\Omega_\rho = \Omega \setminus \overline{\omega_\rho}$ the perturbed domain obtained by removing the hole ω_ρ from Ω.
Generally, an asymptotic expansion of the function j can be obtained in the following form

$$j(\Omega_\rho) = j(\Omega) + f(\rho)\, g(x_0) + o\left(f(\rho)\right),$$

where $f(\rho)$ is an explicit positive function such that

$$\lim_{\rho \to 0} f(\rho) = 0.$$

The sensitivity $g(x_0)$ is called the topological derivative or the topological gradient which indicades where creating new holes is most beneficial. It can be used as a descent direction in an optimization process to solve various problems. Indeed, in order to minimize the criterion j, one has to create holes at some points where g is negative.
On the other hand, the sensitivity g is usually easy to compute using the solution of direct and adjoint problems defined on the initial domain Ω (namely, the safe domain). Hence, the topological gradient method is far more faster than classical optimization methods as an efficient and cheap algorithm can be built. We refer the reader to [68, 81] for a concise overview of the method. These various capabilities of the topological gradient method cited above make it attractive for one aiming to face cavities identification problems.

In order to recover cavities in mechanical structures, we rely on these techniques exposed above.

1.3 Dissertation organization

This manuscript is organized as follows:

The first part, namely the second chapter introduces and reviews in details the Kohn-Vogelius functional selected to formulate the geometrical inverse problems related to cavities identification into a shape optimization problem.

It is essential to emphasize the performance of this functional before discussing the optimization step.
After describing the energy gap functional, we try to answer to the question of detecting cavities in mechanical structures.

The second part of the work is quite original and develops our main results. Indeed, it is concerned with the identification of unknown domains, namely cavities using partial differential equations and overdetermined boundary data in a first step and partially overdetermined boundary data in a second step. Our purpose in this part is to develop a consistent theoretical and numerical approach to recover cavities.

In both third and fourth chapters, we formulate the cavities identification problems as a shape optimization ones by the means of the Kohn-Vogelius misfit functional reported in the second chapter. We compute its shape gradient. Then, we solve numerically the shape optimization problems by combining the gradient information with the level set method in a steepest descent algorithm. We illustrate the approach proposed by numerical results.
It should be noted that in the third chapter, we consider the scalar case, namely the Laplace operator and in the fourth chapter, we discuss the extension to the vectorial case. In fact, we focus on the linear elasticity problem which is of our most interest in this work.

Since overdetermined boundary data are critically important in geometrical inverse problems, our attention in the fifth chapter is restricted to a new framework for a geometrical inverse problem in linear elasticity. Indeed, our aim is to recover cavities from partially overdetermined boundary data. To our knowledge, there is no literature on this particular problem so far. The methodology used to take into account this extra difficulty, namely these non-standards overdetermined boundary data, is based too on the Kohn-Vogelius formulation combined not with the shape gradient method as it was the case for both third and fourth chapters but with the topological gradient method. In fact, an asymptotic expansion for the functional is derived with respect to the creation of a small hole using an adaptation of the adjoint method and a domain truncation.

Finally, the last part of this thesis contains the main conclusions concerning our results and our methods, focusing on the difficulties encountered; as well as some perspectives.

Chapter 2

A survey literature related to the Kohn-Vogelius type cost functional

Contents

Abstract

This chapter is an expansive overview of the Kohn-Vogelius approach which leads to solve a large class of problems in particular inverse ones. Its origin governed by the Wexler algorithm is uncovered and the Kohn-Vogelius suggestion as a variational approach is presented. The effectiveness of this function also known as the energy gap-cost functional was illustrated by exhibiting the various problems solved through its means and its properties.

Keywords: Kohn-Vogelius functional, Wexler algorithm, alternating directions method.

Résumé

Ce chapitre est une revue de littérature résumant l'état de l'art de la fonctionnelle de Kohn et Vogelius. Cette étude met l'accent sur la performance de l'approche Kohn et Vogelius permettant de résoudre une large classe de problèmes en particulier les problèmes inverses. Nous exposons son principe de construction à partir de ses origines notamment de l'algorithme de Wexler. L'efficacité de cette fonctionnelle connue aussi sous le nom de fonctionnelle d'énergie est soulignée par l'énumération des problèmes résolus par son biais.

Mots clés: Fonctionnelle de Kohn et Vogelius, algorithme de Wexler, méthode de directions alternatives.

2.1 Introduction

In the last decades, several new approaches and methods have been developed. In this review, we argue that the Kohn-Vogelius (**KV**) approach is well suited to large scale problems.
This approach was developed in 1987s [67] with roots in the 1985s [94]. Indeed, it is equivalent or closely related to the Wexler algorithm [94].
This work is a survey of some theoretical and numerical studies about KV approach.
The chapter is organized as follows. In the next section, we briefly survey the theory and history of the Wexler algorithm. The third section is devoted to the construction of the KV functional and we review some of its basic properties. The application to a wide variety of problems of recent interest is the core of Section 4, checking the effectiveness of the KV functional. Numerous references are made. The fifth section contains the application of the KV functional to

the identification of domains; while the sixth one contains the application for Cauchy Robin problem. We finish the chapter by practical comments.

2.2 Wexler algorithm

This algorithm was firstly initialized by Wexler et al. in 1985s [94] where the aim was to recover the unknown electrical conductivity (or impedance) inside a body by the impedance computed tomography reconstruction process; that is by means of steady-state voltage and current flux measurements at the boundary, governed by the Poisson equation.
Mathematically, we are concerned with the following elliptic partial differential equation, namely the Poisson equation for continuously inhomogenous media, i.e;

$$\nabla(\gamma \nabla u) = 0 \qquad \text{in } \Omega, \quad \Omega \subset \mathbb{R}^n, \quad n \geq 2$$

where u is the voltage, γ the positive, real valued conductivity, to be determined and $\sigma = \gamma \nabla u$ the vector of current flow; combined with information about the Cauchy data of finitely many solutions.
This inverse problem also called " Electrical Impedance Tomography " (EIT) [33, 95] has attracted great attention in recent years due to the numerous applications from biomedical to geophysical. Indeed, in biomedical community, EIT can be used to the monitoring of breast cancer detection. In geophysical area, it can be useful for locating of seepage from a toxic waste demp site. Finally, EIT can also be used in nondestructive testing, for the detection of small defects such as cracks and voids in metals (see [33, 95] and references cited within).
As a consequence, many approaches had been proposed in literature without mathematical analysis in that time 1987^{S} until that Kohn and Vogelius focus their attention to the Wexler approach [94], alos called the double constraint method [95], which consists in an iterative algorithm; involving successive estimates of potential-conductivity-potential etc. Given N several pairs of measurements $\{\varphi_i, \Psi_i\}_{i=1}^N$, namely Cauchy data, a single cycle of the process can be resumed in the following stages:
The conductivity γ having been determined in a previous step .

i) Solve N Neumann problems (related to the Neumann data Ψ_i)

$$\begin{cases} \nabla(\gamma \nabla w_i) = 0 & \text{in} \quad \Omega, \\ \gamma \nabla w_i \cdot \nu = \Psi_i & \text{on} \quad \partial\Omega. \end{cases} \tag{2.1}$$

i.e. compute the potential w_i with Neumann boundary conditions; and set $\sigma_i = \gamma \nabla w_i$; in other words, w_i having been knowned, the electric field intensity $\overline{E}$ is given by the negative gradient of potential i.e. $\overline{E} = -\nabla w_i$. As a consequence, the electrical current density distribution is given by $\overline{J} = \gamma \overline{E} = -\gamma \nabla w_i$ which is Ohm's law.

ii) Solve N Dirichlet problems (related to the Dirichlet data φ_i)

$$\begin{cases} \nabla(\gamma \nabla u_i) = 0 & \text{in} \quad \Omega, \\ u_i = \varphi_i & \text{on} \quad \partial\Omega. \end{cases} \tag{2.2}$$

i.e. compute the potential u_i with Dirichlet boundary conditions.

iii) Calculation of conductivity: A least-square technique is employed to produce an estimate of the conductivity profile in an average sense. Indeed, with $\{\sigma_i\}_{i=1}^N$ and $\{u_i\}_{i=1}^N$ fixed as obtained by i) and ii), uptade γ by minimizing the function of the corresponding "residual fluxes" $\{\sigma_i - \gamma \nabla u_i\}_{i=1}^N$

$$\Phi(\gamma) = \int_\Omega \sum_{i=1}^N |\sigma_i - \gamma \nabla u_i|^2 dx \qquad \text{over} \quad \gamma \in A_{ad} \tag{2.3}$$

with

$$A_{ad} = \{\gamma \in L^\infty(\Omega) : 0 < \nu \leq \gamma(x) \leq \mu \text{ a.e. in } \Omega\}.$$

The basic idea herein is that Φ is non-negative and that $\Phi \equiv 0$ exactly when $u_i = w_i$ solves

$$\begin{cases} \nabla \cdot (\gamma \nabla u_i) = 0 & \text{in} \quad \Omega, \\ u_i = \varphi_i & \text{on} \quad \partial\Omega, \\ \gamma \nabla u_i \cdot \nu = \Psi_i & \text{on} \quad \partial\Omega. \end{cases} \tag{2.4}$$

for each $i, 1 \leq i \leq N$. γ is then consistent with the given Dirichlet and Neumann measurements.

It should be noted that in [94] the last function was defined by the square of the residual

$$R = \int_\Omega \sum_{i=1}^N \left(\overline{J} + \gamma \nabla u_i\right) \cdot \left(\overline{J} + \gamma \nabla u_i\right). \tag{2.5}$$

where $\{u_i\}_{i=1}^N$ are the potentials.

The performance of Wexler's algorithm is reported in [94]. However, since the functionals are not lower semicontinuous [67], the solution may have spatial oscillations. To overcome this difficulty, Kohn and Vogelius proposed either follow the traditional way and add a regularizing term $\varepsilon |\nabla \gamma|^2$ to the functional or propose an alternative approach based on relaxtion that we will expose in the next section.

2.3 Kohn-Vogelius functional

The numerical solution of the EIT problem has received a lot of attention in the literature and many algorithms, which can be classified as iterative [33] and noniterative [33, 78] have been proposed. The iterative methods can themselves be classified as output least squares [33, 95] and variational ones [33, 94]. In this chapter, we shall focus our attention on the variational approach, also known as the equation-error formulation [66, 67, 94]. For noniterative algorithms as well as for output least squares, we refer the reader to [33].
In this section, the philosophy behind the KV functional is presented.
With the disadvantages of Wexler's algorithm in mind, Kohn and Vogelius proposed and analysed a variational approach [67] closely related to that proposed originally by Wexler et al [94] to impedance computed tomography. Firstly, they suggested [67] a reconstruction algorithm which is a modification of the Wexler algorithm to make it "an alternating directions" one. Indeed, they discussed the minimization of

$$J(\gamma) = \int_\Omega \sum_{i=1}^{N} |\frac{1}{\sqrt{\gamma}}\sigma_i - \sqrt{\gamma}\nabla u_i|^2 dx \qquad \text{over } \Gamma(\alpha,\beta) \tag{2.6}$$

subject to

$$u_{i|_{\partial\Omega}} = \varphi_i; \qquad \text{div } \sigma_i = 0; \qquad \sigma_i \cdot \nu_{|_{\partial\Omega}} = \Psi_i \qquad 1 \le i \le N$$

$$\gamma \le \gamma(x) \le \beta$$

Then, they keep steps i) and ii) of the Wexler process, descriped in the previous Section, unchanged and instead of step iii) they would prefer

iii)$'$ With $\{\sigma_i\}_{i=1}^N$ and $\{u_i\}_{i=1}^N$ fixed as determined by the two first steps of the Wexler algorithm, uptade $\gamma(x)$ so as to minimize

$$J(\gamma) = \int_\Omega \sum_{i=1}^{N} |\frac{1}{\sqrt{\gamma}}\sigma_i - \sqrt{\gamma}\nabla u_i|^2 dx \qquad \text{over } \Gamma(\alpha,\beta) \tag{2.7}$$

subject to the point wise constraint $\gamma(x) \in \Gamma(\alpha,\beta)$ defined by

$$\Gamma(\alpha,\beta) = \{\gamma : \text{ the eigenvalues } \gamma_1 \le \gamma_2 \text{ of } \gamma \text{ satisfy} \\ \alpha \le \gamma_1,\ \gamma_2 \le \beta,\ \alpha\beta \le (\alpha+\beta-\gamma_2)\,\gamma_1\}$$

i.e. the infinimum of J is over an appropriate family of symmetric matrices (Theorem 3.1 [67]).

One of the advantage of this new technique based in relaxation is that it offers an alternative approach by identifying the oscillations and building them into the functional. So, the unknouwn parameter can be stably predicted by boundary measurements as the " relaxed problem " is lower semicontinuous [67]. It is important to note that "the relaxed problem" generally has fewer local minimum than the original one. The second advantage concerns the behavior of the discretized relaxed problem under mesh refinement. Indeed, the minimization of the relaxed functional on a coarse mesh is roughly equivalent to minimization of the original one on a finer mesh.
This new variational method had been implemented by Kohn and McKenney [66].

2.4 Kohn-Vogelius functional applications

In this section, we intended to show the trends of the KV functional allowing the reader to have then an insight on its effectiveness. The range of KV functional applications is very broad indeed. The approach is especially attractive for free boundary problems and inverse problems such as cavities identification problems and data completion ones.
In the sequel, some theoretical and numerical researches solved by the means of KV approach are presented.

2.4.1 Shape optimization problems

The KV functional has been used with considerable success in a wide collection of models. For instance, in the framework of shape optimization problems, the connection of the KV functional with the shape optimization theory enables to solve a various type of problems by the means of gradient method, that turns to be the keystone of the analysis we intend here.
This part is concerned with the identification of unknown domains governed by elliptic partial differential equations. These equations modelise steady state electrical, thermal or mechanical phenomena.
Typically, many physical problems [21, 64] governed by partial differential equation with overdetermined data lead to an optimization problem of the form

$$(Ep)\begin{cases} \min_{\Omega} J(u_{\Omega}, \Omega), \\ \text{subject to } e(u_{\Omega}) = 0. \end{cases} \tag{2.8}$$

where J denotes the functional that depends on a domain Ω as well as on a function u_Ω which is the solution of a partial differential equation $e(u_\Omega) = 0$ posed on Ω.
The KV approach has been successfully applied to solve both interior and exterior Bernoulli problem [21] that can be considered as a prototype of a stationary free boundary problem, as well as the cavities identification problem [64] arising in many applications in industry such as non destructive testing.
In the case of [21, 64], $e(u_\Omega) = \Delta u_\Omega$ in Ω.

2.4.1.1 Free boundary problems

Due to the remarkably wide rang of challenging applications in real life of the Bernoulli problem, it is being extensively studied [15, 16, 17, 18, 21, 49] and particularly solved by minimizing the KV type cost functional over a class of admissible domains subject to two boundary value problems. To this end, two state functions are introduced. Indeed, one satisfies the mixed boundary value problem and the second one satisfies the pure Dirichlet problem. Thus, the particular shape optimization problem under consideration is the minimization of the L^2- distance of the gradients of the state functions.
It is important to note that minimizing a shape functional requires often some gradient information and Hessian. Indeed, the first-order shape derivative of KV functional has already been carried out by using both shape and material derivatives of the states in [21] for both exterior and interior Bernoulli problem and in [16] for only the exterior Bernoulli problem and by using the Hölder continuity of the state variables satisfying the Dirichlet and Neumann problems in [17] but without introducing any adjoint variables. In [49], to numerically solve the exterior Bernoulli problem, the authors used also the KV functional but restricted to starlike domains, while in [21] the obtained optimization problem (Ep) is solved by a steepest descent algorithm using the gradient information combined with the level set method for general domains and for both exterior and interior Bernoulli problems.
All among the Bernoulli problem, the second-order shape derivative was computed via two different ways. One [15] is through the approach of Sokolowski and Zolesio [91] by domain differentiation technique. The other way is based on the boundary differentiation scheme [18]. Furthermore, the second-order shape derivative of the KV functional at the solution of Bernoulli problem is computed using Tiihnen's approach [18].

2.4.1.2 KV functional application to geometric inverse problems : Cavities identification

After its introduction by Kohn and Vogelius [67], this misfit functional received widespread attention within the inverse problem community as it has given a new life to solve such ill posed problems.
In [23], the authors consider the inverse problem of determining defects from overspecified boundary data in order to decide about safety of the material structure. This problem modeled by the Stokes system arises for example in moulds filling. Indeed, many defects in a casting have their origins at the filling-stage since the industrial process may generate flaws consisting of small gas bubbles trapped inside the material while solidifying. Furthermore the problem of determining small cavities become of immense practical benefit to the foundry industry. The authors [23] suggest an alternative approach by rephrasing the geometrical inverse problem into an optimal design one. The optimal design functional to minimize in order to find out the flaws is the KV energy like misfit functional. To minimize this functional, the authors resort to the topological sensitivity analysis.

2.4.2 KV functional application to non geometric inverse problems

In the last three decades, researchers have witnessed rapid progress in the field of inverse problems and one can remark that the KV misfit functional attract more and more attention and not only geometric inverse problems but also inverse problems in general concept are broadly solved using the KV functional.
The key point for solving such inverse problems is to transform them on some minimization problems. Indeed, an optimization framework based on this KV formulation is often established. Moreover, gradient-type iterative algorithms are adopted to find the minimizers, namely the optimal solution.
Firstly, let us mention that the KV functional is used in biomedical imaging concept. Indeed, although, the KV energy functionals have been used for a long time in the electrical impedance tomography [48] as we have just seen in the last section, they have been used [53] in 2014 for the first time in an under-determined inverse source problem known as the BLT (Bioluminescence tomography) problem, which is a new method in biomedical imaging.
Indeed, in [53], rather than using the L2-norm on the boundary for data fidelity,

the determination of the light source function was achieved using the KV formulation with different boundary value problems, namely a Neumann one and a Robin one.
However, instead of adopting an iterative procedure, as is often the case, to solve numerically the BLT problem, a fast solver is introduced without the need of iterations to reconstruct the density of inner light source function [53] by transforming the BLT problem into a system of partial differential equations.

2.4.3 KV functional application to parameters inverse problems : Data completion problems

The KV functional has not only been applied to geometric inverse problems as it was mentioned above, but also to parameter inverse problems.
Indeed, in the context of ill-posed problem related to boundary data recovering, also known as a Cauchy problem, Andrieux et al. [8] make use of the KV approach to solve the problem by the computation of the gradients of the energy-like KV functional. The problem consists in recovering the value of the boundary data on a part Γ_i of the boundary of a domain Ω within which a partial differential operator is known and overspecified data being available on the remaining part Γ_c of the boundary. This kind of problem arises in many applications in the identification of boundary conditions or physical parameters entering into its formulation , the extension of measured surface fields inside a body from partial boundary measurements, but also in the framework of thermostatics where the aim is to recover the temperature in a given domain when its distribution and the heat flux are known over the accessible region of the boundary of the domain of interest namely, to reconstruct both lacking data (the temperature and the corresponding flux) on the remaining part of the boundary. Note that this issue is mathematically identical to the electrostatics case encountered in electric impedance tomography discussed in the second section.

2.5 KV functional application to the identification of domains

The domain identification problem has been an important topic and remains an area of active research since it appears in many industrial and engineer applications. Based on the functional exposed in the previous section and

introduced by Kohn and Vogelius for parameters identifications via linear elliptic problems, a new functional is derived for geometrical inverse problems. Indeed, an equivalent form of the KV functional is given.
We will denote by Θ a family of sets with a commun part of boundary $\partial\Omega_c$. We are interested in finding the unknown part $\partial\Omega_i$ from overdetermined data, namely temparature and "flux" on $\partial\Omega_c$.
We assume that the boundary $\partial\Omega_i$ satisfies

$$q \cdot n = 0 \quad \text{on } \partial\Omega_i \quad \forall \Omega \in \Theta. \tag{2.9}$$

For $\Omega \in \Theta$, let us introduce the following sets

$$T(\Omega) = \left\{ T \in H^1(\Omega); T_{|\partial\Omega_c} = T_m \right\} \tag{2.10}$$

$$Q(\Omega) = \left\{ q \in L^2(\Omega); \text{div } q = 0, q \cdot n_{|\partial\Omega_i} = 0, q \cdot n_{|\partial\Omega_c} = q_m \right\}. \tag{2.11}$$

k being strictly positive function, the KV functional is then defined by

$$F(\Omega, T, q) = \frac{1}{2} \int_\Omega \left(\sqrt{k} \nabla T - \frac{1}{\sqrt{k}} q \right)^2 \quad \forall (T, q) \in T(\Omega) \times Q(\Omega). \tag{2.12}$$

One can get

$$F(\Omega, q, T) = \frac{1}{2} \int_\Omega k \nabla T^2 + \frac{1}{2} \int_\Omega \frac{q^2}{k} + \int_{\partial\Omega_c} q_m \, T_m. \tag{2.13}$$

It is easy to check that the last term is known and independant of Ω.
A positive functional can therefore derived

$$\widehat{F}(\Omega) = \min_{(T,q) \in T(\Omega) \times Q(\Omega)} F(\Omega, q, T). \tag{2.14}$$

Let Ω_0 be the domain to identify, (T^0, q^0) the "real" couple correspondant to Ω_0 and (T_m, q_m) the overdetermined boundary data. So, we get

$$\widehat{F}(\Omega_0) = 0 \tag{2.15}$$

$$T^0 = \text{Arg} \min_{T(\Omega_0)} \frac{1}{2} \int_{\Omega_0} k \, \nabla T^2, \tag{2.16}$$

and

$$q_0 = \text{Arg} \min_{Q(\Omega_0)} \frac{1}{k} q^2. \tag{2.17}$$

So, the problem of the identification of Ω is transformed into an optimization problem, namely the minimization of $\widehat{F}$ over the set of admissible domains Θ. The following property will be needed to provide a new interesting expression for the functional $\widehat{F}$ in order to numerically resolve the optimization problem.

Property 1.

$$\forall \Omega \in \Theta \quad \min_{q \in Q(\Omega)} \frac{1}{2} \int_\Omega \frac{q^2}{k} = - \min_{T \in H^1(\Omega)} \left[\frac{1}{2} \int_\Omega k \, \nabla T^2 + \int_{\partial \Omega_c} q_m \, T \right]. \tag{2.18}$$

Proof. Let $\overline{T}$ be the argument (defined up to a constant) of the minimum in $H^1(\Omega)$ of the functional

$$J(\Omega) = \frac{1}{2} \int_\Omega k \, \nabla T^2 + \int_{\partial \Omega_c} q_m \, T \qquad T \in H^1(\Omega). \tag{2.19}$$

$\overline{T}$ exists due to the coercivity and the convexivity of J. Then, $\forall \varphi \in H^1(\Omega)$, we get

$$\int_\Omega k \nabla \overline{T} \, \nabla \varphi = - \int_{\partial \Omega_c} q_m \, \varphi. \tag{2.20}$$

Moreover, the argument $\overline{q}$ of the minimum on $Q(\Omega)$ of the functional

$$j(q) = \frac{1}{2} \int_\Omega \frac{q^2}{k}, \tag{2.21}$$

satisfies

$$\int_\Omega \frac{1}{k} \overline{q} \cdot (p - \overline{q}) = 0 \qquad \forall p \in Q(\Omega). \tag{2.22}$$

Now, we shall prove that $\overline{q} = -k \, \nabla \overline{T}$.

$$\begin{aligned} A &= \int_\Omega \frac{1}{k} \left(-k \, \nabla \overline{T} \right) \cdot (p - \overline{q}) \qquad p \in Q(\Omega), \\ &= \int_\Omega (\overline{q} - p) \cdot \nabla \overline{T}, \\ &= \int_{\partial \Omega} (\overline{q} - p) \cdot n \, \overline{T} - \int_\Omega \text{div } (\overline{q} - p) \, \overline{T}, \\ &= 0. \end{aligned}$$

Furthermore, we get div $\left(k \, \nabla \overline{T} \right) = 0$ deduced from (2.20). From the unicity of $\overline{q}$, we deduce $\overline{q} = -k \, \nabla \overline{T}$ and form (2.20), we get

$$\min_Q j(q) = j(\overline{q}) = \frac{1}{2} \int_\Omega \frac{\overline{q}^2}{k} = \frac{1}{2} \int_\Omega k \, \nabla \overline{T}^2. \tag{2.23}$$

$$\min_{H^1(\Omega)} J(T) = J(\overline{T}) = \frac{1}{2} \int_{\partial \Omega} k \nabla \overline{T}^2 + \int_{\partial \Omega_c} q_m \, \overline{T} = -\frac{1}{2} \int_\Omega k \nabla \overline{T}^2. \tag{2.24}$$

□

2.6 Application of the Kohn-Vogelius method for Cauchy Robin problem

2.6.1 An energy based least squares method

We consider in this section the Cauchy Robin problem as a model problem.

$$\begin{cases} \triangle u & = & 0 \text{ in } \Omega, \\ \dfrac{\partial u}{\partial n} & = & \Phi \text{ on } \Gamma_N, \text{ prescribed current flux} \\ u & = & f \text{ on } \Gamma_N, \text{ measurements} \\ \dfrac{\partial u}{\partial n} + qu & = & 0 \text{ on } \gamma. \end{cases}$$

Suppose q is determined. Therefore, we have twice too many prescribed data on Γ_N

$$(D)\begin{cases} \triangle u^D & = & 0 \text{ in } \Omega, \\ u^D & = & f \text{ on } \Gamma_N, \\ \dfrac{\partial u^D}{\partial n} + qu^D & = & 0 \text{ on } \gamma. \end{cases}, (N)\begin{cases} \triangle u^N & = & 0 \text{ in } \Omega, \\ \dfrac{\partial u^N}{\partial n} & = & \Phi \text{ on } \Gamma_N, \\ \dfrac{\partial u^N}{\partial n} + qu^N & = & 0 \text{ on } \gamma. \end{cases}$$

Provided q is the true impedance, we have

$$u^D(q) = u^N(q).$$

$\Rightarrow$ Therefore, let us minimize the misfit between u^D and u^N in order to get the true q.

Many misfit function may be proposed.
- Ordinary least squares:

$$\begin{aligned} J(q) &= \int_{\Gamma_N} |u^D(q) - u^N(q)|^2, \\ &= \int_{\Gamma_N} |f - u^N(q)|^2. \end{aligned}$$

- Energy least squares:

$$\int_\Omega |\nabla(u^D - u^N)|^2 + \int_\gamma |u^D - u^N|^2.$$

This idea has been proposed by several authors since Ladevère (early 70_s). Mainly by Kohn and Vogelius in 1989.

Advantages :

- Physical signification : We are not comparing data as measured, but solution as computed from these data.

- Stability : Distributed least squares (not on the boundary). If instability show up, they would impact heartily the misfit function. Therfore, they hopefully would be damped down.

Theorem 1. *There exists a unique solution $q \in Qad$ such that*

$$(O) \quad J(q) \leq J(q') \ \forall q' \in Qad,$$

and q is the solution of the inverse problem

$$(IP) \begin{cases} \text{Find } q \in Qad \text{ such that the solution } u \text{ of} \\ \\ (FP) \begin{cases} \triangle u & = & 0 \text{ in } \Omega, \\ \dfrac{\partial u}{\partial n} & = & \Phi \text{ on } \Gamma_N, \\ \dfrac{\partial u}{\partial n} + qu & = & 0 \text{ on } \gamma. \end{cases} \\ \\ \text{also verifies } u = f \text{ on } \Gamma_N, \end{cases}$$

provided (IP) has a solution (identifiability); $q \in Qad$.

Proof.
• Let q solve (IP) therefore $J(q) = 0$, since $u(q) = u^D$ and also $u(q) = u^N$ (this is (FP))
and

$$J(q) \leq J(q') \ \forall q' \in Qad,$$

• Let us suppose that we have two solutions of (O) q_1 and q_2.
Therefore $u_1^D = u_1^N$ and $u_2^D = u_2^N$ since $J(q_1) = J(q_2) = 0$. It follows that both u_1^N and u_2^N solve the inverse problem and thus $u_1^N = u_2^N$, which yields $q_1 = q_2$. □

2.6.2 The Kohn-Vogelius gradient algorithm

In order to implement the gradient algorithm, we need to compute the gradient $J'(q).r$. To this end, both expansion of u_D^h and u_N^h are needed.

One can prove that:

$$u_N^h = u_N^0 + hu_N^1 + h + \varepsilon(h).$$

and

$$u_D^h = u_D^0 + hu_D^1 + h + \eta(h),$$

where u_D^1 and u_N^1 solve

$$(N_1)\begin{cases} u_N^1 \in V = H^1(\Omega) \\ \displaystyle\int_\Omega \nabla u_N^1 \cdot \nabla v + \int_\gamma q u_N^1 v \;=\; -\int_{\Gamma_N} r u_N^0 v, \qquad \forall v \in H^1(\Omega). \end{cases}$$

$$(D_1)\begin{cases} u_D^1 \in V_0 \qquad\qquad (\Omega) \\ \displaystyle\int_\Omega \nabla u_D^1 \nabla v + \int_\gamma q u_D^1 v \;=\; -\int_{\Gamma_N} r u_D^0 v, \qquad \forall v \in V_0 \end{cases}$$

Theorem 2. *The derivative of the KV-functional is*

$$J'(q).r = \lim_{\lambda \to 0} \frac{J(q+\lambda r) - J(q)}{\lambda} = \int_\gamma r(|u_D^0|^2 - |u_N^0|^2)$$

Proof. We can write

$$J(q) = J_D(q) + J_N(q) + J_{DN}(q)$$

$$\text{where } \begin{cases} J_D(q) &= \displaystyle\int_\Omega |\nabla u_D|^2 + \int_\gamma q|u_D|^2, \\ J_N(q) &= \displaystyle\int_\Omega |\nabla u_N|^2 + \int_\gamma q|u_N|^2, \\ J_{DN}(q) &= \displaystyle -2\left\{\int_\Omega \nabla u_D \nabla u_N + \int_\gamma q u_D u_N\right\}. \end{cases}$$

One can remark that J_{DN} is a constant. Indeed, we have

$$\int_\Omega \nabla u_D \nabla u_N = -\int_\Omega \triangle u_N u_D + \int_\Gamma \frac{\partial u_N}{\partial n} u_D$$

as well as $u_D = f$, $\dfrac{\partial u_N}{\partial n} = \Phi$ on Γ_N and $\triangle u_N = 0$ in Ω.
Therefore,

$$\int_\Omega \nabla u_D \nabla u_N = \int_{\Gamma_N} \Phi f + \int_\gamma \frac{\partial u_N}{\partial n} u_D$$

Since $\frac{\partial u_N}{\partial n} = -qu_N$, we get

$$\int_\Omega \nabla u_D \nabla u_N = \int_{\Gamma_N} \Phi f - \int_\gamma q u_N u_D,$$

and thus

$$\int_\Omega \nabla u_D \nabla u_N + \int_\gamma q u_N u_D = \int_{\Gamma_N} \Phi f = constant.$$

and so $J'_{DN}(q).r$ vanish.
Now, using the asymptotic expansion above, we get that

$$J'_D(q).r = 2\int_\Omega \nabla u_D^0 \nabla u_D^1 + 2\int_\gamma q u_D^0 u_D^1 + \int_\gamma r|u_D^0|^2,$$

and similarly

$$J'_N(q).r = 2\int_\Omega \nabla u_N^0 \nabla u_N^1 + 2\int_\gamma q u_N^0 u_N^1 + \int_\gamma r|u_N^0|^2.$$

Now, using the formulation (N_1) with $v = u_N^0$, we get

$$J'_N(q).r = -2\int_\gamma r|u_N^0|^2 + \int_\gamma r|u_N^0|^2 = -\int_\gamma r|u_N^0|^2.$$

In the same way, using (D_1) with $v = u_D^0$, we get

$$J'_D(q).r = 2\left[\int_\Omega \nabla u_D^0 \nabla u_D^1 + \int_\gamma q u_D^0 u_D^1\right] + \int_\gamma r|u_D^0|^2,$$

However, $\int_\Omega \nabla u_D^0 \nabla u_D^1 + \int_\gamma q u_D^0 u_D^1 = -\int_\Omega \triangle u_D^0 u_D^1 + \int_\Gamma \frac{\partial u_D^0}{\partial n} u_D^1 + \int_\gamma q u_D^0 u_D^1$
u_D^0 verifies $\frac{\partial u_D^0}{\partial n} + q u_D^0 = 0$ on γ and $\frac{\partial u_D^0}{\partial n} = \Phi$ on Γ_N, whereas u_D^1 vanishes on Supp Φ.
Therefore,

$$\int_\Omega \nabla u_D^0 \nabla u_D^1 + \int_\gamma q u_D^0 u_D^1 = 0$$

and thus

$$J'_D(q).r = \int_\gamma r|u_D^0|^2.$$

The dervative is then

$$J'(q).r = \int_\gamma r(|u_D^0|^2 - |u_N^0|^2)$$

□

The K-V algorithm

- Choose $q^0 \in Qad$
- Calculate $u^D(q)$ and $u^N(q)$
- Compute $J'(q)$
- $q^{n+1} = q^n - \rho J'(q^n)$

It is nothing but the gradient algorithm applied to the KV functional

1. As all gradient algorithm, it is slow.
2. Understand why it is?

$$J'(q).r = \int_\gamma r(u_D^2(q) - u_N^2(q))$$

Let us suppose $r = sin(n\sigma)$, therefore $J'(q).sin(n\sigma)$ is the n^{th} Fourier coefficient of $(u_D^2 - u_N^2)$.
Provided u_D and u_N are smooth, these components of the gradient decrease fastly.

$\Rightarrow$ The gradient search is solely a search along the lowest frequencies.

The algorithm is thus expected to squeeze the higher frequencies components, and consequently to behave in a Stable way (since instabilities show up in the higher frequencies)

2.6.3 Stability of the Kohn-Vogelius algorithm (or/and robustiness)

$$(IP)\begin{cases} \text{Find } q \in Qad \text{ such that } u \\ \begin{cases} \triangle u = 0 \text{ in } \Omega, \\ \dfrac{\partial u}{\partial n} = \Phi \text{ on } \Gamma_N, \\ \dfrac{\partial u}{\partial n} + qu = 0 \text{ on } \gamma. \end{cases} \\ \text{also solve } u(q) = f. \end{cases} , (OP)\begin{cases} \text{Find } q \in Qad \text{ such that } u \\ J(q) \leq J(q') \ \forall q' \in Qad \end{cases}$$

1) If the measured data f are "exact" $\Rightarrow [(IP) \Leftrightarrow (OP)]$

2) The measurements are noisy. Thus
(a) The inverse problem has no solution.
(b) The optimization problem may have.

Theorem 3. *Suppose $f_n \in H^{\frac{1}{2}}(\Gamma_N)$ be a sequence of "noisy measurements" such that*
$f_n \to f \in H^{\frac{1}{2}}(\Gamma_N)$.

Therefore
1) $\forall n \in \mathbb{N}$, the optimization problem (OP_n) with data f_n has at least one solution

2) q_n being any solution of (OP_n), we have $\lim_{n\to\infty} ||q_n - q||_{0,\gamma} = 0$

Questions

1) This result is a stability one for the optimization problem, not for the (IP). Indeed, q_n has no correction with any inverse problem, whereas q has.

However, this theorem confirm that one can solve the optimization problem with approximate data (f_n) since we get an approximation q_n of the desired impedance q.

2) BUT usually noisy data f_n are not expected to belong to $H^{\frac{1}{2}}(\Gamma_N)$.
We have $f_\varepsilon = f + \varepsilon,\ \varepsilon \in L^2(\Gamma_N)$ and $||\varepsilon||_{L^2(\Gamma_N)} = \varepsilon$.
What is run usually is

(a) Smooth f_ε by some method, such as cubic splines and get $\tilde{f}_\varepsilon$ which is smooth enough, namely $\tilde{f}_\varepsilon \in H^{\frac{1}{2}}(\Gamma_N)$ (actually $\tilde{f}_\varepsilon \in C^2(\Gamma_N)$).
The central question is how close to the actual data f, $\tilde{f}_\varepsilon$ is?

We can prove that

$$\begin{aligned} ||\tilde{f}_\varepsilon - f||_{0,\infty,\Gamma_N} &\leq c(\varepsilon + h^2), \\ & \qquad h = [\text{ splining path }] \\ ||\tilde{f}_\varepsilon - f||_{1,\infty,\Gamma_N} &\leq c(\frac{\varepsilon}{h} + h). \end{aligned}$$

Therefore, cloosing $h \sim \sqrt{\varepsilon}$, we get

$$||\tilde{f}_\varepsilon - f||_{0,\infty,\Gamma_N} \leq c\varepsilon$$

and

$$||\tilde{f}_\varepsilon - f||_{1,\infty,\Gamma_N} \leq c\sqrt{\varepsilon}$$

(b) Use the smoothed $\tilde{f}_\varepsilon$ data to solve the (OP).

Therefore, we get $\tilde{q}_\varepsilon$ and, using the stability theorem

$$\lim_{\varepsilon \to 0} ||\tilde{q}_\varepsilon - q||_{0,\gamma} = 0.$$

This is a robustines result, though not a quantitative one.

2.7 Comments

The important issue of this chapter was to emphasize the utility of the KV approach.

From the innumerable applications cited, it can be easly seen that the methodology described is effective.

Chapter 3

An energy-gap cost functional for cavities identification

Contents

This chapter builds on the article entitled "**An energy-gap cost functional for cavities identification**" to appear in Nonlinear Studies, 2016. This work was done in collaboration with Sinda Khalfallah.

Abstract

This paper aims to solve an ill-posed cavities identification problem governed by Laplace equation with overdetermined boundary data. We introduce a Dirichlet-Neumann misfit function and we rephrase the inverse problem into a shape optimization one. The obtained problem is solved by a steepest descent algorithm using the gradient information combined with the level set method. The efficiency and accuracy of this approach is illustrated by numerical results.

Keywords: Cavities identification, ill-posed problem, domain perturbation, shape optimization, shape derivative, level set method.

Résumé

Dans ce papier, nous considérons un problème inverse géométrique régi par l'équation de Laplace. En ayant accès à des données surdéterminées sur le bord, notre objectif est de détecter la (ou les) cavité(s) dans la structure. Nous introduisons une approche Dirichlet-Neumann permettant de reformuler le problème en un problème d'optimisation de forme. L'identification est achevée itérativement par le biais d'un algorithme de descente de type gradient combiné avec la méthode level set. Les résultats numériques obtenus essentiellement dans le cas du changement de topologie, relatif à l'identification de deux cavités, prouvent la pertinence et la performance de notre méthode.

Mots clés: Identification de cavités, problème mal posé, perturbation du domaine, optimisation de forme, dérivée de forme, méthode des ensembles de niveaux.

3.1 Introduction

The underlying motivation for this research theme is cavities identification in materials which has become one of the leading branches of engineering science [70, 77]. Indeed, the problem of detecting cavities and localizing damage has acquired practical importance and may occur in many applications in industry such as non destructive testing [23]. Nowadays, the art of computer simulation has reached some maturity that allows new abilities to solve diverse geometrical problems. In fact, significant efforts have been concentrated on developing

computational pricing techniques for models where cavities occur.
The present paper emphasizes understanding and solving such an inverse problem. Indeed, it is devoted to numerical solution of identifying cavities, with possibly multiple connected components, from boundary measurements within the framework of the Laplace equation.
Let $A \subset \mathbb{R}^2$ be a bounded and open domain with boundary Υ_0. Given the heat flux Φ (input) and the temperature f measured on the boundary Υ_0, the problem under consideration consists in finding a bounded domain $\overline{B} \subset A$ with boundary Γ and the solution u of the following problem

$$\begin{cases} \Delta u = 0 & \text{in} \quad \Omega, \\ \dfrac{\partial u}{\partial \nu} = 0 & \text{on} \quad \Gamma, \\ \dfrac{\partial u}{\partial \nu_0} = \Phi & \text{on} \quad \Upsilon_0, \\ u = f & \text{on} \quad \Upsilon_0. \end{cases} \tag{3.1}$$

Above, $\Omega = A \setminus \overline{B}$, ν_0 and ν are the outward unit normals to the boundary of Ω.
The question we are concerned with is how to determine the boundary Γ by means of the data (Φ, f) prescribed on the accessible boundary Υ_0.
One approach to solve the inverse problem of reconstructing an object from boundary measurements is based on shape optimization methods. Such an approach has been extensively applied not only in the framework of inverse problems [2, 19, 37] but also in the framework of free boundary problems [21, 59, 63]. Thus, the shape optimization theory has been shown to be an attractive and successful approach to solve geometrical inverse problems.
Consequently, in a computational view, our cavities identification problem can be addressed as an optimization process in which the objective is to minimize the misfit between the solution of the following Dirichlet problem

$$\begin{cases} \Delta u_D = 0 & \text{in} \quad \Omega, \\ \dfrac{\partial u_D}{\partial \nu} = 0 & \text{on} \quad \Gamma, \\ u_D = f & \text{on} \quad \Upsilon_0, \end{cases} \tag{3.2}$$

and the Neumann one

$$\begin{cases} \Delta u_N = 0 & \text{in} \quad \Omega, \\ \dfrac{\partial u_N}{\partial \nu} = 0 & \text{on} \quad \Gamma, \\ \dfrac{\partial u_N}{\partial \nu_0} = \Phi & \text{on} \quad \Upsilon_0. \end{cases} \tag{3.3}$$

Let us, then, define the error function J depending on the domain Ω by

$$J(\Omega) := \frac{1}{2}\int_{\Omega} |\nabla u_D - \nabla u_N|^2. \tag{3.4}$$

One can remark that if (u, Ω) is a solution of the problem (3.1), then $u_D = u_N = u$. It follows that $J(\Omega) = 0$. Conversely, if $J(\Omega) = 0$, then $u_D = u_N$ up to a constant and $u = u_D = u_N$ is a solution of (3.1). Thus, the problem (3.1) is transformed into a shape optimization one

$$\begin{cases} \text{Find } \Omega \text{ such that} \\ J(\Omega) = \min\limits_{\tilde{\Omega} \subset A} J(\tilde{\Omega}), \end{cases} \tag{3.5}$$

which consists in minimizing the previously defined Kohn-Vogelius cost functional (3.4). The minimum has to be taken over all sufficiently smooth domains Ω suth that $\Omega \subset A$. Previously, this Kohn-Vogelius cost functional has been used in the context of parameter identification [66]. Recently, it has been successfully applied to free boundary problems related to a Bernoulli problem [21]. Let us point out that while the free boundary problem namely the Bernoulli problem is known to be well-posed [49], since the overdetermined boundary data (Dirichlet and Neumann data) are both given at the free boundary, the geometric inverse problem we adress here is well known to be ill-posed. That is, a slight error in the over-specified data may produce an enormous error in the numerical solution [57] which makes the inverse problem investigated in this paper very difficult to be solved. On the other hand, although we follow the same method as in [21], our contribution gives some worthfull results which have not been established in [21]. Indeed, we have achieved convergence in the case where the solution is made of two disconnected cavities and starting from an initial guess with one connected component.
The remainder of this paper is organized as follows: The next section is devoted to the computation of the shape gradient of the energy-gap cost functional J (3.4). The third section deals with the numerical analysis of the problem and presents the outline of the level set method. Numerical results are reported in the fourth section to demonstrate the behavior of our approach and the accuracy of the techniques investigated in previous sections. Our conclusion is drawn in the fifth section.

3.2 Shape derivative of the functional J

The shape optimization concept has several distinctive advantages as it allows us to use one of its fundamental tools, in literature known as the shape deriva-

tive we would like to review in this section [21, 37]. It has been used to prove local Lipschitz results for unknown boundaries in [22] as well as for straight cracks in [9].
In order to give a general idea related to the set of tools needed to define the shape deformation, let us first of all consider an open and bounded domain U such that $U \supset \overline{\Omega}$ and introduce the family of transformations F_t which defines a perturbation of the domain Ω of the form

$$F_t = Id + th,$$

where Id is the identity operator, h is a deformation field belonging to the space

$$Q = \{h \in \mathcal{C}^{1,1}(\overline{U})^2;\ h = 0 \text{ on } \Upsilon_0\}$$

and t is small enough such that F_t is a diffeomorphism from Ω onto its image. The perturbations of Ω and Γ are respectively defined by

$$\Omega_t := F_t(\Omega) \qquad \text{and} \qquad \Gamma_t := F_t(\Gamma).$$

Since h vanishes on Υ_0 for $h \in Q$, then $F_t(\Upsilon_0) = \Upsilon_0$. Thus, for all t, Υ_0 is a part of the boundary of Ω_t. We would consider the solutions $u_{Dt} := u_D(\Omega_t)$ and $u_{Nt} := u_N(\Omega_t)$ of (3.2) and (3.3) respectively formulated on the domain Ω_t instead of Ω and write u_D^t (respectively u_N^t) for the function $u_{Dt} \circ F_t$ (respectively $u_{Nt} \circ F_t$).

Definition 2. *The Eulerian derivative of the functional J at Ω in the direction of an element $h \in Q$ is defined by the quantity, when it exists:*

$$J'(\Omega, h) = \lim_{t \mapsto 0} \frac{J(\Omega_t) - J(\Omega)}{t}.$$

The Eulerian derivative is called shape derivative if $J'(\Omega, h)$ exists for all $h \in Q$ and the mapping $h \mapsto J'(\Omega, h)$ is linear and continuous with respect to the topology of $\mathcal{C}^{1,1}(\overline{\Omega})^2$.

At this stage, let us remind a transformation lemma [91] that would be useful later to determine the shape derivative of the functional J (3.4).

Lemma 1.

i) If $\varphi \in L^1(\Omega_t)$, then $\varphi^t \in L^1(\Omega)$ and we have

$$\int_{\Omega_t} \varphi = \int_{\Omega} \delta_t \varphi^t,$$

where $\delta_t = \det(DF_t)$ and DF_t is the Jacobian matrix of F_t.

ii) If $\varphi \in H^1(\Omega_t)$, *then* $\varphi^t \in H^1(\Omega)$ *and we have*

$$(\nabla\varphi) \circ F_t = M_t \nabla\varphi^t,$$

with $M_t = DF_t^{-T}$.

We can now present the following two results related to the material derivative of the state functions.

Proposition 1. *There exist* u_D^1 *and* $o(t)$ *in* $H^1(\Omega)$ *such that*

$$u_D^t = u_D^0 + t\, u_D^1 + t\, o(t), \tag{3.6}$$

where

i) u_D^0 *is the solution of* (3.2).

ii) $\lim_{t\mapsto 0} ||o(t)||_{H^1(\Omega)} = 0$.

iii) u_D^1 *is the unique solution of the following problem: Find* $u_D^1 \in V_0$ *such that* $\forall\, v \in H^1(\Omega)$

$$\int_\Omega \langle \nabla u_D^1, \nabla v\rangle = \int_\Omega \left[\langle Dh\nabla u_D^0, \nabla v\rangle + \langle \nabla u_D^0, Dh\nabla v\rangle - \langle \nabla u_D^0, \nabla v\rangle div\ h\right], \tag{3.7}$$

where

$$V_0 = \left\{v \in H^1(\Omega); v = 0 \text{ on } \Upsilon_0\right\}.$$

Proof. We proceed in the same way as in [46] for the elasticity problem. □

The calculations for the Neumann problem go along the same line as those of Dirichlet.

Proposition 2. *There exist* u_N^1 *and* $o(t)$ *in* $H^1(\Omega)$ *such that*

$$u_N^t = u_N^0 + t\, u_N^1 + t\, o(t), \tag{3.8}$$

where

i) u_N^0 *is the solution of* (3.3).

ii) $\lim_{t\mapsto 0} ||o(t)||_{H^1(\Omega)} = 0$.

iii) u_N^1 *is the unique solution of the following problem:*
Find $u_N^1 \in H^1(\Omega)$ *such that* $\forall\, v \in H^1(\Omega)$

$$\int_\Omega \langle \nabla u_N^1, \nabla v\rangle = \int_\Omega \left[\langle Dh\nabla u_N^0, \nabla v\rangle + \langle \nabla u_N^0, Dh\nabla v\rangle - \langle \nabla u_N^0, \nabla v\rangle div\ h\right]. \tag{3.9}$$

We now state our main theorem which provides the shape derivative of the misfit functional J (3.4).

Theorem 4. *The mapping $t \mapsto J(\Omega_t)$ is C^1 in a neighborhood of 0, and its derivative at 0, namely the shape gradient, reads as*

$$J'(\Omega, h) = \int_\Gamma G \, \langle h \, , \, \nu \rangle, \tag{3.10}$$

$$\textit{with} \qquad G = \frac{1}{2}\left[\left(\frac{\partial u_D^0}{\partial \tau}\right)^2 - \left(\frac{\partial u_N^0}{\partial \tau}\right)^2\right]. \tag{3.11}$$

where τ is the unit tangent vector to Γ.

Proof. The main difficulty involved in this theorem lies in reaching the Hadamard-Zolesio structure [44] of the functional J, namely (3.10). We can rewrite $J(\Omega)$ as

$$J(\Omega) = J_D(\Omega) + J_N(\Omega) + J_{DN}(\Omega),$$

$$\text{where} \begin{cases} J_D(\Omega) &= \dfrac{1}{2}\displaystyle\int_\Omega |\nabla u_D|^2, \\ J_N(\Omega) &= \dfrac{1}{2}\displaystyle\int_\Omega |\nabla u_N|^2, \\ J_{DN}(\Omega) &= -\displaystyle\int_\Omega \langle \nabla u_D \, , \, \nabla u_N \rangle. \end{cases}$$

Let us denote by $J_D^{'}(\Omega, h)$, $J_N^{'}(\Omega, h)$ and $J_{DN}^{'}(\Omega, h)$ the shape derivatives of respectively $J_D(\Omega)$, $J_N(\Omega)$ and $J_{DN}(\Omega)$ with respect to the domain Ω in direction h.

Integrating by parts, we easily deduce that

$$J_{DN}(\Omega) = -\int_{\Upsilon_0} \Phi \, f,$$

and therefore that $J_{DN}^{'}(\Omega, h) = 0$. Thus,

$$J^{'}(\Omega, h) = J_D^{'}(\Omega, h) + J_N^{'}(\Omega, h). \tag{3.12}$$

Following the same way as in [40], one can compute the shape derivative of both J_D and J_N.

1. **Shape derivative of the functional $J_D(\Omega)$**
   Using lemma 1, we have

$$\begin{aligned} J_D(\Omega_t) &= \frac{1}{2}\int_{\Omega_t} \langle \nabla u_{Dt} \, , \, \nabla u_{Dt} \rangle, \\ &= \frac{1}{2}\int_{\Omega_t} \langle \nabla u_D^t (DF_t)^{-1} \, o \, F_t^{-1} \, , \, \nabla u_D^t (DF_t)^{-1} \, o \, F_t^{-1} \rangle, \\ &= \frac{1}{2}\int_{\Omega} \langle \nabla u_D^t (DF_t)^{-1} \, , \, \nabla u_D^t (DF_t)^{-1} \rangle \det\,(DF_t). \end{aligned}$$

Using the asymptotic expansion of u_D^t, more precisely (3.6) and the fact that

$$\begin{cases} (DF_t)^{-1} &= Id - t\,Dh + t\,o(t), \\ \det(DF_t) &= 1 + t\ \text{div}\ h + t\,o(t), \end{cases}$$

we obtain

$$\begin{aligned} J_D(\Omega_t) =& J_D(\Omega) + t\int_\Omega \left[\langle \nabla u_D^0\,,\,\nabla u_D^1\rangle - \langle Dh\nabla u_D^0\,,\,\nabla u_D^0\rangle\right] \\ &+ t\int_\Omega \frac{1}{2}\langle \nabla u_D^0\,,\,\nabla u_D^0\rangle\ \text{div}\ h + t\,o(t). \end{aligned}$$

Therefore, we get

$$J_D^{'}(\Omega,h) = \int_\Omega \left[\langle \nabla u_D^0\,,\,\nabla u_D^1\rangle - \langle Dh\nabla u_D^0\,,\,\nabla u_D^0\rangle + \frac{1}{2}\,|\nabla u_D^0|^2\ \text{div}\ h\right].$$

Using the variational formulation of the Dirichlet problem (3.2), one can prove that

$$\int_\Omega \langle \nabla u_D^0\,,\,\nabla u_D^1\rangle = 0.$$

Thus, the shape derivative of the functional $J_D(\Omega)$ is

$$J_D^{'}(\Omega,h) = \int_\Omega \left[\frac{1}{2}\,|\nabla u_D^0|^2\ \text{div}\ h - \langle Dh\nabla u_D^0\,,\,\nabla u_D^0\rangle\right].$$

2. **Shape derivative of the functional** $J_N(\Omega)$

   In the same way, using lemma 1 and the asymptotic expansion of u_N^t (3.8), we get that

$$J_N^{'}(\Omega,h) = \int_\Omega \left[\langle \nabla u_N^0\,,\,\nabla u_N^1\rangle - \langle Dh\,\nabla u_N^0\,,\,\nabla u_N^0\rangle + \frac{1}{2}\,|\nabla u_N^0|^2\ \text{div}\ h\right].$$

   Since $u_N^0 \in H^1(\Omega)$ and using (3.9), the shape derivative of the functional $J_N(\Omega)$ becomes

$$J_N^{'}(\Omega,h) = \int_\Omega \left[\langle Dh\,\nabla u_N^0\,,\,\nabla u_N^0\rangle - \frac{1}{2}\,|\nabla u_N^0|^2\ \text{div}\ h\right]. \tag{3.13}$$

We have

$$\int_\Omega \langle Dh\,\nabla u_N^0\,,\,\nabla u_N^0\rangle = \int_\Omega \frac{\partial u_N^0}{\partial x}\langle \nabla h_1\,,\,\nabla u_N^0\rangle + \int_\Omega \frac{\partial u_N^0}{\partial y}\langle \nabla h_2\,,\,\nabla u_N^0\rangle$$

where $h = (h_1, h_2)$. By integrating this equation by parts, we obtain

$$\begin{aligned} \int_\Omega \langle Dh\,\nabla u_N^0\,,\,\nabla u_N^0\rangle =& -\int_\Omega h_1\,\text{div}\left(\frac{\partial u_N^0}{\partial x}\,\nabla u_N^0\right) + \int_{\partial\Omega} h_1\,\frac{\partial u_N^0}{\partial x}\,\frac{\partial u_N^0}{\partial n} \\ &- \int_\Omega h_2\,\text{div}\left(\frac{\partial u_N^0}{\partial y}\,\nabla u_N^0\right) + \int_{\partial\Omega} h_2\,\frac{\partial u_N^0}{\partial y}\,\frac{\partial u_N^0}{\partial n}. \end{aligned}$$

It can be concluded that

$$\int_\Omega \langle Dh\,\nabla u_N^0\,,\,\nabla u_N^0\rangle = -\int_\Omega h_1 \operatorname{div}\left(\frac{\partial u_N^0}{\partial x}\,\nabla u_N^0\right) - \int_\Omega h_2 \operatorname{div}\left(\frac{\partial u_N^0}{\partial y}\,\nabla u_N^0\right) + \int_{\partial\Omega} \frac{\partial u_N^0}{\partial n}\langle h\,,\,\nabla u_N^0\rangle.$$

Or $\dfrac{\partial u_N^0}{\partial \nu} = 0$ on Γ and $h = 0$ on Υ_0, then

$$\int_\Omega \langle Dh\,\nabla u_N^0\,,\,\nabla u_N^0\rangle = -\int_\Omega h_1 \operatorname{div}\left(\frac{\partial u_N^0}{\partial x}\,\nabla u_N^0\right) - \int_\Omega h_2 \operatorname{div}\left(\frac{\partial u_N^0}{\partial y}\,\nabla u_N^0\right). \tag{3.14}$$

According to the generalized Green formula and using the fact that $h_{|\Upsilon_0} = 0$, we have

$$\int_\Omega |\nabla u_N^0|^2 \operatorname{div} h = -\int_\Omega \langle \nabla\left(|\nabla u_N^0|^2\right)\,,\,h\rangle + \int_\Gamma |\nabla u_N^0|^2\,\langle h\,,\,\nu\rangle. \tag{3.15}$$

On the other hand, after a straightforward calculation, it can be deduced that

$$2\operatorname{div}\left(\frac{\partial u_N^0}{\partial x}\,\nabla u_N^0\right) - \frac{\partial}{\partial x}\left(|\nabla u_N^0|^2\right) = 2\,\frac{\partial u_N^0}{\partial x}\,\Delta u_N^0 \tag{3.16}$$

and

$$2\operatorname{div}\left(\frac{\partial u_N^0}{\partial y}\,\nabla u_N^0\right) - \frac{\partial}{\partial y}\left(|\nabla u_N^0|^2\right) = 2\,\frac{\partial u_N^0}{\partial y}\,\Delta u_N^0. \tag{3.17}$$

Using (3.14), (3.15), (3.16) and (3.17) and taking into account the monotonicity of u_N^0, the equation (3.13) becomes

$$J_N^{'}(\Omega, h) = -\frac{1}{2}\int_\Gamma |\nabla u_N^0|^2\,\langle h\,,\,\nu\rangle. \tag{3.18}$$

Proceeding in the same way as the Neumann problem, one can prove that

$$J_D^{'}(\Omega, h) = \frac{1}{2}\int_\Gamma |\nabla u_D^0|^2\,\langle h\,,\,\nu\rangle. \tag{3.19}$$

Using (3.12), (3.18) and (3.19) and taking into account that

$$\frac{\partial u_D^0}{\partial \nu} = 0 \qquad \text{and} \qquad \frac{\partial u_N^0}{\partial \nu} = 0 \quad \text{on } \Gamma,$$

we can conclude that

$$J'(\Omega, h) = \frac{1}{2}\int_\Gamma \left[\left(\frac{\partial u_D^0}{\partial \tau}\right)^2 - \left(\frac{\partial u_N^0}{\partial \tau}\right)^2\right]\,\langle h\,,\,\nu\rangle.$$

□

3.3 Numerical approximation

The main purpose of the present section is to numerically solve the problem (3.1) presented in the introduction, that is to retrieve the cavity B from the data (Φ, f). Therefore, our objective is to numerically confirm the theoretical results, investigated in the previous sections using an iterative method. At the k^{th} iteration, we consider for $t \geq 0$ the deformation of Γ^k as $\Gamma_t^k = F_t(\Gamma^k)$.
Now, we turn to the question of finding a good descent direction. The best possible one would be the following

$$h \in Q \quad \text{such that} \quad h_{|\Gamma} = -G\,\nu,$$

where G is given by (3.11). Thus, the algorithm described in the next second subsection can be seen as a descent method. To numerically implement this iterative process, we use the level set method.

3.3.1 Level set method

Since its introduction in 1988 by the American Mathematicians Stanley Osher and James Sethian [84], the level set method has been at the heart of one of the most active and successful research areas in image processing, computer graphics, optimization and computational fluid dynamics.
Based on a survey of research literature, one can remark that the shape derivative theory has been incorporated with the level set method to investigate shape optimization problems. The motivation to choose this method as a numerical tool to solve our problem is due not only to its connection with the shape derivative concept but also to its ability to automatically handle topology changes without requiring an elaborate mechanism. In this section, we develop the method in a sequence of steps. A good general review can be found in [62, 82]. First of all, we shortly introduce the level set method and briefly discuss the signed distance notion. Then, we enumerate some of the advantages of this method. Finally, we state the level set equation.
Since a number of very powerful tools are available when we introduce an implicit interface representation, we would like to define the interface as the isocontour of some function. In fact, in two dimensions and at any time t, our closed curve Γ_t is represented implicitly as the zero level set of a smooth, lipschitz-continuous scalar function $\varphi(x,t)$ by

$$\Gamma_t = \{x;\ \varphi(x,t) = 0\}.$$

Thus, the level set technique adds "dynamics" to the implicit contour. Although there are infinitely many choices of the implicit function, one would like it to be as smooth as possible. A good choice for that turns out to be the signed distance from the interface defined by $\varphi(x) = \pm\, d(x, \Gamma)$. It is preferred for its stability in numerical computations. The sign (-1) or (+1) depends on which side of the curve the point x lies in. One of the outstanding features of the level set formulation is that the geometrical properties of the interface such as the curvature κ and the normal vector ν are simply obtained in terms of φ, that is

$$\nu = \frac{\nabla\varphi}{|\nabla\varphi|} \qquad \text{and} \qquad \kappa = \nabla \cdot \frac{\nabla\varphi}{|\nabla\varphi|}.$$

The key idea of the level set method is the Hamilton-Jacobi approach [84] to numerical solutions of a time dependent equation for a moving implicit interface. Indeed, the evolution of the function φ is governed by the following Hamilton-Jacobi transport equation

$$\begin{cases} \partial_t\varphi - G\,|\nabla\varphi| &= 0 \qquad t \in (0, T], \\ \varphi(\cdot, 0) &= \varphi_0, \end{cases} \tag{3.20}$$

where φ_0 is a signed distance function corresponding to Γ^0. This equation, also known as "the level set equation", is obtained by the temporal derivative of the equation $\varphi(x, t) = 0$ and taking into account that

$$h_{|\Gamma} = -G\,\nu = -G\,\frac{\nabla\varphi}{|\nabla\varphi|},$$

where G was previously computed in Theorem 4. From (3.20), it could be seen that the implicit function φ is used both to represent the interface and to enable it to "evolve".

3.3.2 Outline of the algorithm

The combination of all these techniques presented previously yields an efficient algorithm which has flexibility in topology shape changing. The derivation of our approach could be represented in the following algorithm stages based on an iterative scheme.

1. Initialize $\varphi(., 0)$ to be the signed distance function associated to the initial contour Γ^0.

2. Compute the solutions u_D and u_N of the Dirichlet problem (3.2) respectively the Neumann one (3.3) using $P1$ finite element method.

3. Compute the speed function G (3.11).

4. Reinitialize the level set function by solving the Hamilton-Jacobi equation (3.20) and get a new function φ.

5. Check the stop condition, which is calculated as the Hausdorff distance between current and previous positions of the contour Γ.

It should be noted that the stopping criterion is reached when the Hausdorff distance between the successive curves Γ^{k-1} and Γ^k is sufficiently low; namely

$$d_H(\Gamma^k, \Gamma^{k-1}) < C\,\delta x^2,$$

where C is a constant independent of the grid spacing δx. Let us remind that the Hausdorff distance for two sets $A, B \subset \mathbb{R}^2$ is defined by

$$d_H(A,B) = \max\left(\sup_{a\in A} d(a,B)\ ,\ \sup_{b\in B} d(b,A)\right)$$

where

$$d(a,B) = \inf_{b\in B} |a-b|.$$

For various relative properties related to the Hausdorff distance concept, one can refer to [61].
In the next section, this iterative algorithm is tested over three different cases of situations including even multiple cavities on a square region.

3.4 Numerical tests

For numerical purposes, we consider the square $U = [-1,1] \times [-1,1]$ as a computational domain for all the following numerical simulations.
A series of pictures are presented in each case to show the shape evolution during the iterations. The diverse numerical scenarios, carried out using the previously presented theoretical and numerical tools, are described to evaluate the performance of our proposed algorithm.

3.4.1 First case

We evaluate our proposed approach on a first case for which an exact solution is known. Just like Υ_0, we consider the circle centered at the origin with the radius $r = 0.9$ and we initialize our algorithm with

$$\Gamma = \{x;\ |x| = 0.8\}. \tag{3.21}$$

The solution is the circle centered at the origin with a radius $r_{exact} = 0.35$ and the explicit expression u_{exact} of u is given by

$$u_{exact}(x, y) = x \left(\frac{1}{r_{exact}^2} + \frac{1}{x^2 + y^2} \right).$$

For the initial guess, we choose Γ (3.21) big enough to include the unknown cavity. Convergence is obtained after 354 iterations with $J(\Gamma^{354}) = 0.00009$ for 41×41 mesh grid. The cavity identification result is shown in Figure 3.1.

The topological flexibility has long been claimed as a major advantage of the level set method. The next two numerical cases emphasize such flexibility which is so desirable to so many applications.

3.4.2 Second case

For the numerical reconstruction in this case, we consider a disconnected initial guess: the union of the three disjointed circles of radius $R = 0.15$ centered respectively at $(-0.4, 0)$, $(0, 0)$ and $(0.4, 0)$ and a connected solution; namely the circle of radius $r_{exact} = 0.3$ centered at the origin as shown in Figure 3.2. The reconstruction is very good. Indeed, the three separate contours merge and one single curve is produced as the final result. We obtain convergence after 385 iterations for 30×30 mesh grid with $J(\Gamma^{385}) = 0.0022$.

3.4.3 Third case

This last test is the most challenging one. In fact, the inverse problem of identification of two cavities considered in this case has an extra difficulty with respect to those studied in other works found in the literature. In contrast to the last case, we consider disconnected cavities: the union of the two disjointed circles of radius 0.15 centered at $(-0.35, 0)$ and $(0.35, 0)$ and a connected initial guess : the circle of radius 0.65 centered at the origin. This numerical simulation illustrates how the curve changes topology and splits into two separate curves. Figure 3.3 shows the evolution of the boundary Γ^k for 31×31 mesh grid at different iterations; until convergence.

Thus, these last two cases demonstrate the effectiveness of the level set method in handling topology changes. From these numerical illustrations, it is obvious that the reconstruction of the cavity is perfect.

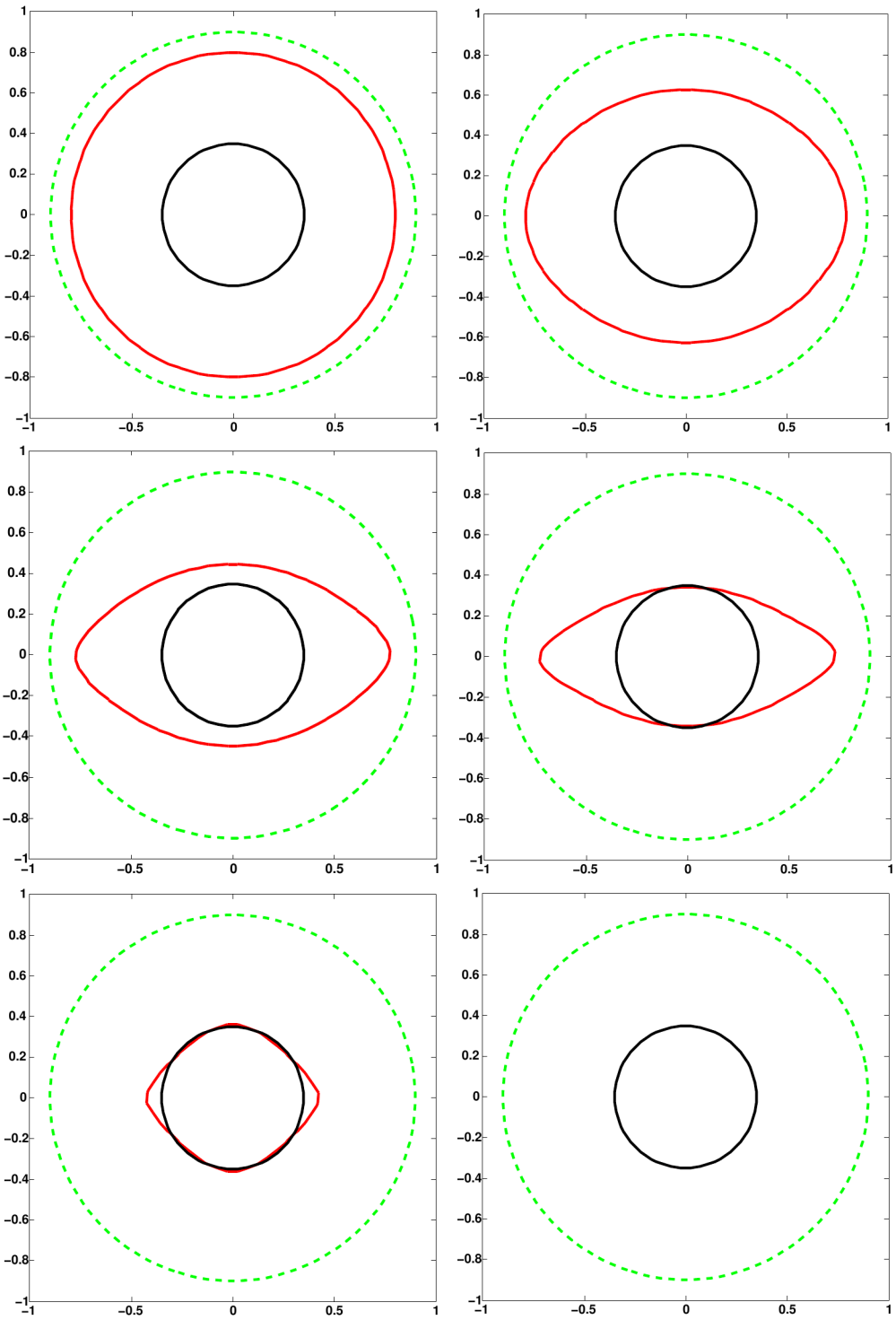

Figure 3.1: Υ_0 the exterior boundary (the dashed green line), Γ the exact solution (the black line), evolution of the boundary Γ^k (the red line) for $k = 0, 2, 4, 6, 67, 354$ (left to right, top to bottom).

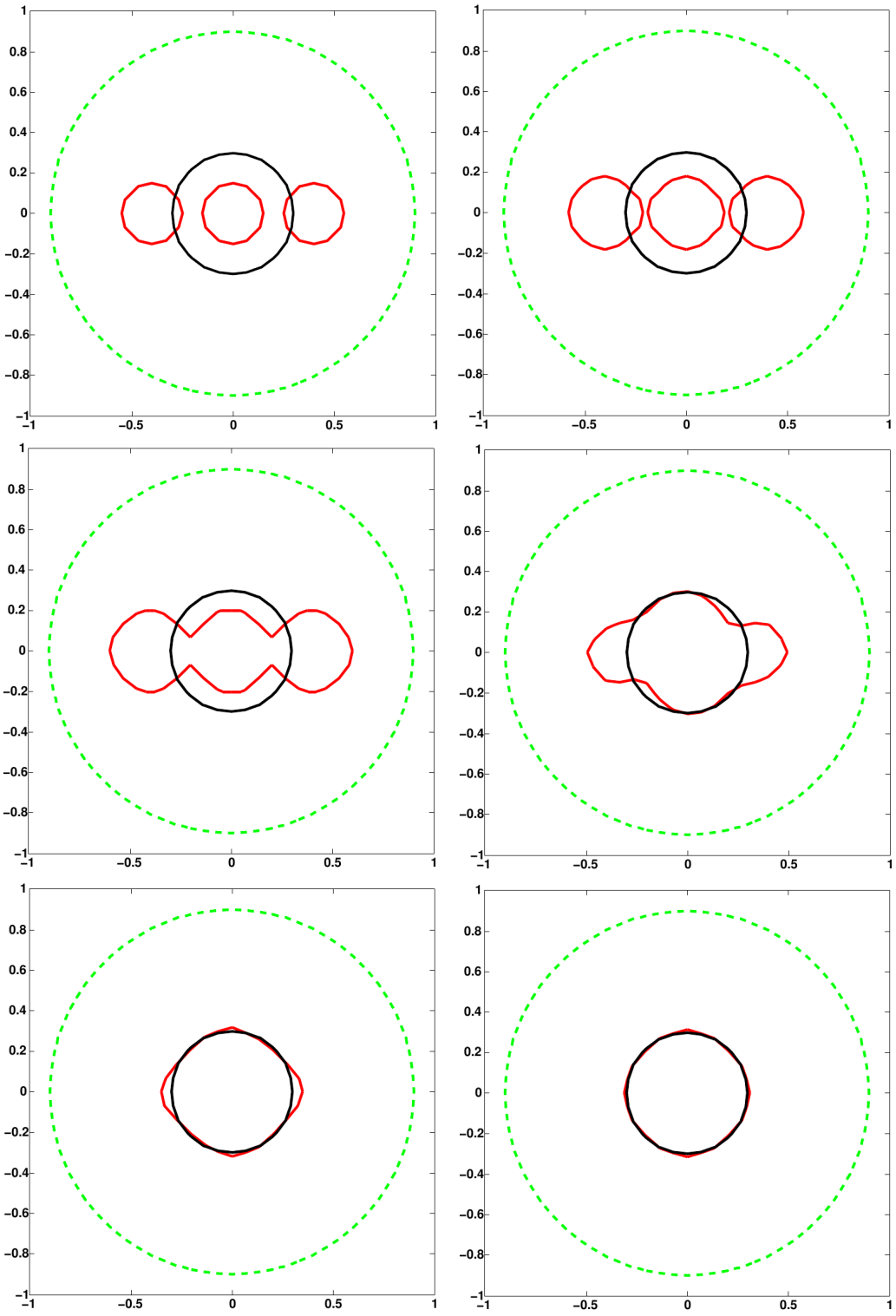

Figure 3.2: Topology change test: Υ_0 the exterior boundary (the dashed green line), Γ the exact solution (the black line), evolution of the boundary Γ^k (the red line) for $k = 0, 1, 2, 8, 85, 385$ (left to right, top to bottom).

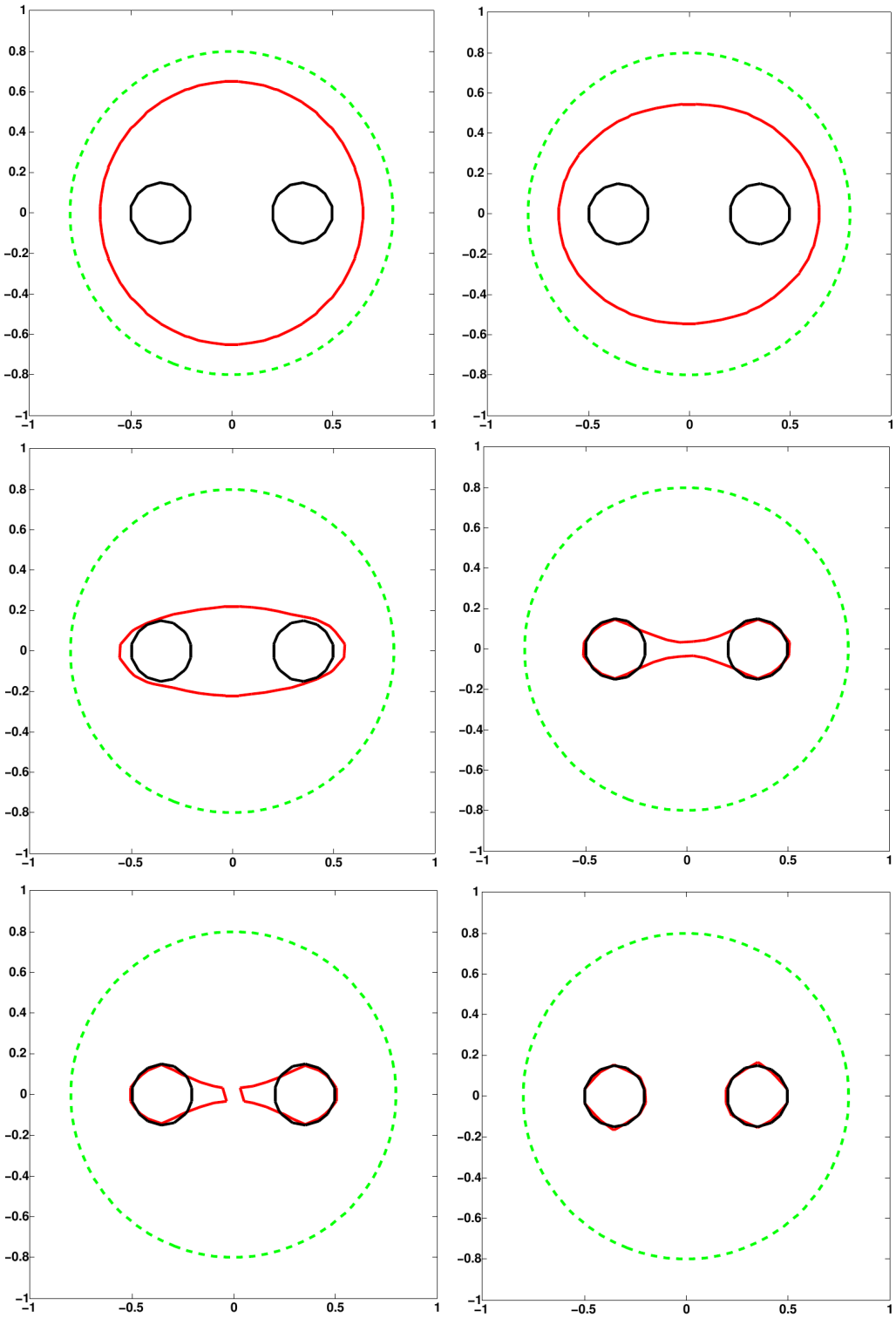

Figure 3.3: Topology change test: Υ_0 the exterior boundary (the dashed green line), Γ the exact solution (the black line), evolution of the boundary Γ^k (the red line) for $k = 0, 1, 5, 55, 56, 111$ (left to right, top to bottom).

3.5 Conclusion

In this paper, we have presented a gradient method to solve an ill-posed geometrical inverse problem of detecting cavities. For this purpose, an energy-gap cost functional rephrasing the inverse problem into a shape optimization one is proposed. Using appropriate techniques, the numerical tests show a significant agreement between the exact cavity shape and its reconstruction, thus demonstrating the validity of our approach as a robust solution tool for this class of problems from theoretical and computational viewpoints. Further work is currently being achieved to extend these techniques to elasticity problems since identifying cavities in mechanical structures has become crucial for engineers.

Chapter 4

An energy gap functional: Cavities identification in linear elasticity

Contents

This chapter builds on the article entitled "**An energy gap functional: Cavities identification in linear elasticity**" This work was done in collaboration with Amel Ben Abda, Sinda Khalfallah and Abdelmalek Zine.

Abstract

The aim of this work is an analysis of some geometrical inverse problems related to the identification of cavities in linear elasticity framework.
We rephrase the inverse problem into a shape optimization one using an energetic least-squares functional. The shape derivative of this cost functional is combined with the level set method in a steepest descent algorithm to solve the shape optimization problem. The efficiency of this approach is illustrated by several numerical results.

Keywords: Geometrical inverse problems, linear elasticity, cavities identification, shape optimization, shape derivative, level set method.

Résumé

Nous nous intéressons dans ce travail à l'analyse d'un problème inverse géométrique d'identification de cavités en élasticité linéaire. En introduisant une approche Dirichlet-Neumann, nous transformons notre problème sous la forme d'un problème d'optimisation de forme. La combinaison de la notion de dérivée par rapport au domaine et de la méthode level set, nous a permis la mise en oeuvre d'un algorithme de descente de type gradient pour la résolution numérique du problème inverse en question. L'efficacité de notre approche a été prouvée par les différents résultats numériques obtenus que ce soit dans le cas d'identification d'une seule cavité ou du plusieurs cavités.

Mots clés: Problèmes inverses géométriques, élasticité linéaire, identification de cavités, optimisation de forme, dérivée par rapport au domaine, méthode level set.

4.1 Introduction

Elastic cavities detection is a challenging problem from both the theoretical and the numerical point of view, as it is important to check the integrity of mechanical structures, see for example [70, 77]. The motivation of this work is to solve such inverse problems in the case of linear elasticity.
To this end, throughout this paper we consider a bounded domain $B \subset \mathbb{R}^2$,

with boundary Υ, occupied by a linear elastic material and we assume that there exists a cavity, namely a bounded domain $\overline{A} \subset B$ with boundary Γ. Let us denote by Ω the domain $B \setminus \overline{A}$. The forward linear elastic problem is therefore given by

$$\begin{cases} \operatorname{div} \sigma(u) &= 0 & \text{in } \Omega, \\ \sigma(u) &= \lambda \operatorname{tr} \varepsilon(u) \operatorname{Id} + 2\mu \varepsilon(u) & \text{in } \Omega, \\ \sigma(u)\, n &= 0 & \text{on } \Gamma, \\ \sigma(u)\, n_\Upsilon &= g & \text{on } \Upsilon, \end{cases}$$

where n_Υ and n are the outward unit normals to the boundary of Ω as it is

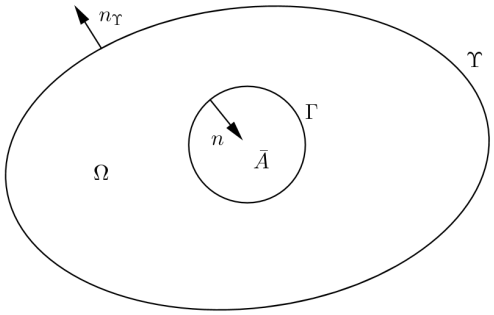

Figure 4.1: The domain Ω.

shown in Figure 4.1. The vector u denotes the displacement field, $\sigma(u)$ is the associated Cauchy stress tensor and $\varepsilon(u)$ is the linearized strain tensor given by

$$\varepsilon(u) = \frac{1}{2}\left(\nabla u + \nabla u^T\right).$$

σ and ε are related by the Hooke constitutive law, the medium being assumed to be homogeneous and isotropic. Therefore,

$$\sigma(u) = \lambda \operatorname{tr} \varepsilon(u) \operatorname{Id} + 2\mu \varepsilon(u)$$

and conversely

$$\varepsilon(u) = \frac{1+\nu}{E}\sigma(u) - \frac{\nu}{E}\left(\operatorname{tr} \sigma(u)\right) \operatorname{Id}.$$

Above, tr denotes the trace of matrix and λ, μ are the Lamé coefficients related to Young's modulus E and Poisson's ratio ν via

$$\mu = \frac{E}{2(1+\nu)} \qquad \text{and} \qquad \lambda = \frac{E\,\nu}{(1-2\nu)(1+\nu)}.$$

The geometrical inverse problem under consideration consists so in recovering the cavity A, namely the unknown shape Γ by applying some prescribed load

g on Υ and measuring the induced displacement on the same part Υ, i.e

$$\begin{cases} \sigma(u)\, n_\Upsilon &= g & \text{on } \Upsilon, \\ u &= f & \text{on } \Upsilon. \end{cases}$$

For the remainder of this paper, let us consider the following problem of recovering the cavity A

$$\begin{cases} \operatorname{div} \sigma(u) &= 0 & \text{in } \Omega, \\ \sigma(u) &= \lambda \operatorname{tr} \varepsilon(u) \operatorname{Id} + 2\mu\, \varepsilon(u) & \text{in } \Omega, \\ \sigma(u)\, n &= 0 & \text{on } \Gamma, \\ u &= f & \text{on } \Upsilon, \\ \sigma(u)\, n_\Upsilon &= g & \text{on } \Upsilon. \end{cases} \tag{4.1}$$

The identifiability of cavities as well as the local directional stability estimates were discussed in [28] where the authors use the so-called Almansi lemma [80] to prove the uniqueness question for the inverse problem.
A classical way to solve this problem is to formulate it as a shape optimization one. In fact, in [28], the cavity identification problem was transformed into a least-squares optimization problem

$$\arg \min_{\Sigma \in \mathcal{H}} \underbrace{\frac{1}{2}\left(\int_{\Gamma_M} |u - u^{\text{obs}}|^2 \text{ds}\right)}_{:= J_0(\Sigma)}$$

where $\mathcal{H}$ is some admissible set of geometries and u^{obs} denotes the observed data on some part Γ_M of the boundary. In [28], Ben Ameur et al. compute the shape derivative of the functional J_0 using the adjoint method. In [29], a regularization procedure was performed to recover cavities with minimal geometrical assumptions and the level set method is used to numerically solve the problem. As in [28, 29], we are interested in formulating the cavity identification problem (4.1) as a shape optimization one. To this end, we split the initial problem (4.1) into two sub-problems. Indeed, for a given Ω, let (σ_D, u_D) and (σ_N, u_N) be the solutions of the following Dirichlet, respectively Neumann problem

$$\begin{cases} \operatorname{div} \sigma_D &= 0 & \text{in } \Omega, \\ \varepsilon_D &= \frac{1+\nu}{E}\, \sigma_D - \frac{\nu}{E} (\operatorname{tr} \sigma_D) \operatorname{Id} & \text{in } \Omega, \\ \sigma_D\, n &= 0 & \text{on } \Gamma, \\ u_D &= f & \text{on } \Upsilon, \end{cases} \tag{4.2}$$

and

$$\begin{cases} \operatorname{div}\sigma_N &= 0 & \text{in } \Omega, \\ \varepsilon_N &= \frac{1+\nu}{E}\,\sigma_N - \frac{\nu}{E}\,(\operatorname{tr}\,\sigma_N)\,\mathrm{Id} & \text{in } \Omega, \\ \sigma_N\, n &= 0 & \text{on } \Gamma, \\ \sigma_N\, n_\Upsilon &= g & \text{on } \Upsilon. \end{cases} \tag{4.3}$$

It should be noted that writing both Dirichlet and Neumann problems in such a way is related to the use of the Hellinger-Reissner principle [93] recalled in the begining of the next section.

One can remark that the cavity to recover A^* is reached ($A = A^*$) when there is no misfit between both Dirichlet and Neumann solutions, that is, when $\sigma_D = \sigma_N$ and $u_D = u_N$. According to this observation, we propose an identification process based on the minimization of the following error functional J depending on the domain Ω

$$J(\Omega) := \frac{1}{2}\int_\Omega (\sigma_D - \sigma_N) : (\varepsilon(u_D) - \varepsilon(u_N)). \tag{4.4}$$

Thus, the cavities identification problem (4.1) can be formulated as a shape optimization one as follows

$$\begin{cases} \text{Find } \Omega \text{ such that} \\ J(\Omega) = \min\limits_{\tilde{\Omega}\subset B} J(\tilde{\Omega}). \end{cases} \tag{4.5}$$

The main contribution of the present paper relies on the use of the error functional (4.4) that can be interpreted as an energetic least-squares one based on fields computed from the measured data on the exterior boundary. Let us briefly browse history of this functional. Its main idea was introduced in 1985 by Wexler [94] who proposed an algorithm to recover the unknown impedance from the knowledge of solutions on the boundary of the spatial domain. In 1987, this algorithm has attracted the attention of Kohn and Vogelius [67] who suggested a modification of Wexler's algorithm to make it an alternating direction one by proposing a new misfit gap-cost functional. In the past two decades, this formulation has emerged as an effective tool for the treatment of various inverse problems. Indeed, it has been widely explored in the context of free boundary problems [17, 18, 21, 49], inclusion [76] and cracks [6] detection as well as cavities identification [23, 64]. It takes also advantage of being a self-regularizing way to proceed [8, 39].

The present research aims to develop an efficient method to numerically solve the shape optimization problem (4.5) by computing the shape derivative of the energy like misfit functional (4.4) in order to retrieve cavities in linear elasticity

framework.
The remainder of the paper is organized as follows: the upcoming section briefly presents the variational formulations in two fields for both Dirichlet and Neumann problems. In the third section , we introduce the concept of shape derivative and give its analytical expression for the functional J. The level set method as well as the optimization algorithm is described in the fourth section. We test the numerical behavior of our Dirichlet-Neumann approach combining with the level set method in several numerical examples presented in the fifth section. The last section is devoted to some comments.

4.2 Variational formulations in two fields

4.2.1 The Dirichlet problem

We adopted the formulation in two fields, namely the Hellinger-Reissner principle [93]. It consists to write both equilibrium equation and Hooke's law in variational form and not to inject Hooke's law in the equilibrium equation. The unknown is then the couple (σ, u).
Let us recall our Dirichlet problem (4.2),

$$\begin{cases} \operatorname{div}\sigma_D &= 0 & \text{in } \Omega, \\ \varepsilon_D &= \frac{1+\nu}{E}\,\sigma_D - \frac{\nu}{E}\,(\operatorname{tr}\,\sigma_D)\,\mathrm{Id} & \text{in } \Omega, \\ \sigma_D\, n &= 0 & \text{on } \Gamma, \\ u_D &= f & \text{on } \Upsilon. \end{cases}$$

Then, we introduce the following space V

$$V = \left\{ v \in \left[H^1(\Omega)\right]^2 ; v = 0 \text{ on } \Upsilon \right\}. \tag{4.6}$$

Let $v \in V$

$$\begin{aligned} & \int_\Omega -\operatorname{div}\,\sigma_D \cdot v = 0, \\ \Longrightarrow \quad & \int_\Omega \sigma_D : \varepsilon(v) - \int_{\partial\Omega} (\sigma_D\, n)\cdot v = 0, \\ \Longrightarrow \quad & \int_\Omega \operatorname{tr}\left[\sigma_D\, \varepsilon(v)\right] = 0, \end{aligned}$$

where " : " is the doubly contracted product.
The variational formulation of the equilibrium equation is then

$$\forall v \in V \qquad \int_\Omega \operatorname{tr}(\sigma_D\, \nabla v) = 0,$$

and using Hooke's law, we get

$$\forall \tau \in L^2_s(\Omega) \qquad \int_\Omega \left[\frac{1+\nu}{E}\,\mathrm{tr}(\sigma_D\,\tau) - \frac{\nu}{E}\,\mathrm{tr}(\sigma_D)\,\mathrm{tr}(\tau)\right] - \int_\Omega \mathrm{tr}(\tau\,\nabla u_D) = 0,$$

where

$$L^2_s(\Omega) = \left\{\tau = (\tau_{\alpha\,\beta}) \in \left[L^2(\Omega)\right]^4 ; \tau_{\alpha\,\beta} = \tau_{\beta\,\alpha}\right\}. \tag{4.7}$$

In fact, let $\tau \in L^2_s(\Omega)$

$$\begin{aligned} & \int_\Omega \varepsilon_D : \tau = \int_\Omega \left[\frac{1+\nu}{E}(\sigma_D : \tau) - \frac{\nu}{E}\,\mathrm{tr}(\sigma_D)(\mathrm{Id} : \tau)\right], \\ \Longrightarrow \quad & \int_\Omega \mathrm{tr}(\tau\,\varepsilon_D) = \int_\Omega \left[\frac{1+\nu}{E}\,\mathrm{tr}(\sigma_D\,\tau) - \frac{\nu}{E}\,\mathrm{tr}(\sigma_D)\,\mathrm{tr}(\tau)\right], \\ \Longrightarrow \quad & \int_\Omega \left[\frac{1+\nu}{E}\,\mathrm{tr}(\sigma_D\,\tau) - \frac{\nu}{E}\,\mathrm{tr}(\sigma_D)\,\mathrm{tr}(\tau)\right] - \int_\Omega \mathrm{tr}(\tau\,\nabla u_D) = 0. \end{aligned}$$

Finally, we obtain the formulation in two fields of the Dirichlet problem (4.2). Find $(\sigma_D, u_D) \in L^2_s(\Omega) \times \left[H^1(\Omega)\right]^2 ; u_D = f$ on Υ such that

$$\begin{cases} \forall \tau \in L^2_s(\Omega), & \displaystyle\int_\Omega \left[\frac{1+\nu}{E}\,\mathrm{tr}(\sigma_D\,\tau) - \frac{\nu}{E}\,\mathrm{tr}(\sigma_D)\,\mathrm{tr}(\tau)\right] - \int_\Omega \mathrm{tr}(\tau\,\nabla u_D) = 0, \\ \forall v \in V, & \displaystyle\int_\Omega \mathrm{tr}(\sigma_D\,\nabla v) = 0. \end{cases} \tag{4.8}$$

Let us define for $(\sigma, \tau) \in \left[L^2_s(\Omega)\right]^2$ and $v \in \left[H^1(\Omega)\right]^2$ the bilinear symmetric form $a(.,.)$ and the bilinear form $b(.,.)$ as following

$$a(\sigma, \tau) = \int_\Omega \left[\frac{1+\nu}{E}\mathrm{tr}(\sigma\,\tau) - \frac{\nu}{E}\mathrm{tr}(\sigma)\mathrm{tr}(\tau)\right],$$

and

$$b(\tau, v) = -\int_\Omega \mathrm{tr}(\tau\,\nabla v).$$

The formulation in two fields (4.8) can so be rewritten as:
Find $(\sigma_D, u_D) \in L^2_s(\Omega) \times \left[H^1(\Omega)\right]^2 ; u_D = f$ on Υ such that

$$\begin{cases} \forall \tau \in L^2_s(\Omega), & a(\sigma_D, \tau) + b(\tau, u_D) = 0, \\ \forall v \in V, & b(\sigma_D, v) = 0. \end{cases} \tag{4.9}$$

The first equation reflects the constitutive law and the second the equilibrium equation.

4.2.2 The Neumann problem

Proceeding in the same way as the Dirichlet problem, the formulation in two fields of the Neumann problem (4.3) is: Find $(\sigma_N, u_N) \in L^2_s(\Omega) \times [H^1(\Omega)]^2$ such that

$$\begin{cases} \forall \tau \in L^2_s(\Omega), \ \displaystyle\int_\Omega \left[\frac{1+\nu}{E}\,\mathrm{tr}(\sigma_N\,\tau) - \frac{\nu}{E}\,\mathrm{tr}(\sigma_N)\,\mathrm{tr}(\tau)\right] - \int_\Omega \mathrm{tr}(\tau\,\nabla u_N) = 0, \\ \forall v \in \left[H^1(\Omega)\right]^2, \ \displaystyle\int_\Omega \mathrm{tr}(\sigma_N\,\nabla v) = \int_\Upsilon g \cdot v. \end{cases}$$

In other words, by using the bilinear forms a and b, the formulation in two fields in the case of the Neumann problem is then: Find $(\sigma_N, u_N) \in L^2_s(\Omega) \times [H^1(\Omega)]^2$ such that

$$\begin{cases} \forall \tau \in L^2_s(\Omega), & a(\sigma_N, \tau) + b(\tau, u_N) = 0, \\ \forall v \in \left[H^1(\Omega)\right]^2, & b(\sigma_N, v) = -\displaystyle\int_\Upsilon g \cdot v. \end{cases} \tag{4.10}$$

4.3 Shape derivative of the functional J

Many studies in the field of structural optimization have been undertaken for the last two decades. The main part of this section is concerned with the shape sensitivity analysis of the mapping $\Omega \longmapsto J(\Omega)$; J being given by (4.4). Let us first begin with a review of some concepts related to the shape optimization theory [91].

In order to apply a gradient method to the minimization problem (4.5), we recall the concept of shape derivative. We prove its existence for the functional J and give its analytical expression.

To carry out the sensitivity analysis of the shape functional J, one needs to introduce a family of perturbations $\{\Omega_t\}$ of a given domain $\Omega \subset \mathbb{R}^2$. We make use of the transformations which are defined as the perturbations of the identity mapping id. Indeed, let us consider an open and bounded domain $U \supset \overline{\Omega}$ and construct a family of transformations F_t as follows

$$F_t = id + th,$$

where h is a deformation field belonging to the space

$$Q = \{h \in \mathcal{C}^{1,1}(\overline{U})^2;\ h = 0 \text{ on } \Upsilon\},$$

and t is sufficiently small such that F_t is a diffeomorphism from Ω onto its image.

The family of domains $\{\Omega_t\}$ and $\{\Gamma_t\}$ are then defined by

$$\Omega_t := F_t(\Omega) \qquad \text{and} \qquad \Gamma_t := F_t(\Gamma).$$

The condition $h_{|\Upsilon} = 0$ means that the boundary Υ is clamped during the iterative process described in the next section. Thus, for all t, Υ is a part of the boundary of Ω_t.
Then, we shall consider the couples (σ_{Dt}, u_{Dt}) and (σ_{Nt}, u_{Nt}) as the respective solutions of the problems (4.2) and (4.3) defined on the perturbed domain Ω_t, i.e. $(\sigma_{Dt}, u_{Dt}) := (\sigma_D(\Omega_t), u_D(\Omega_t))$ and $(\sigma_{Nt}, u_{Nt}) := (\sigma_N(\Omega_t), u_N(\Omega_t))$. More precisely, these couples are solutions of the following problems

$$\begin{cases} \operatorname{div} \sigma_{Dt} = 0 & \text{in } \Omega_t, \\ \varepsilon_{Dt} = \dfrac{1+\nu}{E}\,\sigma_{Dt} - \dfrac{\nu}{E}\,(\operatorname{tr}\,\sigma_{Dt})\,\mathrm{Id} & \text{in } \Omega_t, \\ \sigma_{Dt}\, n_t = 0 & \text{on } \Gamma_t, \\ u_{Dt} = f & \text{on } \Upsilon, \end{cases}$$

and

$$\begin{cases} \operatorname{div} \sigma_{Nt} = 0 & \text{in } \Omega_t, \\ \varepsilon_{Nt} = \dfrac{1+\nu}{E}\,\sigma_{Nt} - \dfrac{\nu}{E}\,(\operatorname{tr}\,\sigma_{Nt})\,\mathrm{Id} & \text{in } \Omega_t, \\ \sigma_{Nt}\, n_t = 0 & \text{on } \Gamma_t, \\ \sigma_{Nt}\, n_\Upsilon = g & \text{on } \Upsilon, \end{cases}$$

where as mentioned earlier n_Υ and n_t are the outward unit normals to the boundary of Ω_t.

Definition 3. *The Eulerian derivative of the functional J at Ω in the direction of an element $h \in Q$ is defined by the quantity, when it exists*

$$J'(\Omega, h) = \lim_{t \mapsto 0} \frac{J(\Omega_t) - J(\Omega)}{t}.$$

The Eulerian derivative is called shape derivative if $J'(\Omega, h)$ exists for all $h \in Q$ and the mapping $h \mapsto J'(\Omega, h)$ is linear and continuous with respect to the topology of $\mathcal{C}^{1,1}(\overline{\Omega})^2$.

Let us now recall the Zolesio-Hadamard structure theorem (see [44]).

Theorem 5. *There exists a function G defined on Γ such that*

$$J'(\Omega, h) = \int_\Gamma G(h \cdot n).$$

In the remainder of this section, we prove the existence of the shape derivative and formulate the explicit expression of the function G. It might be interesting to point out that the last theorem allows choosing the gradient flow as follows

$$h \in Q \qquad \text{such that} \qquad h_{|\Gamma} = -G\,n,$$

since the shape derivative depends only on the normal component of the vector field h and such descent direction guarantees a decreasing of the value of J. In the fifth section, we will use this normal velocity and the level set method to numerically solve the shape optimization problem (4.5). To determine the shape derivative, we first recall some transformation and differentiation formulas in the following two lemmas [91].
In the sequel, the following notations will be adapted. If φ_t is a function defined on the perturbed domain Ω_t or boundary Γ_t, we note φ^t the function $\varphi_t \circ F_t$ which is defined on the reference domain Ω or boundary Γ. We denote by DF_t the Jacobian matrix of F_t and by DF_t^T the transpose of DF_t. It is easy to see that $(DF_t^T)^{-1} = (DF_t^{-1})^T$; so for the sake of simplicity, we shall write DF_t^{-T}.
Let us now recall the following useful results which can be proved by applying the chain rule.

Lemma 2. *[91]*

i) If $\varphi_t \in L^1(\Omega_t)$, then $\varphi^t \in L^1(\Omega)$ and we have

$$\int_{\Omega_t} \varphi_t = \int_{\Omega} \delta_t\, \varphi^t,$$

where $\delta_t = \det(DF_t) = \det(Id + t\,\nabla h^{\mathsf{T}})$.

ii) If $\varphi_t \in H^1(\Omega_t)$, then $\varphi^t \in H^1(\Omega)$ and we have

$$(\nabla \varphi_t) \circ F_t = M_t \nabla \varphi^t,$$

with $M_t = DF_t^{-T}$.

Lemma 3. *[91] The mappings $t \mapsto \delta_t$ and $t \mapsto M_t$ with values in $\mathcal{C}(\Omega)$ and $\mathcal{C}(\Omega)^{2\times 2}$ respectively, are $\mathcal{C}^1$ in a neighborhood of 0 and we have*

$$\begin{cases} \dfrac{d\delta_t}{dt}\,|_{t=0} & = \operatorname{div} h, \\ \dfrac{dM_t}{dt}\,|_{t=0} & = -\nabla h. \end{cases}$$

4.3.1 Asymptotic expansions

4.3.1.1 The Dirichlet problem

In the remainder of this paper, we denote by (σ_D^0, u_D^0) the solution of the Dirichlet problem (4.2) in the reference domain Ω. Let us define in Ω_t the space V_t respectively $L^2_{st}(\Omega_t)$ in the same way as in (4.6) respectively (4.7)

$$V_t = \left\{ v \in \left[H^1(\Omega_t)\right]^2 ; v = 0 \text{ on } \Upsilon \right\}$$

and

$$L^2_{st}(\Omega_t) = \left\{ \tau = (\tau_{\alpha\,\beta}) \in \left[L^2(\Omega_t)\right]^4 ; \tau_{\alpha\,\beta} = \tau_{\beta\,\alpha} \right\}.$$

Following the same procedure used to find the variational formulation (4.8) in two fields of the Dirichlet problem defined on the reference domain Ω, we obtain the corresponding one in Ω_t. Find $(\sigma_{Dt}, u_{Dt}) \in L^2_{st}(\Omega_t) \times [H^1(\Omega_t)]^2 ; u_{Dt} = f$ on Υ such that

$$\begin{cases} \forall \tau \in L^2_{st}(\Omega_t), \ \displaystyle\int_{\Omega_t} \left[\frac{1+\nu}{E} \operatorname{tr}(\sigma_{Dt}\,\tau) - \frac{\nu}{E} \operatorname{tr}(\sigma_{Dt}) \operatorname{tr}(\tau) \right] - \int_{\Omega_t} \operatorname{tr}(\tau\, \nabla u_{Dt}) = 0, \\ \qquad \forall v \in V_t, \ \displaystyle\int_{\Omega_t} \operatorname{tr}(\sigma_{Dt}\, \nabla v) = 0. \end{cases} \tag{4.11}$$

For this solution (σ_{Dt}, u_{Dt}) defined on the perturbed domain Ω_t, let us associate throughout this paper the couple (σ_D^t, u_D^t) which is the solution transported to the fixed domain Ω by

$$\begin{cases} \sigma_D^t = \sigma_{Dt}\, o\, F_t, \\ u_D^t = u_{Dt}\, o\, F_t. \end{cases} \tag{4.12}$$

It is a standard notation used by the shape optimization community. The couple (σ_D^t, u_D^t) has no mechanical meaning. It has only the advantage to bring back fields defined on the perturbed domain Ω_t to the reference domain Ω. Using the equalities (4.12), the transformation formulas (lemma 2) and the fact that $u_{Dt} = u_D^t = u_D^0$ and $f_t = f^t = f$ on Υ, we get the formulation in two fields of the perturbed Dirichlet problem, brought to the reference domain: Find $(\sigma_D^t, u_D^t) \in L^2_s(\Omega) \times [H^1(\Omega)]^2 ; u_D^t = f$ on Υ such that

$$\begin{cases} \forall\, \tau \in L^2_s(\Omega), & \displaystyle\int_\Omega \left[\frac{1+\nu}{E} \operatorname{tr}(\sigma_D^t\, \tau) - \frac{\nu}{E} \operatorname{tr}(\sigma_D^t) \operatorname{tr}(\tau) \right] \det\,(DF_t) \\ & \displaystyle - \int_\Omega \operatorname{tr}\left[\tau\, (\nabla u_D^t (DF_t)^{-1}) \right] \det\,(DF_t) = 0, \\ \forall\, v \in V, & \displaystyle\int_\Omega \operatorname{tr}\left[\sigma_D^t\, \left(\nabla v\, (DF_t)^{-1} \right) \right] \det\,(DF_t) = 0. \end{cases} \tag{4.13}$$

4.3.1.2 The Neumann problem

We proceed in the same way as for the Dirichlet problem. Note that, as $v_t = v^t$ and $g_t = g^t = g$ on Υ, the formulation in two fields of the perturbed Neumann problem, brought to the reference domain Ω, is then:
Find $(\sigma_N^t, u_N^t) \in L_s^2(\Omega) \times [H^1(\Omega)]^2$ such that

$$\begin{cases} \forall \tau \in L_s^2(\Omega), & \displaystyle\int_\Omega \left[\frac{1+\nu}{E}\mathrm{tr}\left(\sigma_N^t\,\tau\right) - \frac{\nu}{E}\,\mathrm{tr}(\sigma_N^t)\,\mathrm{tr}(\tau)\right]\det\,(DF_t) \\ & \displaystyle -\int_\Omega \mathrm{tr}\left[\tau\,\left(\nabla u_N^t (DF_t)^{-1}\right)\right]\det\,(DF_t) = 0, \\ \forall v \in \left[H^1(\Omega)\right]^2, & \displaystyle\int_\Omega \mathrm{tr}\left[\sigma_N^t\,\left(\nabla v\,(DF_t)^{-1}\right)\right]\det\,(DF_t) = \int_\Upsilon g\cdot v. \end{cases}$$

Before proceeding further with the calculus of the shape derivative of the functional J, we present the following two results related to the asymptotic expansions, namely the material derivative of the state functions.

Theorem 6. (Related to the Dirichlet problem)
There exists $\eta_0 > 0$ such that, if $t < \eta_0$, we get

$$(\sigma_D^t, u_D^t) = (\sigma_D^0, u_D^0) + t\,(\sigma_D^1, u_D^1) + t\,o(t), \tag{4.14}$$

where $(\sigma_D^0, u_D^0), (\sigma_D^1, u_D^1)$ and $o(t)$ are elements of $L_s^2(\Omega) \times [H^1(\Omega)]^2$ satisfying

i) (σ_D^0, u_D^0) is the solution of the linear elasticity Dirichlet problem (4.9) hanging in Ω.

ii) $\lim\limits_{t\mapsto 0} ||o(t)||_{L_s^2(\Omega)\times V} = 0$.

iii) $(\sigma_D^1, u_D^1) \in L_s^2(\Omega) \times V$ is the unique solution of the following problem

$$\begin{cases} \forall \tau \in L_s^2(\Omega),\ a\left(\sigma_D^1, \tau\right) + b\left(\tau, u_D^1\right) = -\displaystyle\int_\Omega tr\left[\tau\left(\nabla u_D^0\,\nabla h\right)\right], \\ \qquad \forall v \in V,\ b\left(\sigma_D^1, v\right) = -\displaystyle\int_\Omega tr\left[\sigma_D^0\,\left(\nabla v\,\nabla h\right)\right] + \int_\Omega tr\left(\sigma_D^0\,\nabla v\right) div\ h. \end{cases} \tag{4.15}$$

Proof. Let Φ be the function

$$\Phi : \mathbb{R} \times L_s^2(\Omega) \times \left[H^1(\Omega)\right]^2 \longrightarrow L_s^2(\Omega) \times \left(\left[H^1(\Omega)\right]^2\right)'$$

defined as following

$$\Phi(t, \sigma, u) = \begin{cases} A(t)\,\sigma + \overline{B(t)}\,u \\ B(t)\,\sigma \end{cases}$$

where we have adopted the following notations

$$A(t)\,\sigma = \left(\frac{1+\nu}{E}\,\sigma - \frac{\nu}{E}\,(\text{tr }\sigma)\ \text{Id}\right)\ \det\,(DF_t),$$

$$< B(t)\,\sigma, v >= -\int_\Omega \text{tr}\left[\sigma\,(\nabla v\,(DF_t)^{-1})\right]\det\,(DF_t).$$

Then $\overline{B(t)}$ (which is the transpose of $B(t)$) will be defined by

$$\overline{B(t)}\,v = -\frac{1}{2}\left[(\text{Id} + t\overline{\nabla h})^{-1}\,\overline{\nabla v} + \nabla v\,(\text{Id} + t\,\nabla h)^{-1}\right]\det\,(DF_t).$$

So, the equations (4.13) can be written as the following

$$\begin{cases} \text{Find } (\sigma_D^t, u_D^t) \in L_s^2(\Omega) \times \left[H^1(\Omega)\right]^2;\ u_D^t = f \text{ on } \Upsilon \text{ such that} \\ \Phi(t, \sigma_D^t, u_D^t) = 0. \end{cases}$$

Φ is a linear application on (σ, u) and differentiable on t. We have also $\Phi(0, \sigma_D^0, u_D^0) = 0$, which reflects that (σ_D^0, u_D^0) is the solution of the problem (4.9) defined on the reference domain Ω. The derivative of Φ, with respect to the variable (σ, u) is Φ itself which leads to

$$\begin{aligned} \frac{\partial \Phi}{\partial(\sigma,u)}(0,\sigma^0,u^0)(\sigma,u) &= \Phi(0,\sigma,u) \\ &= \begin{cases} A(0)\,\sigma + \overline{B(0)}\,u \\ B(0)\,\sigma \end{cases} \\ &= \begin{cases} (\frac{1+\nu}{E}\sigma - \frac{\nu}{E}\,(\text{tr }\sigma)\ \text{Id}) - \frac{1}{2}(\overline{\nabla u} + \nabla u) \\ B(0)\,\sigma. \end{cases} \end{aligned}$$

The partial derivative of Φ, with respect to (σ, u), is then, according to the theorem of Brezzi, a bijection from $L_s^2(\Omega)\times[H^1(\Omega)]^2$ to $L_s^2(\Omega)\times\left([H^1(\Omega)]^2\right)'$. In addition, Φ is linear and continuous. The open mapping theorem provides that Φ is an isomorphism from $L_s^2(\Omega)\times[H^1(\Omega)]^2$ to $L_s^2(\Omega)\times\left([H^1(\Omega)]^2\right)'$. It follows from the implicit function theorem that there exists a positive number η_0 and a neighborhood ϑ of (σ_D^0, u_D^0) in $L_s^2(\Omega)\times[H^1(\Omega)]^2$ such that $\forall\, t \in]-\eta_0, \eta_0[$, there exists a unique couple (σ_D^t, u_D^t) in $L_s^2(\Omega)\times[H^1(\Omega)]^2$ such that

$$\Phi(t, \sigma_D^t, u_D^t) = 0.$$

Moreover, the application $t \mapsto (\sigma^t, u^t)$ is C^1, from $]-\eta_0, \eta_0[$ to ϑ. Then, we have

$$(\sigma_D^t, u_D^t) = (\sigma_D^0, u_D^0) + t\,(\sigma_D^1, u_D^1) + t\,o(t),$$

where

$$\lim_{t\mapsto 0} ||o(t)||_{L_s^2(\Omega)\times V} = 0.$$

iii) Postponing the equality (4.14) in the equations (4.13), using the fact that (σ_D^0, u_D^0) is the solution of the problem (4.9) and identifying the terms of the same order t, we acquire that (σ_D^1, u_D^1) is the solution of the problem (4.15).

□

Similar results can be expected for the Neumann problem. In fact, following the same way as the Dirichlet problem, one can prove the following theorem.

Theorem 7. (Related to the Neumann problem)
There exists $\delta_0 > 0$ such that, if $t < \delta_0$, we get

$$(\sigma_N^t, u_N^t) = (\sigma_N^0, u_N^0) + t\,(\sigma_N^1, u_N^1) + t\,o(t), \tag{4.16}$$

where $(\sigma_N^0, u_N^0), (\sigma_N^1, u_N^1)$ and $o(t)$ are elements of $L_s^2(\Omega) \times [H^1(\Omega)]^2$ satisfying

i) (σ_N^0, u_N^0) is the solution of the linear elasticity Neumann problem (4.10) hanging in Ω.

ii) $\lim\limits_{t \mapsto 0} ||o(t)||_{L_s^2(\Omega)\times[H^1(\Omega)]^2} = 0$.

iii) $(\sigma_N^1, u_N^1) \in L_s^2(\Omega) \times [H^1(\Omega)]^2$ is the unique solution of the following problem

$$\begin{cases} \forall \tau \in L_s^2(\Omega), & a\left(\sigma_N^1, \tau\right) + b\left(\tau, u_N^1\right) = -\displaystyle\int_\Omega tr\left[\tau\left(\nabla u_N^0\, \nabla h\right)\right], \\ \forall v \in \left[H^1(\Omega)\right]^2, & b\left(\sigma_N^1, v\right) = -\displaystyle\int_\Omega tr\left[\sigma_N^0\left(\nabla v\, \nabla h\right)\right] \\ & \qquad + \displaystyle\int_\Omega tr\left(\sigma_N^0\, \nabla v\right) div\ h. \end{cases} \tag{4.17}$$

Lemma 4. *[46]*

$$\overline{div\ \left(\sigma_D^0\, \nabla u_D^0\right)} = \frac{1}{2}\ grad\ \left[tr\ \left(\sigma_D^0\, \nabla u_D^0\right)\right].$$

$$\overline{div\ \left(\sigma_N^0\, \nabla u_N^0\right)} = \frac{1}{2}\ grad\ \left[tr\ \left(\sigma_N^0\, \nabla u_N^0\right)\right].$$

Now, we are able to prove the main result of this section.

Theorem 8. *The mapping $t \mapsto J(\Omega_t)$ is $\mathcal{C}^1$ in a neighborhood of 0 and its derivative at 0 is given by*

$$J'(\Omega, h) = \int_\Gamma G\,(h \cdot n),$$

with

$$G = \frac{1}{2}\left[\left(\sigma_D^0 : \varepsilon(u_D^0)\right) - \left(\sigma_N^0 : \varepsilon(u_N^0)\right)\right]. \tag{4.18}$$

Proof. Using (4.14),(4.16), the transformation formulas (see lemma 2) and the fact that

$$\det(DF_t) = 1 + t\,\mathrm{div}\ h + o(t) \qquad \text{and} \qquad (DF_t)^{-1} = \mathrm{Id} - t\,\nabla h + o(t),$$

(see lemma 3), we get

$$\begin{aligned} J'(\Omega,h) =& \int_\Omega \left[\frac{1+\nu}{E}\left(\sigma_D^0 - \sigma_N^0\right) : \left(\sigma_D^1 - \sigma_N^1\right) - \frac{\nu}{E}\,\mathrm{tr}\left(\sigma_D^0 - \sigma_N^0\right)\,\mathrm{tr}\left(\sigma_D^1 - \sigma_N^1\right)\right] \\ &+ \frac{1}{2}\int_\Omega \mathrm{div}\ h\left[\frac{1+\nu}{E}\left(\sigma_D^0 - \sigma_N^0\right) : \left(\sigma_D^0 - \sigma_N^0\right) - \frac{\nu}{E}\left[\mathrm{tr}\left(\sigma_D^0 - \sigma_N^0\right)\right]^2\right] \\ =& a\left(\sigma_D^0 - \sigma_N^0, \sigma_D^1 - \sigma_N^1\right) \\ &+ \frac{1}{2}\int_\Omega \mathrm{div}\ h\left[\frac{1+\nu}{E}\left(\sigma_D^0 - \sigma_N^0\right) : \left(\sigma_D^0 - \sigma_N^0\right) - \frac{\nu}{E}\left[\mathrm{tr}\left(\sigma_D^0 - \sigma_N^0\right)\right]^2\right] \end{aligned}$$

Using (4.9), (4.10), (4.15) and (4.17), we get

$$\begin{aligned} & a\left(\sigma_D^0 - \sigma_N^0, \sigma_N^1\right) \\ =& - b\left(\sigma_N^1, u_D^0 - u_N^0\right), \\ =& \int_\Omega \mathrm{tr}\left[\sigma_N^0\ \left(\nabla\left(u_D^0 - u_N^0\right)\nabla h\right)\right] - \int_\Omega \mathrm{tr}\left[\sigma_N^0\,\nabla\left(u_D^0 - u_N^0\right)\right]\ \mathrm{div}\ h \end{aligned}$$

and

$$a\left(\sigma_D^1, \sigma_D^0 - \sigma_N^0\right) = \int_\Omega \mathrm{tr}\ \left[\left(\sigma_D^0 - \sigma_N^0\right)\ \nabla u_D^1\right] - \int_\Omega \mathrm{tr}\left[\left(\sigma_D^0 - \sigma_N^0\right)\ \left(\nabla u_D^0\,\nabla h\right)\right].$$

One can prove that

$$\int_\Omega \mathrm{tr}\ \left[\left(\sigma_D^0 - \sigma_N^0\right)\ \nabla u_D^1\right] = 0.$$

Thus, we get

$$\begin{aligned} J'(\Omega,h) \ =\ & \int_\Omega \mathrm{tr}\left[\sigma_N^0\left(\nabla u_N^0\,\nabla h\right)\right] - \int_\Omega \mathrm{tr}\left[\sigma_D^0\left(\nabla u_D^0 \nabla h\right)\right] \\ & -\frac{1}{2}\int_\Omega \left[\varepsilon(u_N^0) : \sigma_N^0\right]\ \mathrm{div}\ h + \frac{1}{2}\int_\Omega \left[\varepsilon(u_D^0) : \sigma_D^0\right]\mathrm{div}\ h. \end{aligned}$$

Using generalized Green's formula, we get

$$\begin{aligned} -\frac{1}{2}\int_\Omega \left[\sigma_N^0 : \varepsilon(u_N^0)\right]\ \mathrm{div}\ h =& -\frac{1}{2}\int_{\partial\Omega} \left[\sigma_N^0 : \varepsilon(u_N^0)\right]\ h\cdot n \\ & + \frac{1}{2}\int_\Omega \mathrm{grad}\ \left[\mathrm{tr}\ \left(\sigma_N^0\,\nabla u_N^0\right)\right]\cdot h \end{aligned}$$

$$\frac{1}{2}\int_\Omega \left[\sigma_D^0 : \varepsilon(u_D^0)\right] \text{ div } h = \frac{1}{2}\int_{\partial\Omega} \left[\sigma_D^0 : \varepsilon(u_D^0)\right]\ h\cdot n - \frac{1}{2}\int_\Omega \text{grad } \left[\text{tr } \left(\sigma_D^0\,\nabla u_D^0\right)\right]\cdot h,$$

$$\int_\Omega \text{tr}\left[\sigma_N^0\ \left(\nabla u_N^0\,\nabla h\right)\right] = \int_{\partial\Omega}\left(n^T\,\sigma_N^0\right)\cdot\left(\nabla u_N^0\,h\right) - \int_\Omega \text{div}\left(\sigma_N^0\,\nabla u_N^0\right)\cdot h,$$

and

$$-\int_\Omega \text{tr}\left[\sigma_D^0\left(\nabla u_D^0\,\nabla h\right)\right] = -\int_{\partial\Omega}\left(n^T\,\sigma_D^0\right)\cdot\left(\nabla u_D^0\,h\right) + \int_\Omega \text{div}\left(\sigma_D^0\,\nabla u_D^0\right)\cdot h.$$

Then, using lemma 4, we can deduce a simple formula of the derivative of J

$$\begin{aligned} J'(\Omega,h) &= \frac{1}{2}\int_{\partial\Omega}\left[\sigma_D^0 : \varepsilon(u_D^0)\right] h\cdot n - \frac{1}{2}\int_{\partial\Omega}\left[\sigma_N^0 : \varepsilon(u_N^0)\right]\ h\cdot n \\ &\quad + \int_{\partial\Omega}\left(n^T\,\sigma_N^0\right)\cdot\left(\nabla u_N^0\,h\right) - \int_{\partial\Omega}\left(n^T\,\sigma_D^0\right)\cdot\left(\nabla u_D^0\,h\right). \end{aligned}$$

Hence, due to the following identities

$$h = 0 \text{ on } \Upsilon, \qquad \text{and} \qquad \sigma_D^0\,n = \sigma_N^0\,n = 0 \quad \text{on} \quad \Gamma,$$

we obtain the desired result

$$J'(\Omega,h) = \int_\Gamma \left[\frac{1}{2}\left[\left(\sigma_D^0 : \varepsilon(u_D^0)\right) - \left(\sigma_N^0 : \varepsilon(u_N^0)\right)\right]\right] h\cdot n.$$

□

4.4 Numerical approximation

This part aims to develop an algorithm to numerically solve the shape optimization problem. Indeed, the last theorem suggests the implementation of a numerical minimization algorithm using the gradient method.
We consider for $t \geq 0$ the deformation of Γ, as in the previous section

$$\Gamma_t^k := \Gamma_t = F_t(\Gamma) = \{x + t\,h(x);\ x \in \Gamma\},$$

where k is related to the k^{th} iteration and h is chosen in such a way that the shape functional J decreases; more precisely, we can choose a descent direction of the functional J as follows

$$h \in Q \quad \text{such that} \quad h_{|\Gamma} = -G\,n.$$

The expression of G is given in (4.18). To numerically implement this iterative procedure, we resort to the level set method.

4.4.1 Level set method

In this subsection, we shortly discuss the level set approach allowing readers to quickly grasp the key ideas. First, the basic ideas of the method are outlined. Then, the signed distance function concept is introduced. Finally, we describe how to combine this method with the shape derivative to obtain numerical solutions for the shape optimization problem. A good general review can be found in [62, 82].

The level set method is a numerical technique for tracking interfaces and shapes developed in 1988 by Osher and Sethian [84]. Over the past few decades, this method has found applications in various fields. Indeed, it has successfully been applied for several problems arising in image processing, computer graphics, optimization and computational physics [82].

The main idea of the level set approach is to represent a closed curve or a surface in a higher dimension, as the zero level set of a time-dependent and smooth function $\Phi(.,t)$, the so-called level set function, that is

$$\Gamma_t = \{x;\ \Phi(x,t) = 0\}. \tag{4.19}$$

So, the level set approach represents the curve Γ implicitly through the function Φ which is assumed to be zero on the curve Γ, to take negative values inside the region delimited by Γ and positive values outside. Basically, if we define a curve as the zero level set of a function Φ then one of the advantages is that the outward unit normal n to Γ and the curvature κ may be easily approximated through the level set function, that is

$$n = \frac{\nabla\Phi}{|\nabla\Phi|} \qquad \text{and} \qquad \kappa = \nabla \cdot \frac{\nabla\Phi}{|\nabla\Phi|}.$$

A suitable initial function $\Phi(x,0)$ has to be determined. We notice that the simplest choice for the initialization is the signed distance from the interface, defined by

$$\Phi(x,.) = \pm\, d(x,\Gamma).$$

The sign (-1) or (+1) depends on which side of the curve the point x lies in.

Let us now explain how to evolve the function Φ in order to mimic a curve evolution.

By definition (4.19), for any time t, the function Φ is zero at all points on the curve Γ_t. As consequence, the temporal derivative of this expression must vanish; and taking into account that

$$h_{|\Gamma} = -G\, n = -G\, \frac{\nabla\Phi}{|\nabla\Phi|},$$

one can deduce the following partial differential equation, in particular a Hamilton Jacobi equation

$$\begin{cases} \partial_t \Phi - G\,|\nabla \Phi| &= 0 \qquad t \in (0,T], \\ \Phi(\cdot,0) &= \Phi_0, \end{cases} \tag{4.20}$$

where Φ_0 is a level set function, in particular a signed distance function corresponding to Γ_0. Thus, curves and surfaces can be evolved by iterating this equation called the level set equation.
Through the iterations, the topology can change and the benefit that occurs when using the level set method is that it makes easy to follow shapes that split in two, develops holes or the inverse of these operations.
Another advantage of the level set approach is that one can perform numerical computations involving curves and surfaces on a fixed cartesian grid without having to parameterize these objects; which simplifies the whole numerical part.
However, the numerical solution requires sophisticated techniques. As a result, the level set method is solved numerically by the fifth-order WENO scheme [65, 82] for the spatial discretization and the third-order Runge-Kutta scheme [54, 82] for the temporal one.

4.4.2 Stopping criterion

Among the many available distances on sets, we consider one of most common which is the Hausdorff distance.
It is defined for two sets $A, B \subset \mathbb{R}^2$ by

$$d_H(A,B) = \max\left(\sup_{a\in A} d(a,B)\ ,\ \sup_{b\in B} d(b,A)\right),$$

where

$$d(a,B) = \inf_{b\in B} |a-b|.$$

The distances $d(a,b)$ are available via the level set functions. The stopping criterion of the algorithm is

$$d_H\left(\Gamma^k, \Gamma^{k-1}\right) < C\,\delta x^2, \tag{4.21}$$

where C is a constant independent of the grid parameter δx.
Before going into numerical tests in the next section, we close this one by outlining the proposed algorithm.

4.4.3 The algorithm

Collecting all the techniques mentioned in previous sections, we are able now to present the algorithm to be implemented for solving the shape optimization problem (4.5) and examine performance on a series of tests in the next section. Let us assume that we know the interface $\Gamma^k := \Gamma$ and a level set function Φ^k associated to $\Gamma^k := \Gamma$.

1. Compute the solutions (σ_D, u_D) and (σ_N, u_N) of the problems (4.2) and (4.3).
2. Compute the velocity function G on Γ, given by (4.18).
3. Update the level set function Φ by solving the level set equation (4.20).
4. Set the stopping criterion given by (4.21).

4.5 Numerical tests

The proposed approach is tested by several cavities detection problems. In the following tests, the square $U = [-1, 1] \times [-1, 1]$ is considered as computational domain.

4.5.1 First case

The first case concerns the reconstruction of a single cavity. Let us consider

$$\Upsilon = \{x;\ |x| = r_0\}.$$

In this case, the solution is the circle C_{exact} centered at the origin with radius R_{exact} and the explicit expression u_{exact} of the solution u of (4.1) is given by

$$u_{\text{exact}}(r) = \frac{C1}{2} r + \frac{C2}{r}$$

where

$$C1 = \frac{2(1+\nu)(1-2\nu)}{E}\, A \qquad \text{and} \qquad C2 = \frac{1+\nu}{E}\, B.$$

Above, the constants A and B are determined by the boundary conditions, namely

$$A = \frac{P_1\, r_1^2 - P_2\, r_0^2}{r_0^2 - r_1^2} \qquad \text{and} \qquad B = \frac{P_1 - P_2}{r_0^2 - r_1^2}\, r_1^2\, r_0^2$$

where $r_1 = R_{\text{exact}}$, $\sigma_r(r_1) = -P_1 = 0$ and $\sigma_r(r_0) = -P_2$ (σ_r is the radial stress).
We have chosen $r_0 = 0.9$, $R_{\text{exact}} = 0.35$ and as an initial guess the circle centered at the origin of radius $R = 0.8$ as it is presented in Figure 4.2. We obtain convergence after 17 iterations with $J(\Gamma^{17}) = 0.0294$ for 30×30 mesh grid .

4.5.2 Second case

In this case, the cavity is a connected domain; the disc of radius $R_{\text{exact}} = 0.3$ centered at the origin; but we consider a disconnected initial guess, namely Γ^0 is the union of the three disjointed circles of radius R equal respectively to 0.14, 0.17 and 0.14 (left to right), centered respectively at $(-0.4, 0)$, $(0, 0)$ and $(0.4, 0)$ as it is shown in Figure 4.3 . The "true" cavity has been successfully reconstructed and the convergence is obtained after 9 iterations for 30×30 mesh grid. This example illustrates how the level set method merges three components into one. Indeed, it shows how the topology of the domain changes during the optimization process.
The both theoretical and numerical proposed techniques in this paper are also able to deal with multiple cavities detection. In fact, in the following tests, we consider the case of a mechanical structure with multiple cavities.

4.5.3 Third case

In this case, we aim to recover two cavities in the structure, namely two disconnected components. Indeed, the solution is the union of the two disjointed circles of radius $R_{\text{exact}} = 0.15$ and centered respectively at $(-0.45, 0)$ and $(0.45, 0)$. We choose as initial guess the circle of radius $R = 0.7$ centered at the origin as it is shown in Figure 4.4.
During the identification process, the shape changes topology and splits into seperate curves. The convergence is obtained after 541 iterations for 31×31 mesh grid.

4.5.4 Fourth case

In this last test, three cavities are buried in the mechanical structure, namely the three disjointed circles of radius $R_{\text{exact}} = 0.14$ and centered respectively at $(-0.44, 0)$, $(0, 0)$ and $(0.44, 0)$. We choose the circle centered at the origin of radius $R = 0.65$ as an initial guess. At each iteration, the level set function

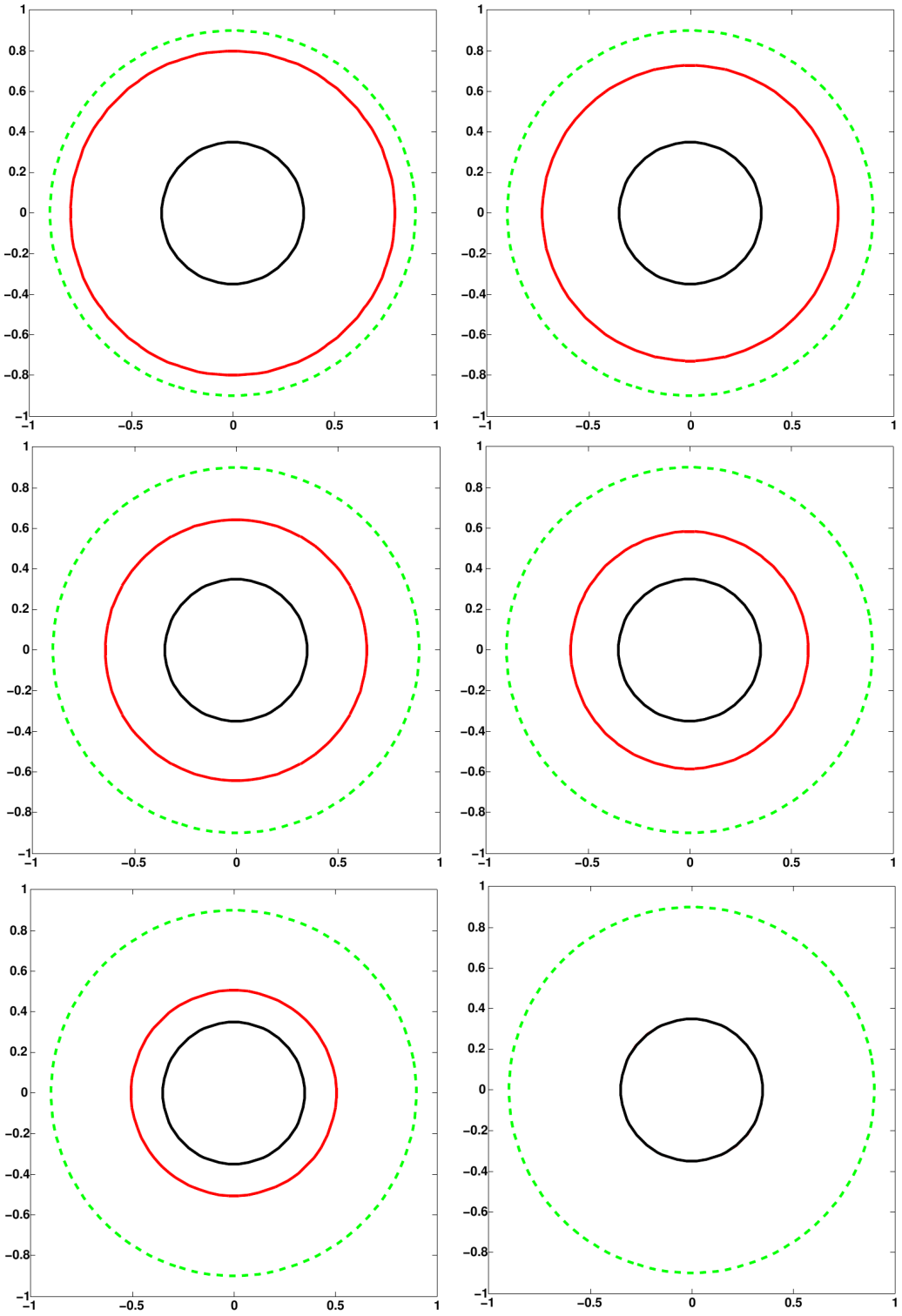

Figure 4.2: Υ the exterior boundary (the dashed green line), Γ the exact solution (the black line), evolution of the boundary Γ^k (the red line) for $k = 0, 6, 10, 12, 14, 17$ (left to right, top to bottom).

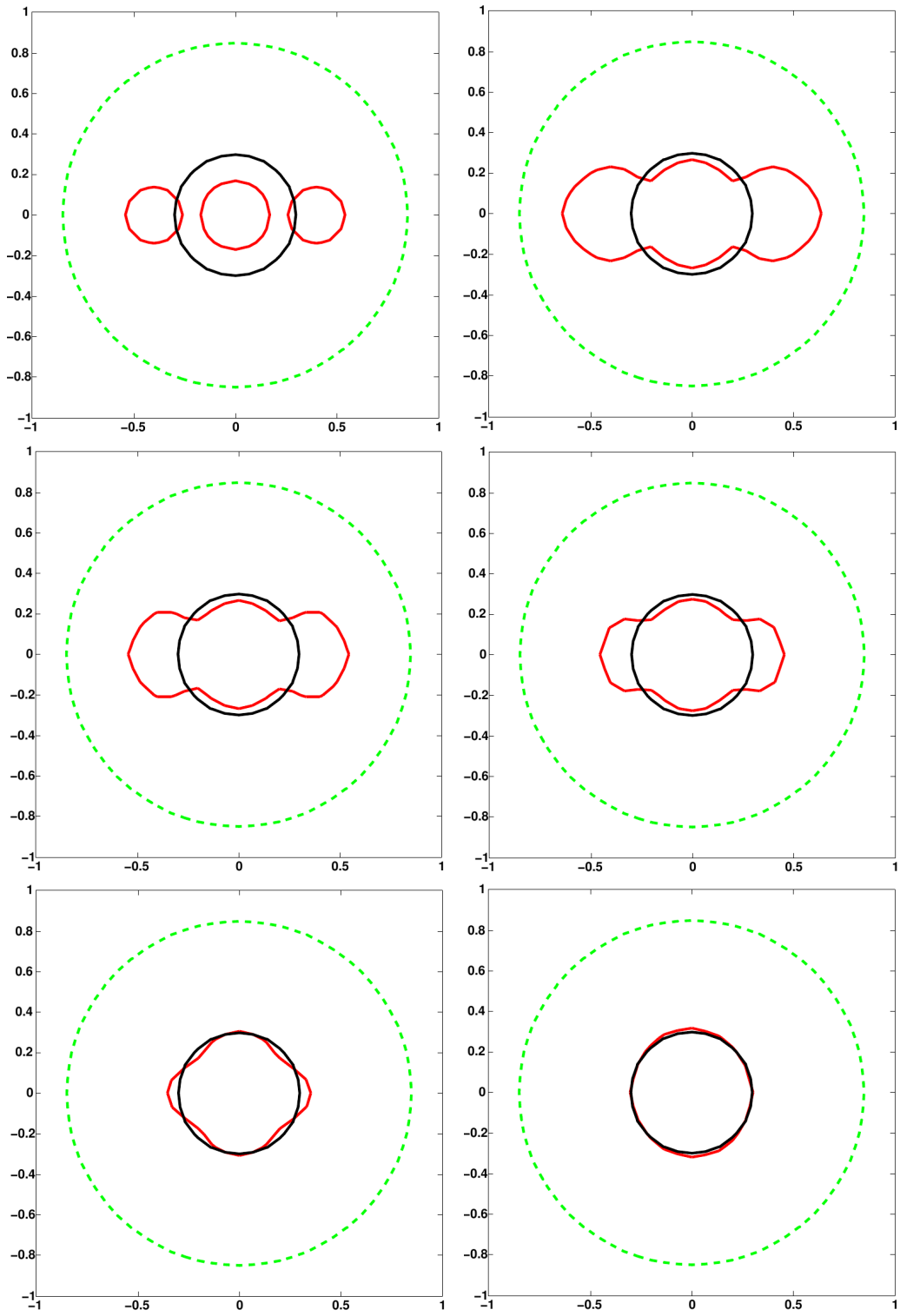

Figure 4.3: Topology change test: Υ the exterior boundary (the dashed green line), Γ the exact solution (the black line), evolution of the boundary Γ^k (the red line) for $k = 0, 1, 2, 3, 4, 9$ (left to right, top to bottom).

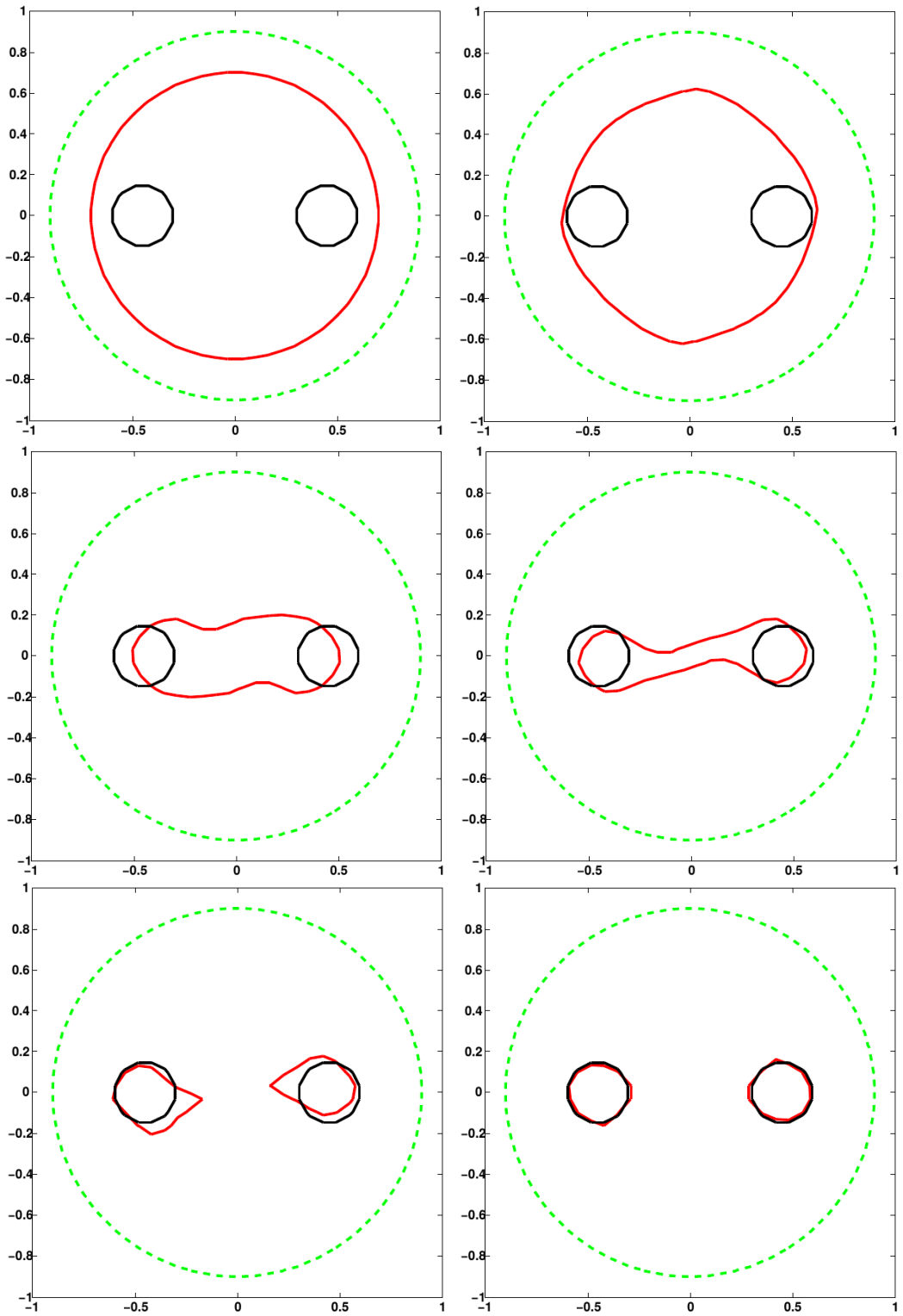

Figure 4.4: Topology change test: Υ the exterior boundary (the dashed green line), Γ the exact solution (the black line), evolution of the boundary Γ^k (the red line) for $k = 0, 210, 422, 442, 456, 541$ (left to right, top to bottom).

is updated by solving the Hamilton-Jacobi equation (4.20). From Figure 4.5, one can remark that the cavity centered at the origin is not well reached. This may be explained by the fact that, compared to the two others cavities, the central one is father away from the exterior boundary Υ, where overdetermined boundary data are prescribed.

4.5.5 The reconstruction with noisy data

The issue discussed in this subsection deals with noisy data.
First of all, it should be noted that numerical results conducted in the previous parts are executed with uncontaminated data. However, in practice, the available data are corrupted by some noise as they are known from measurements. Since it is necessary to see how the reconstructions are influenced when data are noisy, our main objective herein is to retrieve cavities from noisy data instead of exact one.
The reconstruction for all previous cases and for different amplitudes λ of noise, namely $5\%, 10\%, 15\%$ and 20% is plotted in Figure 4.6, Figure 4.7, Figure 4.8 and Figure 4.9 correspondent respectively to the first case, second case, third case and fourth case. Noise has been generated by a random variable.
Let us conclude this subsection by the following summarizing remarks. The recovered cavities depend on noise. Indeed, in the absence of any noise, the reconstruction in Figure 4.2, Figure 4.3, Figure 4.4 and Figure 4.5 is perfect. On the other hand, when noise is not amplified, the reconstructed geometry is quite accurate.

4.6 Comments

The paper extends investigations of cavities reconstruction problems by shape optimization methods for Laplace system [64] to the case of linear elasticity one.
We have proposed an approach based theoretically on the so-called Kohn and Vogelius misfit functional and numerically on the level set method. The numerical results highlight the efficiency of the proposed approach. A future direction of investigation should therefore involve our approach for the nonlinear elasticity theory as it seems that the main ideas can be exploited.

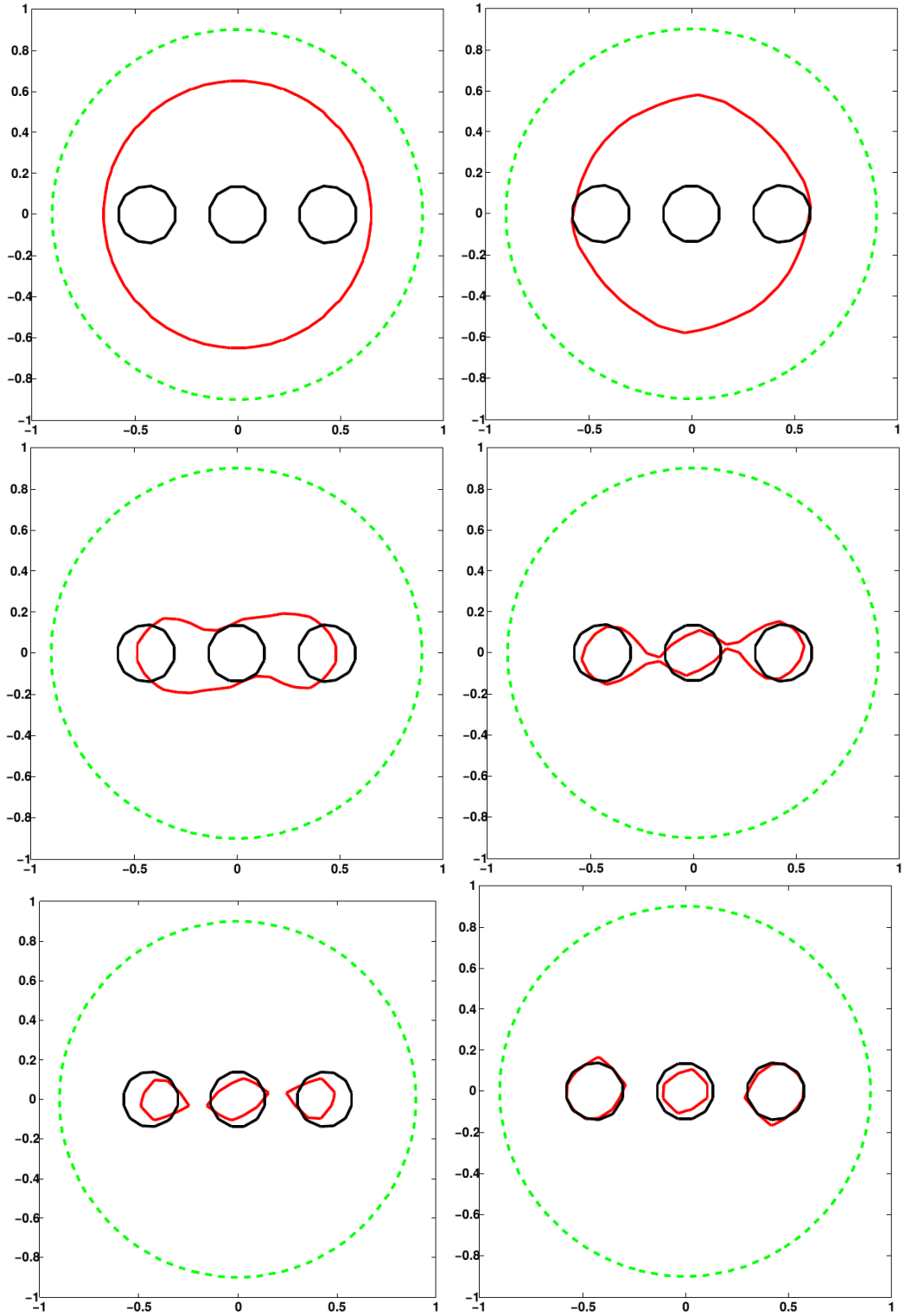

Figure 4.5: Topology change test: Υ the exterior boundary (the dashed green line), Γ the exact solution (the black line), evolution of the boundary Γ^k (the red line) for $k = 0, 145, 308, 420, 421, 751$ (left to right, top to bottom).

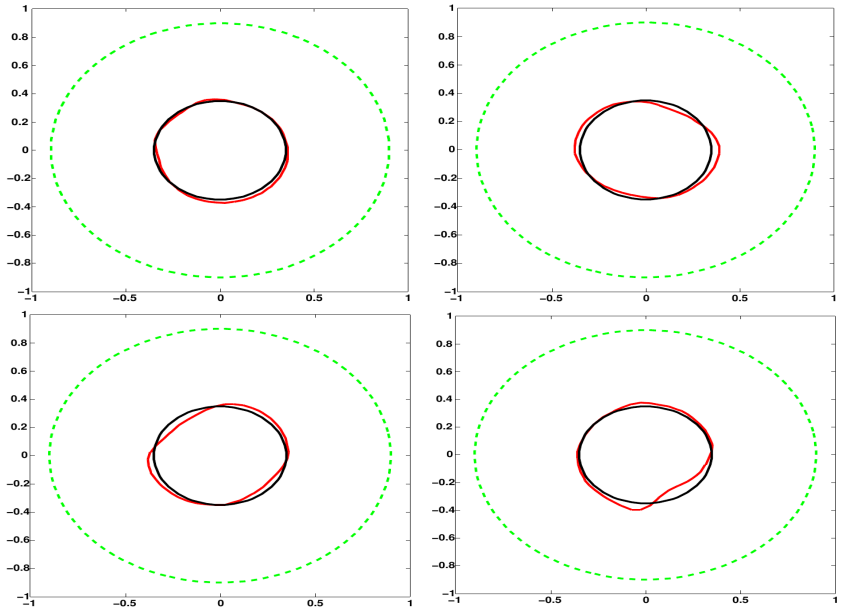

Figure 4.6: Υ the exterior boundary (the dashed green line), Γ the exact solution (the black line), the boundary Γ^k (the red line): the solution of the iterative algorithm correspondent to the first case with noisy data $5\%, 10\%, 15\%, 20\%$ (left to right, top to bottom).

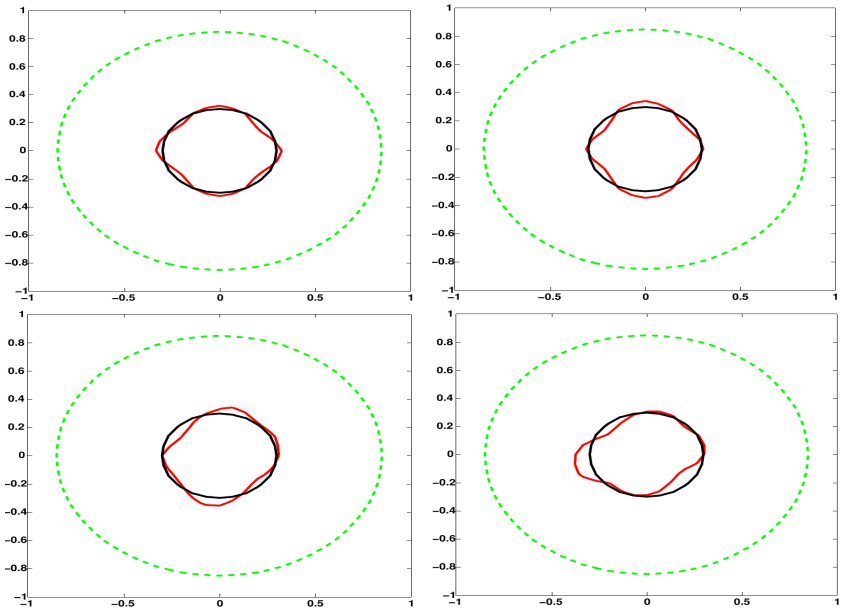

Figure 4.7: Υ the exterior boundary (the dashed green line), Γ the exact solution (the black line), the boundary Γ^k (the red line): the solution of the iterative algorithm correspondent to the second case with noisy data $5\%, 10\%, 15\%, 20\%$ (left to right, top to bottom).

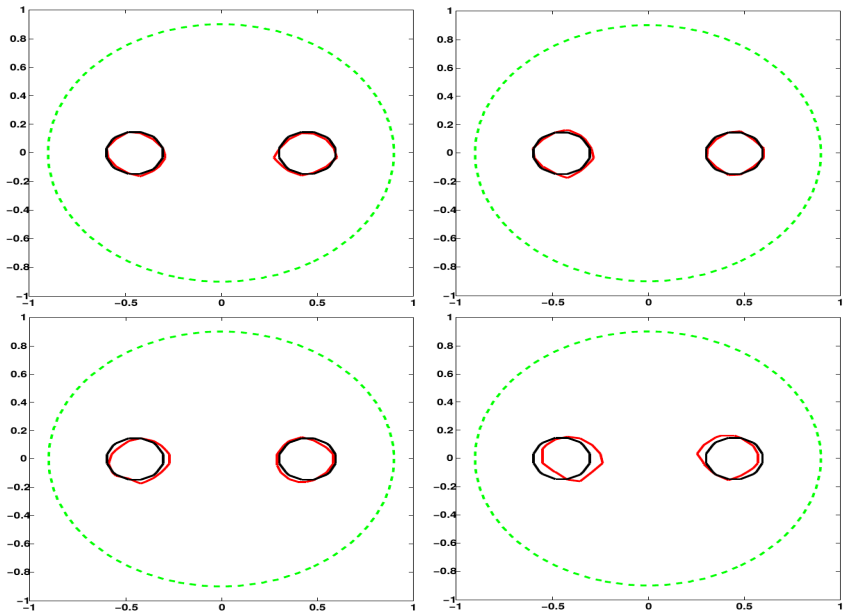

Figure 4.8: Υ the exterior boundary (the dashed green line), Γ the exact solution (the black line), the boundary Γ^k (the red line): the solution of the iterative algorithm correspondent to the third case with noisy data $5\%, 10\%, 15\%, 20\%$ (left to right, top to bottom).

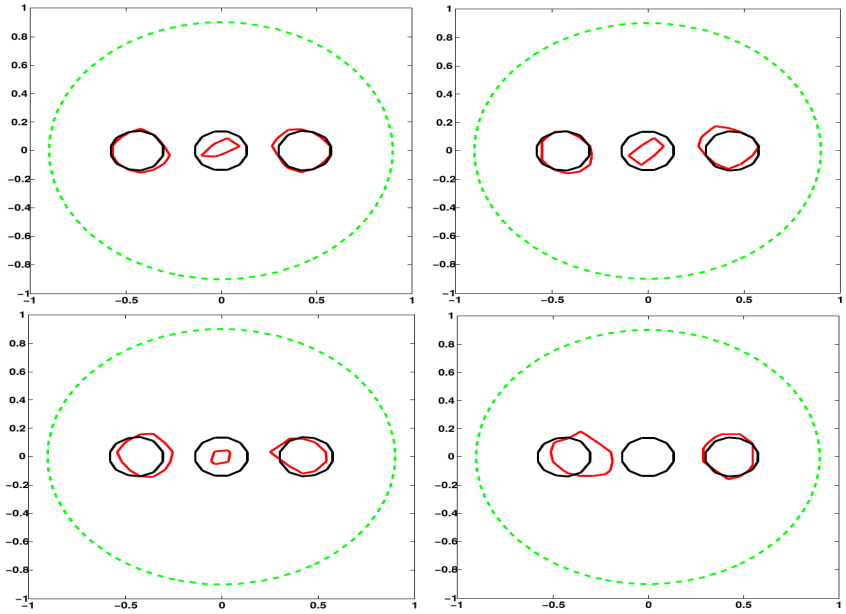

Figure 4.9: Υ the exterior boundary (the dashed green line), Γ the exact solution (the black line), the boundary Γ^k (the red line): the solution of the iterative algorithm correspondent to the fourth case with noisy data $5\%, 10\%, 15\%, 20\%$ (left to right, top to bottom).

Chapter 5

Cavities identification from partially overdetermined boundary data in linear elasticity

Contents

This chapter builds on a detailed version of the article entitled "**Cavities identification from partially overdetermined boundary data in linear elasticity**" published in the Journal of Applied and Computational Mathematics, (5:295. doi:10.4172/2168-9679.1000295), 2016. This work was done in collaboration with Amel Ben Abda and Badreddine Rjaibi.

Abstract

A new framework for a geometric inverse problem in linear elasticity is investigated. The problem concerns the recovery of cavities from the knowledge of partially overdetermined boundary data. The boundary data available for the reconstruction are given by the displacement field and the normal component of the normal stress, whereas no information is given on the shear stress. We propose an identification method based on a Kohn-Vogelius error functional combined with the topological gradient method. Special focus is put on the identification of cavities and a uniqueness result is proved in the case of monotonous cavities. An asymptotic expansion for the energy function is derived with respect to the creation of a small hole. A one-shot reconstruction algorithm based on the topological sensitivity analysis is implemented. Some numerical experiments concerning the cavities identification are finally reported, highlighting the ability of the method to identify multiple cavities.
Keywords: Geometrical inverse problems, cavities identification, linear elasticity, partially overdetermined boundary data, identifiability, Kohn-Vogelius error functional, topological derivative, asymptotic expansion.

Résumé

Lors de cette étude, un nouveau cadre pour un problème inverse géométrique est examiné. Le problème concerne la détection de cavités en élasticité linéaire à partir de données aux limites partiellement surdéterminées. Pour la reconstruction, nous disposons du champ de déplacement et de la partie normale de la contrainte normale; tandis qu'aucune information n'est disponible en ce qui concerne la contrainte de cisaillement. Un résultat d'identifiabilité est prouvé dans le cas de cavités monotones.

Pour la résolution de notre problème inverse, nous proposons une méthode d'identification basée sur une fonctionnelle d'écart énergétique combinée avec la méthode du gradient topologique. Un développement asymptotique pour cette fonctionnelle est obtenue en utilisant la méthode adjointe généralisée.

Les différents résultats numériques obtenus par la mise en oeuvre d'un algorithme en une seule itération, prouvent la fiabilité de notre approche que ce soit dans le cas d'identification d'une seule cavité ou de plusieurs cavités.
Mots clés: Problèmes inverses géométriques, identification de cavités, élasticité linéaire, données partiellement surdéterminées, identifiabilité, fonctionnelle d'écart énergétique, gradient topologique, développement asymptotique.

5.1 Introduction

Shape reconstruction of cavities (namely holes) is a challenging subject with application to diverse areas such as exploration geophysics, medical imaging and non-destructive testing. In industrial framework for example, it is essential for engineers to check the structure integrity and to establish the behavior of mechanical components before critical damage occurs [70, 77].
To such identification tasks (namely to deduce the properties of the hidden interior), boundary data are required. In the context of geometrical inverse problem, it is a question about overdetermined boundary data, namely data provided by measurements distributed on the exterior boundary of the domain of interest [24, 64]. To the author's best knowledge, all geometric inverse problems in linear elasticity, investigated in the literature, have in common to be defined by complete overdetermined boundary data (see for example [24, 28, 29]).
Driven by the needs from applications in both industry and other sciences, we consider in the present work, the geometrical inverse problem of recovering cavities in elasticity framework. The problem is compounded by missing data which is the main motivation. Indeed, the displacement field and the normal component of the normal stress are accessible whereas no information is given on the shear stress.
The problem under consideration might be formulated as follows:
Let $\Omega \subset \mathbb{R}^2$ denotes an open and bounded domain with boundary Υ occupied by a linear elastic material, the medium being assumed to be homogeneous and isotropic. Given the normal component of the normal stress imposed g and the displacement field f measured on the boundary Υ

$$\begin{cases} \sigma(u)\, n_\Upsilon \cdot n_\Upsilon & = g \qquad \text{on } \Upsilon, \\ u & = f \qquad \text{on } \Upsilon, \end{cases}$$

namely the exterior boundary measurements, the linear elasticity inverse problem consists in finding the boundary Γ of a bounded domain $\overline{\mathcal{O}} \subset \Omega$ and the

displacement field u satisfying

$$\begin{cases} -\operatorname{div}\sigma(u) & = 0 & \text{in } \Omega \setminus \overline{\mathcal{O}}, \\ \sigma(u)\, n & = 0 & \text{on } \Gamma, \\ u & = f & \text{on } \Upsilon, \\ \sigma(u)\, n_\Upsilon \cdot n_\Upsilon & = g & \text{on } \Upsilon, \end{cases} \tag{5.1}$$

where n_Υ and n are the outward unit normals to the boundary of $\Omega \setminus \overline{\mathcal{O}}$. The stress tensor σ and the strain tensor ε are given by

$$\sigma_{ij}(u) = \lambda \operatorname{div}(u)\, \delta_{ij} + 2\,\mu\, \varepsilon_{ij}(u)$$

$$\text{and} \qquad \varepsilon_{ij}(u) = \frac{1}{2}\left(\frac{\partial u_i}{\partial x_j} + \frac{\partial u_j}{\partial x_i}\right), \qquad 1 \le i, j \le 2.$$

Above, δ_{ij} is the Kronecker symbol and λ, μ are the Lamé coefficients related to Young's modulus E and Poisson's ratio ν via

$$\mu = \frac{E}{2\,(1+\nu)} \qquad \text{and} \qquad \lambda = \frac{E\,\nu}{(1-2\,\nu)\,(1+\nu)}\,.$$

The rest of this chapter is organized as follows: in the next section, we discuss the identifiability of cavities and prove a uniqueness result only for monotonous cavities, highlighting the importance of the geometric inverse problem under consideration. In the third section, the inverse problem is transformed into a topology optimization one using a Kohn-Vogelius error functional. Then, in the fourth section, we give a brief review of the topological gradient method and then present its application to the cavities localization problem in the fifth section. The main result in this part is providing the topological asymptotic expansion by the means of a generalized adjoint method, previously recalled in the fourth section, and a domain truncation. The sixth section is devoted to numerical implementation using one-iteration algorithm. Indeed, we explore the efficiency of the proposed method by several numerical experiments. The last section contains some comments.

5.2 Identifiability

From the theoretical point of view, there are several relevant questions about this geometric inverse problem due, on one hand, to its ill-posedness and, on the other hand, to the missing boundary measurements. Indeed, solving such a partially overdetermined boundary value problem is a non trivial task since,

to the best of our knowledge, the question of uniqueness is at present far from being solved. Hence, it poses a great challenge. In the following, we discuss the identifiability of cavities, i.e. the uniqueness question for the inverse problem in the case of monotonous cavities.

For $\Omega \subset \mathbb{R}^2$ an open and bounded domain with boundary Υ, let C_1 and C_2 be two connected domain such that $\overline{C_1} \subset C_2$ and $\overline{C_2} \subset \Omega$ (see Figure 5.1). For $i = 1, 2$, let u_i be the solution of the problem

$$\begin{cases} -\operatorname{div}\sigma(u_i) & = 0 & \text{in } \Omega \setminus \overline{C_i}, \\ \sigma(u_i)\, n & = 0 & \text{on } \partial C_i, \\ \sigma(u_i)\, n_\Upsilon \cdot n_\Upsilon & = g & \text{on } \Sigma, \\ u_i \cdot \tau & = f \cdot \tau & \text{on } \Sigma, \\ \sigma(u_i)\, n_\Upsilon & = 0 & \text{on } \Upsilon \setminus \Sigma, \end{cases} \tag{5.2}$$

where ∂C_i is the boundary of C_i, $\Sigma \subset \Upsilon$, n_Υ respectively n are the outward unit normals to the boundary of $\Omega \setminus \overline{C_i}$ on Υ respectively ∂C_i and τ is the tangent vector to the boundary Υ.

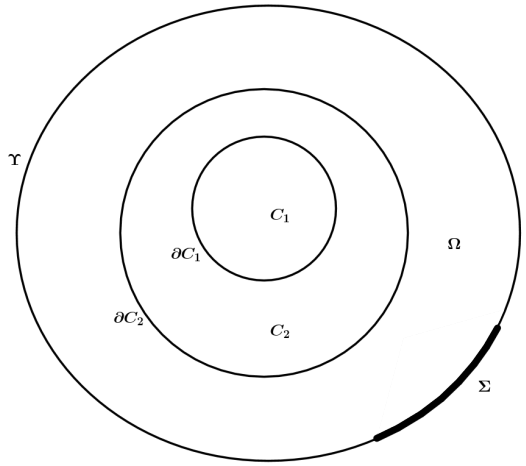

Figure 5.1: The domain with monotonous cavities.

Proposition 3. *Let C_1 and C_2 be two cavities such that $\overline{C_1} \subset C_2$ and for i=1,2, let u_i be the solution of the direct problem (5.2) defined on $\Omega \setminus \overline{C_i}$. Then, if C_1 and C_2 both lead to the same measured normal displacement on Σ, namely $u_1 \cdot n_\Upsilon = u_2 \cdot n_\Upsilon = f \cdot n_\Upsilon$ on Σ, we have $C_1 = C_2$.*

Proof. For the proof, we suppose for simplicity that $f \cdot \tau = 0$ on Σ. u_2 is then the solution of the following problem

$$\min_{v \in \mathcal{V}_2} \frac{1}{2} \int_{\Omega \setminus \overline{C2}} \sigma(v) : \varepsilon(v) dx - \int_\Sigma g(v \cdot n_\Upsilon) ds,$$

where

$$\mathcal{V}_2 = \{v \in \left[H^1(\Omega \setminus \overline{C_2})\right]^2; \qquad v \cdot \tau = 0 \text{ on } \Sigma\}.$$

Hence, u_2 verifies $\forall v \in \mathcal{V}_2$

$$\frac{1}{2}\int_{\Omega\setminus\overline{C_2}} \sigma(u_2) : \varepsilon(u_2)dx - \int_\Sigma g(u_2 \cdot n_\Upsilon)ds \leqslant \frac{1}{2}\int_{\Omega\setminus\overline{C_2}} \sigma(v) : \varepsilon(v)dx - \int_\Sigma g(v \cdot n_\Upsilon)ds.$$

In particular, since $\overline{C_1} \subset C_2$ and $u_1 \cdot \tau = f \cdot \tau = 0$ on Σ, we have

$$\frac{1}{2}\int_{\Omega\setminus\overline{C_2}} \sigma(u_2) : \varepsilon(u_2)dx - \int_\Sigma g(u_2 \cdot n_\Upsilon)ds \leqslant \frac{1}{2}\int_{\Omega\setminus\overline{C_2}} \sigma(u_1) : \varepsilon(u_1)dx - \int_\Sigma g(u_1 \cdot n_\Upsilon)ds. \tag{5.3}$$

Then, since $u_1 \cdot n_\Upsilon = u_2 \cdot n_\Upsilon$ on Σ, we obtain from (5.3)

$$\begin{aligned}\int_{\Omega\setminus\overline{C2}} \sigma(u_2) : \varepsilon(u_2)dx &\leqslant \int_{\Omega\setminus\overline{C_2}} \sigma(u_1) : \varepsilon(u_1)dx, \\ &\leqslant \int_{\Omega\setminus\overline{C1}} \sigma(u_1) : \varepsilon(u_1)dx - \int_{C2\setminus\overline{C1}} \sigma(u_1) : \varepsilon(u_1)dx. \end{aligned} \tag{5.4}$$

Using the Green formula, we have on one hand from the problem (5.2) related to u_2

$$\int_{\Omega\setminus\overline{C2}} \sigma(u_2) : \varepsilon(v)dx = \int_\Sigma g(v \cdot n_\Upsilon)ds, \quad \forall v \in \mathcal{V}_2$$

and on the other hand from the problem (5.2) related to u_1

$$\int_{\Omega\setminus\overline{C1}} \sigma(u_1) : \varepsilon(v)dx = \int_\Sigma g(v \cdot n_\Upsilon)ds, \quad \forall v \in \mathcal{V}_1,$$

where

$$\mathcal{V}_1 = \{v \in \left[H^1(\Omega \setminus \overline{C_1})\right]^2; \qquad v \cdot \tau = 0 \text{ on } \Sigma\}.$$

Then, we have from (5.4)

$$\int_\Sigma g(u_2 \cdot n_\Upsilon)ds \leqslant \int_\Sigma g(u_1 \cdot n_\Upsilon)ds - \int_{C2\setminus\overline{C1}} \sigma(u_1) : \varepsilon(u_1)dx$$

Hence, since $u_1 \cdot n_\Upsilon = u_2 \cdot n_\Upsilon$ on Σ, it follows that

$$0 \leqslant -\int_{C_2\setminus\overline{C1}} \sigma(u_1) : \varepsilon(u_1)dx.$$

We get so that mes $(C_2 \setminus \overline{C_1}) = 0$, that is $C_2 = C_1$. □

So, one can distinguish two cavities C_1 and C_2 such that $\overline{C_1} \subset C_2$ from partially overdetermined boundary data on Σ.

5.3 Formulation as a topology optimization problem

In order to solve our geometrical inverse problem (5.1), we propose a Dirichlet-Neumann approach by the means of a self regularization technique, namely the Kohn-Vogelius formulation [21, 24, 64]. Indeed, it leads to define two direct problems. One of them is related to the Dirichlet data (the displacement field f) (5.5) and the other one is associated to the "Neumann" data (the normal component of the normal stress g) (5.6)

$$\begin{cases} -\operatorname{div}\sigma(u^D) &= 0 & \text{in } \Omega\setminus\overline{\mathcal{O}}, \\ \sigma(u^D)\,n &= 0 & \text{on } \Gamma, \\ u^D &= f & \text{on } \Upsilon \end{cases} \tag{5.5}$$

and

$$\begin{cases} -\operatorname{div}\sigma(u^N) &= 0 & \text{in } \Omega\setminus\overline{\mathcal{O}}, \\ \sigma(u^N)\,n &= 0 & \text{on } \Gamma, \\ \sigma(u^N)\,n_\Upsilon\cdot n_\Upsilon &= g & \text{on } \Upsilon, \\ u^N\cdot\tau &= f\cdot\tau & \text{on } \Upsilon. \end{cases} \tag{5.6}$$

The main idea of the proposed approach relies on the use of a Kohn-Vogelius functional defined by

$$\mathcal{J}(u^D,u^N) := \frac{1}{2}\int_{\Omega\setminus\overline{\mathcal{O}}} \big(\sigma(u^D)-\sigma(u^N)\big) : \big(\varepsilon(u^D)-\varepsilon(u^N)\big)\,, \tag{5.7}$$

as it will be explained below. Thus, the geometrical inverse problem (5.1) is formulated as a topology optimization one

$$\min_{\overline{\mathcal{O}}\subset\Omega} \mathcal{J}(u^D,u^N). \tag{5.8}$$

One of promising techniques that can be designed to such shape reconstruction problem is the level set method combined with the shape gradient method [21, 24, 64]. However, one can remark that although the level set method is able to automatically handle topology changes and reconstruct the precise geometry of the cavities [21, 24, 64], it requires an iterative procedure where at each iteration step, one needs to solve a sequence of forward solutions. As a consequence, the level set method seems to be a slow and expensive process. To overcome this difficulty when solving our geometrical inverse problem, we resort to a one iteration algorithm based on the topological gradient method.

It is a recent numerical method of shape and topology optimization of structures, introduced by A. Schumacher in 1995 [89] in the context of compliance minimization in linear elasticity and which makes possible topology changes. Indeed, unlike the classical shape optimization, the topology of the domain may change during the optimization process. A change in topology means removing a small ball from the domain of integration. Our aim is so to find an optimal shape without any a priori assumption about its topology.

5.4 The topological gradient method

As it does not impose restriction on the topology of the domain, the topological gradient method has been widely applied in literature to different and broad cases of problems as the elasticity framework [52, 90], the Stokes system [23, 36], the Helmholtz equation [86], the image processing problems [10, 20] and many others. We refer to [5, 36, 68] for a concise overview of the method.
Let us present the basic idea of this approach. We consider a variable, open and bounded domain Ω of $\mathbb{R}^2$ and a cost functional $j(\Omega) = \mathcal{J}(u_\Omega)$ to be minimized, where u_Ω is solution to a given PDE defined over Ω. For a small parameter $\rho > 0$, let $\Omega_\rho = \Omega \setminus (\overline{x_0 + \rho\,\omega})$ be the perturbed domain obtained by removing a small part $\omega_\rho = x_0 + \rho\,\omega$ from Ω, where $x_0 \in \Omega$ and $\omega \subset \mathbb{R}^2$ is a fixed open and bounded subset containing the origin, whose boundary $\partial\omega$ is connected and piecewise of class C^1 (see Figure 5.2). If $\rho = 0$ then $\omega_\rho = \emptyset$.

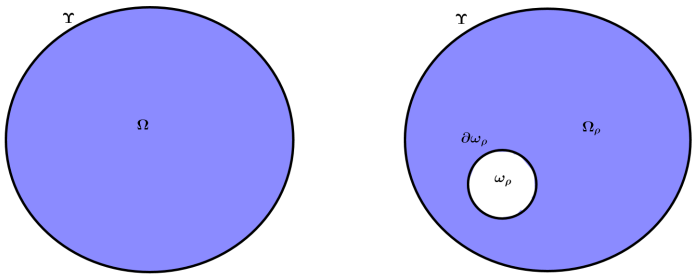

Figure 5.2: The initial domain and the same domain after the inclusion of the hole.

Then, a so-called topological asymptotic expansion of the function j is provided by the topological sensitivity theory in the following form

$$j(\Omega_\rho) = j(\Omega) + f(\rho)\, g(x_0) + o\left(f(\rho)\right),$$
$$\text{where} \qquad \lim_{\rho \to 0} f(\rho) = 0 \qquad \text{and} \qquad f(\rho) > 0.$$

In other words, the purpose is to study the variations of the objective function $j(\Omega_\rho)$ as $\rho \to 0$. The topological sensitivity $g(x_0)$, also called the topological gradient can be used like a descent direction in an optimization process. Indeed, to minimize the criterion j, one has to create holes at some points where the topological gradient g is negative. $g(x_0)$ is usually computed using the solution of direct and adjoint problems defined on the initial domain and it will be the case in our problem as it will be demonstrated in the forthcoming sections.

5.4.1 A generalized adjoint method

The following generalized adjoint method [52, 86] is applied to the above problem.

Let $\mathcal{V}$ be a fixed Hilbert space. For $\rho \geqslant 0$, let a_ρ be a bilinear, symmetric, uniformly continuous and coercive form on $\mathcal{V}$ and let l_ρ be a linear and uniformly contiunous form on $\mathcal{V}$. We assume that there exist a bilinear and continuous form δ_a, a linear and continuous form δ_l and a real function $f(\rho) > 0$ defined on $\mathbb{R}_+$ such that

$$\begin{cases} \lim\limits_{\rho \to 0} f(\rho) = 0, \\ ||a_\rho - a_0 - f(\rho)\delta_a||_{\mathcal{L}_2(\mathcal{V})} = o(f(\rho)), \\ ||l_\rho - l_0 - f(\rho)\delta_l||_{\mathcal{L}(\mathcal{V})} = o(f(\rho)), \end{cases}$$

where $\mathcal{L}(\mathcal{V})$ (respectively $\mathcal{L}_2(\mathcal{V})$) denotes the space of continuous and linear (respectively bilinear) forms on $\mathcal{V}$.

These assumptions will be satisfied in the topology optimization context in the next section. For $\rho \geqslant 0$, let u_ρ be the unique solution [52] to the following problem:

$$a_\rho(u_\rho, v) = l_\rho(v) \quad \forall v \in \mathcal{V}. \tag{5.9}$$

Now, let us consider a function $j(\Omega_\rho) = \mathcal{J}_\rho(u_\rho)$, where $\mathcal{J}_0$ is differentiable with respect to u, its derivative being denoted by $D\mathcal{J}(u)$. Moreover, we suppose that there exists a function $\delta_\mathcal{J}$ defined on $\mathcal{V}$ such that

$$\mathcal{J}_\rho(v) - \mathcal{J}_0(u) = D\mathcal{J}(u)(v-u) + f(\rho)\delta_\mathcal{J}(u) + o(||v-u|| + f(\rho)) \qquad \forall u, v \in \mathcal{V}.$$

For $\rho > 0$, we define the Lagrangian operator $\mathcal{L}_\rho$ by

$$\mathcal{L}_\rho(u, v) = \mathcal{J}_\rho(u) + a_\rho(u, v) - l_\rho(v) \qquad \forall u, v \in \mathcal{V}.$$

Its variation with respect to ρ is given by

$$\delta_{\mathcal{L}}(u,v) = \delta_{\mathcal{J}}(u) + \delta_a(u,v) - \delta_l(v) \qquad \forall u, v \in \mathcal{V}$$

and we have

$$\mathcal{L}_\rho(u,v) - \mathcal{L}_0(u,v) = f(\rho)\delta_{\mathcal{L}}(u,v) + o(f(\rho)) \qquad \forall u, v \in \mathcal{V}.$$

Theorem 9. *[52] The function j has the asymptotic expansion*

$$j(\Omega_\rho) = j(\Omega) + f(\rho)\delta_{\mathcal{L}}(u_0, v_0) + o(f(\rho)), \tag{5.10}$$

where u_0 is the solution to the problem (5.9) with $\rho = 0$ and v_0 is the solution to the adjoint problem: find $v_0 \in \mathcal{V}$ such that

$$a_0(w, v_0) = -D\mathcal{J}(u_0)w \qquad \forall w \in \mathcal{V}. \tag{5.11}$$

5.5 Application to cavities identification

Let Ω be defined in the same way as in the introduction. The linear elasticity Dirichlet respectively "Neumann" problems, defined on the whole domain Ω, are the following: Find u_0^D respectively u_0^N solution of

$$\begin{cases} -\operatorname{div}\sigma(u_0^D) &= 0 & \text{in } \Omega, \\ u_0^D &= f & \text{on } \Upsilon, \end{cases} \tag{5.12}$$

respectively

$$\begin{cases} -\operatorname{div}\sigma(u_0^N) &= 0 & \text{in } \Omega, \\ \sigma(u_0^N)\, n_\Upsilon \cdot n_\Upsilon &= g & \text{on } \Upsilon, \\ u_0^N \cdot \tau &= f \cdot \tau & \text{on } \Upsilon, \end{cases} \tag{5.13}$$

where $\sigma, \Upsilon, n_\Upsilon$ and τ are as already defined in the first section. Let us also consider Ω_ρ as previously specified in the previous section and the displacements $u_{\Omega_\rho}^D$ and $u_{\Omega_\rho}^N$ defined as the solutions of the following Dirichlet (5.14) and "Neumann" (5.15) problems, on the perforated domain Ω_ρ, by

$$\begin{cases} -\operatorname{div}\sigma(u_{\Omega_\rho}^D) &= 0 & \text{in } \Omega_\rho, \\ u_{\Omega_\rho}^D &= f & \text{on } \Upsilon, \\ \sigma(u_{\Omega_\rho}^D)\, n &= 0 & \text{on } \partial\omega_\rho \end{cases} \tag{5.14}$$

and

$$\begin{cases} -\operatorname{div}\sigma(u_{\Omega_\rho}^N) &= 0 & \text{in } \Omega_\rho, \\ \sigma(u_{\Omega_\rho}^N)\, n_\Upsilon \cdot n_\Upsilon &= g & \text{on } \Upsilon, \\ u_{\Omega_\rho}^N \cdot \tau &= f \cdot \tau & \text{on } \Upsilon, \\ \sigma(u_{\Omega_\rho}^N)\, n &= 0 & \text{on } \partial\omega_\rho, \end{cases} \tag{5.15}$$

where n denotes the outward normal to Ω_ρ on the boundary $\partial\omega_\rho$. It should be reminded that for $\rho = 0$, we have $\omega_\rho = \emptyset$ and $\Omega_0 = \Omega$.
One can remark that ω_ρ coincides with the actual cavity $\mathcal{O}$ (5.1) where there is no misfit between both Dirichlet (5.14) and "Neumann" (5.15) problems, that is when $u^D_{\Omega_\rho} = u^N_{\Omega_\rho}$ in Ω_ρ. According to this observation, we propose to recover $\mathcal{O}$ by minimizing an energy gap cost functional, namely the following misfit Kohn-Vogelius functional (5.7) defined by

$$j(\Omega_\rho) = \mathcal{J}(u^D_{\Omega_\rho}, u^N_{\Omega_\rho}) = \frac{1}{2}\int_{\Omega_\rho} \Big(\sigma(u^D_{\Omega_\rho}) - \sigma(u^N_{\Omega_\rho})\Big) : \Big(\varepsilon(u^D_{\Omega_\rho}) - \varepsilon(u^N_{\Omega_\rho})\Big)\, dx, \tag{5.16}$$

in the presence of a single hole $\omega_\rho \subset \Omega$. Above, for both Dirichlet (5.14) and "Neumann" (5.15) problems, we impose a homogeneous Neumann boundary condition on $\partial\omega_\rho$ which means that ω_ρ represents a perforation, namely a cavity in mathematical concept.
The so-called Kohn-Vogelius criterion [67] (5.16) has already been investigated in the topological gradient context for the detection of cracks [6] in the steady-state heat equation, for the localization of small cavities in Stokes flow [23] and for the shape reconstruction of inclusions in an inverse conductivity problem [41].
The computation of the topological gradient exposed below is inspired by the paper [52] and let us point out that the main contribution in our work relies not only on the detection of cavities from partially overdetermined boundary data but also on the use of the error functional (5.16), also known as an energetic least-squares functional [21, 24, 64]. Indeed, the aim here is to derive an asymptotic expansion for the cost functional j (5.16) following the same procedure outlined in the previous section, that is, to study the variation of the design functional $\mathcal{J}$ with respect to the creation of small hole. However, the tools presented in the previous section cannot be applied directly as a fixed functional space $\mathcal{V}$ is required. Indeed, the displacements $u^D_{\Omega_\rho}$ (5.14) and $u^N_{\Omega_\rho}$ (5.15) are defined on the variable domain Ω_ρ dependant on ρ.
Let us mention that this question can be solved in the context of shape gradient method by the means of a fixed domain [21, 24, 64, 79], the so-called reference domain Ω and a bi-Lipshitz map between this reference domain Ω and the perturbed one.
Nevertheless, a domain truncation technique [52, 86] comes to help in the topological gradient context which allows us to construct a functional space independent of ρ. Hence, the topological gradient method can be viewed as an extension of the classical shape gradient method [21, 24, 64, 79] with a difficulty

concerning the lack of homeomorphism map between the safe domain Ω and the perforated one Ω_ρ since the domains Ω and Ω_ρ haven't the same topology.

5.5.1 Domain truncation technique

Let $R > 0$ be such that $\overline{B(x_0, R)} \subset \Omega$ and $\omega_\rho \subset B(x_0, R)$. Then, the truncated open set Ω_R (see Figure 5.3) is defined by

$$\Omega_R = \Omega \setminus \overline{B(x_0, R)}.$$

Let us denote by D_ρ the open set $B(x_0, R) \setminus \overline{\omega_\rho}$ (see Figure 5.3).
In order to provide an asymptotic expansion of the functional j (5.16), we need, first of all, an asymptotic expansion of both problems (5.14) and (5.15).

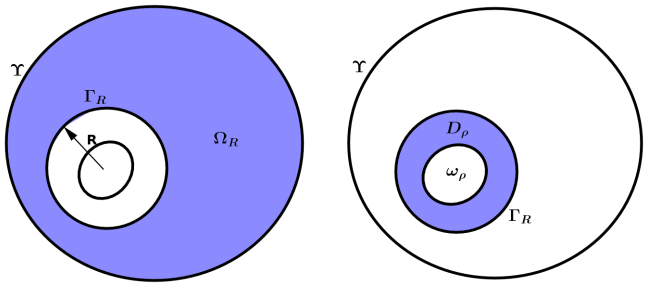

Figure 5.3: The truncated domain.

5.5.1.1 The Dirichlet problem:

For $\rho \geqslant 0$, let us define the Dirichlet-to-Neumann operator T_ρ, needed in the sequel, by

$$\begin{array}{rccl} T_\rho : & H^{\frac{1}{2}}(\Gamma_R)^2 & \longrightarrow & H^{-\frac{1}{2}}(\Gamma_R)^2 \\ & \varphi & \longmapsto & T_\rho\varphi = \sigma(u_\rho^\varphi)n, \end{array}$$

where u_ρ^φ is the solution to the problem

$$\begin{cases} -\operatorname{div}\sigma(u_\rho^\varphi) & = 0 & \text{in } D_\rho, \\ u_\rho^\varphi & = \varphi & \text{on } \Gamma_R, \\ \sigma(u_\rho^\varphi)\, n & = 0 & \text{on } \partial\omega_\rho. \end{cases}$$

Above, Γ_R is the boundary of $B(x_0, R)$. The normal n is chosen outward to D_ρ on $\partial\omega_\rho$ and Γ_R, regardless of whether D_ρ or Ω_R are considered.
Hence, the displacement u_ρ^D is defined for $\rho \geqslant 0$ as the solution of the truncated

problem: Find u_ρ^D such that

$$\begin{cases} -\operatorname{div}\sigma(u_\rho^D) &= 0 & \text{in } \Omega_R, \\ u_\rho^D &= f & \text{on } \Upsilon, \\ \sigma(u_\rho^D)\, n &= T_\rho\, u_\rho^D & \text{on } \Gamma_R. \end{cases} \tag{5.17}$$

The problem (5.17) can be stated in its variational formulation as following: Find $u_\rho^D \in [H^1(\Omega_R)]^2 ; u_\rho^D = f$ on Υ such that

$$a_\rho^D(u_\rho^D, v) = l^D(v) \qquad \forall v \in \mathcal{V}_R^D, \tag{5.18}$$

where the functional space $\mathcal{V}_R^D$ and the bilinear form a_ρ^D are defined by

$$\begin{aligned} & \mathcal{V}_R^D = \{u \in \left[H^1(\Omega_R)\right]^2 ; \quad u = 0 \text{ on } \Upsilon\} \\ \text{and} \qquad & a_\rho^D(u,v) = \int_{\Omega_R} \sigma(u) : \varepsilon(v) dx + \int_{\Gamma_R} T_\rho\, u \cdot v\, d\gamma(x). \end{aligned} \tag{5.19}$$

Here, $l^D \equiv 0$.
The reader is referred to [52] to prove the symmetry, continuity and coercivity of a_ρ^D. Let us remind a standard result in PDE theory.

Proposition 4. *[52] Problems (5.14) and (5.17) have a unique solution. Moreover, the solution u_ρ^D to problem (5.17) is the restriction to Ω_R of the solution $u_{\Omega_\rho}^D$ to problem (5.14).*

Proof. One can follow the same lines as in the Helmholtz problem [86]. □

5.5.1.2 The "Neumann" problem:

Let Ω_R, Γ_R, D_ρ and the operator T_ρ be as previously defined. Then, the displacement u_ρ^N is defined for $\rho \geqslant 0$ as the solution of the truncated problem: Find u_ρ^N such that

$$\begin{cases} -\operatorname{div}\sigma(u_\rho^N) &= 0 & \text{in } \Omega_R, \\ \sigma(u_\rho^N)\, n_\Upsilon \cdot n_\Upsilon &= g & \text{on } \Upsilon, \\ u_\rho^N \cdot \tau &= f \cdot \tau & \text{on } \Upsilon, \\ \sigma(u_\rho^N)\, n &= T_\rho\, u_\rho^N & \text{on } \Gamma_R. \end{cases} \tag{5.20}$$

The variational formulation associated to problem (5.20) is the following: Find $u_\rho^N \in [H^1(\Omega_R)]^2 ; u_\rho^N \cdot \tau = f \cdot \tau$ on Υ such that

$$a_\rho^N(u_\rho^N, v) = l^N(v) \qquad \forall v \in \mathcal{V}_R^N \tag{5.21}$$

where the functional space $\mathcal{V}_R^N$, the bilinear form a_ρ^N and the linear form l^N are defined by

$$\mathcal{V}_R^N = \{u \in \left[H^1(\Omega_R)\right]^2; \quad u \cdot \tau = 0 \text{ on } \Upsilon\},$$
$$a_\rho^N(u,v) = \int_{\Omega_R} \sigma(u) : \varepsilon(v) dx + \int_{\Gamma_R} T_\rho\, u \cdot v\, d\gamma(x) \tag{5.22}$$
$$\text{and} \quad l^N(v) = \int_\Upsilon g\,(v \cdot n_\Upsilon). \tag{5.23}$$

Since $a_\rho^N \equiv a_\rho^D$, a_ρ^N is symmetric, continuous and coercive and one can easily prove the continuity of the linear form l^N.
Then, we have the same standard result as the one related to the Dirichlet problem (Proposition 4), that is:

Proposition 5. *Problems (5.15) and (5.20) have a unique solution. Moreover, the solution u_ρ^N to problem (5.20) is the restriction to Ω_R of the solution $u_{\Omega_\rho}^N$ to problem (5.15).*

The fixed Hilbert space $[H^1(\Omega_R)]^2$ required by the adjoint method previously presented in the fourth section is now available. For $u_\rho^D \in [H^1(\Omega_R)]^2$, let $\widetilde{u_\rho^D} \in [H^1(\Omega_\rho)]^2$ be the extension of u_ρ^D which coincides with u_ρ^D on Ω_R and Γ_R and which satisfies

$$\begin{cases} -\operatorname{div}\sigma(\widetilde{u_\rho^D}) &= 0 \qquad \text{in } D_\rho, \\ \sigma(\widetilde{u_\rho^D})\, n &= 0 \qquad \text{on } \partial\omega_\rho. \end{cases}$$

In the same way, for $u_\rho^N \in [H^1(\Omega_R)]^2$, let $\widetilde{u_\rho^N} \in [H^1(\Omega_\rho)]^2$ be the extension of u_ρ^N which coincides with u_ρ^N on Ω_R and Γ_R and which satisfies

$$\begin{cases} -\operatorname{div}\sigma(\widetilde{u_\rho^N}) &= 0 \qquad \text{in } D_\rho, \\ \sigma(\widetilde{u_\rho^N})\, n &= 0 \qquad \text{on } \partial\omega_\rho. \end{cases}$$

Then, a function $\mathcal{J}_\rho$ can be defined on $[H^1(\Omega_R)]^2 \times [H^1(\Omega_R)]^2$ by

$$\mathcal{J}_\rho(u_\rho^D, u_\rho^N) = \mathcal{J}(\widetilde{u_\rho^D}, \widetilde{u_\rho^N})$$

and from the previous proposition 4 and 5, it follows that

$$j(\Omega_\rho) = \mathcal{J}(u_{\Omega_\rho}^D, u_{\Omega_\rho}^N) = \mathcal{J}_\rho(u_\rho^D, u_\rho^N).$$

5.5.2 The main result

We are now able to prove the main result of our work available in the case of spherical hole.

Theorem 10. *The function j has the following asymptotic expansion*

$$j(\Omega_\rho) = j(\Omega) + \rho^2 \left[\delta_{a^D}(u_0^D, v_0^D) + \delta_{a^N}(u_0^N, v_0^N) + \delta_{\mathcal{J}}(u_0^D, u_0^N)\right] + o(\rho^2), \quad (5.24)$$

where

$$\delta_{a^D}(u_0^D, v_0^D) = -\frac{\pi\,(\mu+\eta)}{2\,\eta\,\mu}\left[4\,\mu\,\sigma(u_0^D) : \varepsilon(v_0^D) + (\eta - 2\,\mu)\; tr\;\sigma(u_0^D)\; tr\;\varepsilon(v_0^D)\right], \quad (5.25)$$

$$\delta_{a^N}(u_0^N, v_0^N) = -\frac{\pi\,(\mu+\eta)}{2\,\eta\,\mu}\left[4\,\mu\,\sigma(u_0^N) : \varepsilon(v_0^N) + (\eta - 2\,\mu)\; tr\;\sigma(u_0^N)\; tr\;\varepsilon(v_0^N)\right] \quad (5.26)$$

and

$$\delta_{\mathcal{J}}(u_0^D, u_0^N) = -\frac{\pi}{2}\left[\sigma(u_0^D)(x_0) : \varepsilon(u_0^D)(x_0) + \sigma(u_0^N)(x_0) : \varepsilon(u_0^N)(x_0)\right]. \quad (5.27)$$

Above,

$$\eta = \lambda + \mu \qquad (\textit{plane strain}),$$

$v_0^D \in \mathcal{V}_0^D$ is the solution to the adjoint equation associated to the Dirichlet problem (5.12)

$$a_0^D(w, v_0^D) = -\partial_{u_0^D}\mathcal{J}(u_0^D, u_0^N)\, w \qquad \forall w \in \mathcal{V}_0^D, \quad (5.28)$$

$v_0^N \in \mathcal{V}_0^N$ is the solution to the adjoint equation associated to the Neumann problem (5.13)

$$a_0^N(w, v_0^N) = -\partial_{u_0^N}\mathcal{J}(u_0^D, u_0^N)\, w \qquad \forall w \in \mathcal{V}_0^N. \quad (5.29)$$

Proof. 1. **Variation of the bilinear form a_ρ^D (Dirichlet problem)**

The variation of the bilinear form a_ρ^D (5.19) defined by

$$a_\rho^D(u, v) = \int_{\Omega_R} \sigma(u) : \varepsilon(v) dx + \int_{\Gamma_R} T_\rho\, u \cdot v\, d\gamma(x)$$

reads

$$a_\rho^D(u, v) - a_0^D(u, v) = \int_{\Gamma_R} (T_\rho - T_0)\, u \cdot v\, d\gamma(x).$$

As a consequence, one has only to examine $(T_\rho - T_0)\varphi$ for $\varphi \in \left[H^{\frac{1}{2}}(\Gamma_R)\right]^2$. Indeed, one would like to find an operator $\delta_T \in \mathcal{L}(H^{\frac{1}{2}}(\Gamma_R)^2; H^{-\frac{1}{2}}(\Gamma_R)^2)$ such that

$$||T_\rho - T_0 - \rho^2\,\delta_T||_{\mathcal{L}(H^{\frac{1}{2}}(\Gamma_R)^2; H^{-\frac{1}{2}}(\Gamma_R)^2)} = o(\rho^3).$$

Hence, we define δ_{a^D} by

$$\delta_{a^D}(u,v) = \int_{\Gamma_R} \delta_T\, u \cdot v \, d\gamma(x) \qquad \forall u, v \in \left[H^1(\Omega_R)\right]^2$$

and we get that

$$||a_\rho^D - a_0^D - \rho^2\, \delta_{a^D}||_{\mathcal{L}_2([H^1(\Omega_R)]^2)} = o(\rho^3).$$

Making use of the same procedure outlined in [52], one can get the expression (5.25).

2. **Variation of the bilinear form a_ρ^N (Neumann problem)**
We remark that the same bilinear form a_ρ is available for the Dirichlet and the Neumann problem, namely $a_\rho^D \equiv a_\rho^N$. As a consequence, the same variation (5.26) of a_ρ^N follows.

3. **Variation of the linear form l^D and l^N**
Since l^N is independent of ρ, it follows trivially that $\delta_{l^N} \equiv 0$ and since $l^D \equiv 0$, then $\delta_{l^D} \equiv 0$.

4. **Variation of the cost functional**
Let us now focus our attention on the variation of the Kohn-Vogelius functional given by

$$\mathcal{J}(u^D_{\Omega_\rho}, u^N_{\Omega_\rho}) = \frac{1}{2}\int_{\Omega_\rho} \Big(\sigma(u^D_{\Omega_\rho}) - \sigma(u^N_{\Omega_\rho})\Big) : \Big(\varepsilon(u^D_{\Omega_\rho}) - \varepsilon(u^N_{\Omega_\rho})\Big)\, dx.$$

This functional $\mathcal{J}$ can be decomposed as

$$\mathcal{J}(u^D_{\Omega_\rho}, u^N_{\Omega_\rho}) = \mathcal{J}_D(u^D_{\Omega_\rho}) + \mathcal{J}_N(u^N_{\Omega_\rho}) + \mathcal{J}_{DN}(u^D_{\Omega_\rho}, u^N_{\Omega_\rho}),$$

$$\text{where} \quad \begin{cases} \mathcal{J}_D(u^D_{\Omega_\rho}) = \dfrac{1}{2}\displaystyle\int_{\Omega_\rho} \sigma(u^D_{\Omega_\rho}) : \varepsilon(u^D_{\Omega_\rho})\, dx, \\ \mathcal{J}_N(u^N_{\Omega_\rho}) = \dfrac{1}{2}\displaystyle\int_{\Omega_\rho} \sigma(u^N_{\Omega_\rho}) : \varepsilon(u^N_{\Omega_\rho})\, dx, \\ \mathcal{J}_{DN}(u^D_{\Omega_\rho}, u^N_{\Omega_\rho}) = -\displaystyle\int_{\Omega_\rho} \sigma(u^D_{\Omega_\rho}) : \varepsilon(u^N_{\Omega_\rho})\, dx. \end{cases}$$

(i) *Variation of $\mathcal{J}_D$:* The variation of $\mathcal{J}_D$ reads

$$\begin{aligned} &\mathcal{J}_D(u^D_{\Omega_\rho}) - \mathcal{J}_D(u_0^D) \\ =&\frac{1}{2}\int_{\Omega_\rho} \sigma(u^D_{\Omega_\rho}) : \varepsilon(u^D_{\Omega_\rho})\, dx - \frac{1}{2}\int_{\Omega} \sigma(u_0^D) : \varepsilon(u_0^D)\, dx, \\ =&\frac{1}{2}\int_{\Omega_\rho} \sigma(u^D_{\Omega_\rho} - u_0^D) : \varepsilon(u^D_{\Omega_\rho})\, dx + \frac{1}{2}\int_{\Omega_\rho} \sigma(u^D_{\Omega_\rho} - u_0^D) : \varepsilon(u_0^D)\, dx \\ &- \frac{1}{2}\int_{\omega_\rho} \sigma(u_0^D) : \varepsilon(u_0^D)\, dx. \end{aligned}$$

Using the Green formula, one can get from (5.14) that

$$\frac{1}{2}\int_{\Omega_\rho}\sigma(u^D_{\Omega_\rho}-u^D_0):\varepsilon(u^D_{\Omega_\rho})\,dx=0.$$

Then, it follows that

$$\begin{aligned}\mathcal{J}_D(u^D_{\Omega_\rho})-\mathcal{J}_D(u^D_0)=&\frac{1}{2}\int_{\Omega_\rho}\sigma(u^D_{\Omega_\rho}-u^D_0):\varepsilon(u^D_0)\,dx\\&-\frac{1}{2}\int_{\omega_\rho}\sigma(u^D_0):\varepsilon(u^D_0)\,dx.\end{aligned}\tag{5.30}$$

(ii) *Variation of $\mathcal{J}_N$:* The variation of $\mathcal{J}_N$ reads

$$\begin{aligned}&\mathcal{J}_N(u^N_{\Omega_\rho})-\mathcal{J}_N(u^N_0)\\=&\frac{1}{2}\int_{\Omega_\rho}\sigma(u^N_{\Omega_\rho}):\varepsilon(u^N_{\Omega_\rho})\,dx-\frac{1}{2}\int_{\Omega}\sigma(u^N_0):\varepsilon(u^N_0)\,dx,\\=&\frac{1}{2}\int_{\Omega_\rho}\sigma(u^N_{\Omega_\rho}-u^N_0):\varepsilon(u^N_{\Omega_\rho})\,dx+\frac{1}{2}\int_{\Omega_\rho}\sigma(u^N_{\Omega_\rho}-u^N_0):\varepsilon(u^N_0)\,dx\\&-\frac{1}{2}\int_{\omega_\rho}\sigma(u^N_0):\varepsilon(u^N_0)\,dx.\end{aligned}$$

Using the Green formula applied to the problem (5.15), we obtain

$$\frac{1}{2}\int_{\Omega_\rho}\sigma(u^N_{\Omega_\rho}-u^N_0):\varepsilon(u^N_{\Omega_\rho})\,dx=\frac{1}{2}\int_{\Upsilon}\sigma(u^N_{\Omega_\rho})\,n_\Upsilon\cdot(u^N_{\Omega_\rho}-u^N_0)ds.$$

Since $u^N_{\Omega_\rho}\cdot\tau=u^N_0\cdot\tau=f\cdot\tau$ and $\sigma(u^N_{\Omega_\rho})\,n_\Upsilon\cdot n_\Upsilon=g$ on Υ, we have

$$\frac{1}{2}\int_{\Upsilon}\sigma(u^N_{\Omega_\rho})\,n_\Upsilon\cdot(u^N_{\Omega_\rho}-u^N_0)ds=\frac{1}{2}\int_{\Upsilon}g\left[(u^N_{\Omega_\rho}-u^N_0)\cdot n_\Upsilon\right]ds.$$

Then, the following equality holds

$$\frac{1}{2}\int_{\Omega_\rho}\sigma(u^N_{\Omega_\rho}-u^N_0):\varepsilon(u^N_{\Omega_\rho})\,dx=\frac{1}{2}\int_{\Upsilon}g\left[(u^N_{\Omega_\rho}-u^N_0)\cdot n_\Upsilon\right]ds.$$

Hence, we get

$$\begin{aligned}&\mathcal{J}_N(u^N_{\Omega_\rho})-\mathcal{J}_N(u^N_0)\\=&\frac{1}{2}\int_{\Omega_\rho}\sigma(u^N_{\Omega_\rho}-u^N_0):\varepsilon(u^N_0)\,dx+\frac{1}{2}\int_{\Upsilon}g\left[(u^N_{\Omega_\rho}-u^N_0)\cdot n_\Upsilon\right]ds\\&-\frac{1}{2}\int_{\omega_\rho}\sigma(u^N_0):\varepsilon(u^N_0)\,dx.\end{aligned}\tag{5.31}$$

(iii) *Variation of $\mathcal{J}_{DN}$:* The variation of $\mathcal{J}_{DN}$ reads

$$\mathcal{J}_{DN}(u^D_{\Omega_\rho}, u^N_{\Omega_\rho}) - \mathcal{J}_{DN}(u^D_0, u^N_0) = -\int_{\Omega_\rho} \sigma(u^D_{\Omega_\rho}) : \varepsilon(u^N_{\Omega_\rho})\, dx + \int_{\Omega} \sigma(u^D_0) : \varepsilon(u^N_0)\, dx.$$

Using the Green formula applied, on one hand, to the problem (5.15) we obtain

$$-\int_{\Omega_\rho} \sigma(u^D_{\Omega_\rho}) : \varepsilon(u^N_{\Omega_\rho})\, dx = -\int_{\Upsilon} \sigma(u^N_{\Omega_\rho}) n_\Upsilon \cdot f\, ds$$

and on the other hand, to the problem (5.13) we get

$$\int_{\Omega} \sigma(u^D_0) : \varepsilon(u^N_0)\, dx = \int_{\Upsilon} \sigma(u^N_0) n_\Upsilon \cdot f\, ds.$$

Then, we have

$$\mathcal{J}_{DN}(u^D_{\Omega_\rho}, u^N_{\Omega_\rho}) - \mathcal{J}_{DN}(u^D_0, u^N_0) = \int_{\Upsilon} \sigma(u^N_0 - u^N_{\Omega_\rho}) n_\Upsilon \cdot f\, ds.$$

Since $\sigma(u^N_0) n_\Upsilon \cdot n_\Upsilon = \sigma(u^N_{\Omega_\rho}) n_\Upsilon \cdot n_\Upsilon = g$ on Υ, it follows that

$$\mathcal{J}_{DN}(u^D_{\Omega_\rho}, u^N_{\Omega_\rho}) - \mathcal{J}_{DN}(u^D_0, u^N_0) = \int_{\Upsilon} \Big[\sigma(u^N_0 - u^N_{\Omega_\rho}) n_\Upsilon \cdot \tau\Big] (f \cdot \tau)\ ds. \tag{5.32}$$

Combining the variations (5.30), (5.31) and (5.32), the variation of the functional $\mathcal{J}$ becomes

$$\begin{aligned}
&\mathcal{J}(u^D_{\Omega_\rho}, u^N_{\Omega_\rho}) - \mathcal{J}(u^D_0, u^N_0)\\
=&\mathcal{J}_D(u^D_{\Omega_\rho}) - \mathcal{J}_D(u^D_0) + \mathcal{J}_{DN}(u^D_{\Omega_\rho}, u^N_{\Omega_\rho}) - \mathcal{J}_{DN}(u^D_0, u^N_0) + \mathcal{J}_N(u^N_{\Omega_\rho})\\
&- \mathcal{J}_N(u^N_0),\\
=&\frac{1}{2}\int_{\Omega_\rho} \sigma(u^D_{\Omega_\rho} - u^D_0) : \varepsilon(u^D_0)\, dx - \frac{1}{2}\int_{\omega_\rho} \sigma(u^D_0) : \varepsilon(u^D_0)\, dx\\
&+ \int_{\Upsilon} \Big[\sigma(u^N_0 - u^N_{\Omega_\rho}) n_\Upsilon \cdot \tau\Big] (f \cdot \tau)\ ds + \frac{1}{2}\int_{\Omega_\rho} \sigma(u^N_{\Omega_\rho} - u^N_0) : \varepsilon(u^N_0)\, dx\\
&+ \frac{1}{2}\int_{\Upsilon} g \Big[(u^N_{\Omega_\rho} - u^N_0) \cdot n_\Upsilon\Big]\, ds - \frac{1}{2}\int_{\omega_\rho} \sigma(u^N_0) : \varepsilon(u^N_0)\, dx,\\
=&D\mathcal{J}(u^D_0, u^N_0)(u^D_{\Omega_\rho} - u^D_0, u^N_{\Omega_\rho} - u^N_0) - \frac{1}{2}\int_{\omega_\rho} \sigma(u^D_0) : \varepsilon(u^D_0)\, dx\\
&- \frac{1}{2}\int_{\omega_\rho} \sigma(u^N_0) : \varepsilon(u^N_0)\, dx,
\end{aligned}$$

where

$$\begin{aligned}
&D\mathcal{J}(u_0^D, u_0^N)(u_{\Omega_\rho}^D - u_0^D, u_{\Omega_\rho}^N - u_0^N) \\
=&\frac{1}{2}\int_{\Omega_\rho} \sigma(u_{\Omega_\rho}^D - u_0^D) : \varepsilon(u_0^D)\, dx + \frac{1}{2}\int_{\Omega_\rho} \sigma(u_{\Omega_\rho}^N - u_0^N) : \varepsilon(u_0^N)\, dx \\
&- \int_\Upsilon \left[\sigma(u_{\Omega_\rho}^N - u_0^N) n_\Upsilon \cdot \tau\right] (f \cdot \tau)\ ds + \frac{1}{2}\int_\Upsilon g \left[(u_{\Omega_\rho}^N - u_0^N) \cdot n_\Upsilon\right] ds.
\end{aligned}$$

Using the change of variables $x = x_0 + \rho\, y$ with $x_0 = 0$, one can write

$$\begin{aligned}
&\int_{\omega_\rho} \sigma(u_0^D) : \varepsilon(u_0^D)\, dx \\
=&\rho^2 \int_\omega \sigma(u_0^D)(\rho\, y) : \varepsilon(u_0^D)(\rho\, y)\, dy, \\
=&\rho^2 \int_\omega \sigma(u_0^D)(0) : \varepsilon(u_0^D)(0)\, dy \\
&+ 2\,\rho^2 \int_\omega \left[\sigma(u_0^D)(\rho\, y) - \sigma(u_0^D)(0)\right] : \varepsilon(u_0^D)(0)\, dy \\
&+ \rho^2 \int_\omega \left[\sigma(u_0^D)(\rho\, y) - \sigma(u_0^D)(0)\right] : \left[\varepsilon(u_0^D)(\rho\, y) - \varepsilon(u_0^D)(0)\right]\, dy, \\
=&\rho^2 \int_\omega \sigma(u_0^D)(0) : \varepsilon(u_0^D)(0)\, dy + E_1(\rho) + E_2(\rho),
\end{aligned}$$

where

$$E_1(\rho) = 2\,\rho^2 \int_\omega \left[\sigma(u_0^D)(\rho\, y) - \sigma(u_0^D)(0)\right] : \varepsilon(u_0^D)(0)\, dy$$

and

$$E_2(\rho) = \rho^2 \int_\omega \left[\sigma(u_0^D)(\rho\, y) - \sigma(u_0^D)(0)\right] : \left[\varepsilon(u_0^D)(\rho\, y) - \varepsilon(u_0^D)(0)\right]\, dy.$$

By the Taylor expansion, using the fact that u_0^D is regular in a neighborhood of 0, namely $u_0^D \in C^2(\omega_\rho)$, one can prove that

$$\int_\omega \left[\sigma(u_0^D)(\rho\, y) - \sigma(u_0^D)(0)\right] : \varepsilon(u_0^D)(0)\, dy = O(\rho)$$

and so we obtain $E_1(\rho) = o(\rho^2)$.
In the same way, using the Taylor expansion and the regularity of u_0^D in a neighborhood of the origin, we get that

$$\int_\omega \left[\sigma(u_0^D)(\rho\, y) - \sigma(u_0^D)(0)\right] : \left[\varepsilon(u_0^D)(\rho\, y) - \varepsilon(u_0^D)(0)\right]\, dy = O(\rho^2)$$

and so $E_2(\rho) = o(\rho^2)$. Then, it follows that

$$\frac{1}{2}\int_{\omega_\rho} \sigma(u_0^D) : \varepsilon(u_0^D)\, dx = \frac{1}{2}\,\rho^2 \int_\omega \sigma(u_0^D)(0) : \varepsilon(u_0^D)(0)\, dx + o(\rho^2).$$

Following the same lines outlined above, we derive

$$\frac{1}{2}\int_{\omega_\rho} \sigma(u_0^N) : \varepsilon(u_0^N)\, dx = \frac{1}{2}\,\rho^2 \int_{\omega} \sigma(u_0^N)(0) : \varepsilon(u_0^N)(0)\, dx + o(\rho^2).$$

Thus,

$$\delta_{\mathcal{J}}(u_0^D, u_0^N) = -\frac{\pi}{2}\left[\sigma(u_0^D)(x_0) : \varepsilon(u_0^D)(x_0) + \sigma(u_0^N)(x_0) : \varepsilon(u_0^N)(x_0)\right].$$

All the assumptions of the adjoint method are satisfied and the topological asymptotic expansion is given by Theorem 9. □

5.6 Numerical experiments

In spite of the lack of identifiability of the inverse problem under consideration (in the second section, the identifiability was only proved in the case of monotonous cavities), it is nevertheless useful to evaluate the efficiency of the proposed method through numerical experiments.
Therefore, this part aims to develop a one-shot reconstruction algorithm to numerically solve our cavities identification problem from partially overdetermined boundary data using the topological gradient method. In order to evaluate the topological gradient g, it is practically sufficient to solve the Dirichlet (5.12) and Neumann (5.13) state equations as well as the appropriate adjoint Dirichlet (5.28) and Neumann (5.29) state equations in the safe domain Ω. Hence, an efficient and cheap topology optimization algorithm can be implemented in our case as one only needs to compute the solution of both Dirichlet and Neumann direct and adjoint problems. Since the function j has to be minimized, one has to create holes at some points x_0 where the topological gradient $g(x_0)$, giving by

$$g(x_0) = \delta_{a^D}(u_0^D, v_0^D) + \delta_{a^N}(u_0^N, v_0^N) + \delta_{\mathcal{J}}(u_0^D, u_0^N). \tag{5.33}$$

is the most negative. In order to point out this feature, let us enumerate the steps of the topological optimization algorithm to be implemented.

5.6.1 Algorithm

Let Ω^{true} be a domain containing a cavity whose location and shape are to be retrieved from boundary measurements. The displacement f and the normal component of the normal stress g are generated by a numerical computation of a direct problem over the domain Ω^{true} containing the cavity to recover

(synthetic data).
Since the partially overdetermined boundary data (f, g) are overspecified, the numerical procedure could be represented in the following algorithm stages.

1. Provide the initial domain Ω_0 (the safe domain).
2. Solve the Dirichlet (5.12) and Neumann (5.13) direct problems in the safe domain Ω_0.
3. Solve the Dirichlet (5.28) and Neumann (5.29) adjoint problems in the safe domain Ω_0.
4. Compute the topological gradient g (5.33).
5. Create holes at the points where the topological derivative is the most negative.

5.6.2 Numerical tests

In this subsection, we provide some numerical results related to the identification of cavities carried out with the algorithm described above.
We consider for all the following tests the same initial domain Ω_0, namely the disc centered at the origin of radius $r_0 = 2$.

5.6.2.1 First case

In this case, the solution, namely the boundary of the cavity to recover, is the circle C_{exact} centered at the origin with radius $R_{\text{exact}} = 0.45$ and the partially overdetermined boundary data, that is the displacement field and the normal component of the normal stress are taken from the analytical expression u_{exact}, of the solution u of the elasticity problem with complete data [24], given by

$$u_{\text{exact}}(r) = \frac{C1}{2} r + \frac{C2}{r}$$

where

$$C1 = \frac{2(1+\nu)(1-2\nu)}{E} A \qquad \text{and} \qquad C2 = \frac{1+\nu}{E} B.$$

Above, the constants A and B are determined by the boundary conditions, namely

$$A = \frac{P_1 r_1^2 - P_2 r_0^2}{r_0^2 - r_1^2} \qquad \text{and} \qquad B = \frac{P_1 - P_2}{r_0^2 - r_1^2} r_1^2 r_0^2$$

where $r_1 = R_{\text{exact}}$, $\sigma_r(r_1) = -P_1 = 0$ and $\sigma_r(r_0) = -P_2$ (σ_r is the radial stress). Figure 5.4 shows the level lines of the topological gradient g (5.33). We remark that the level set curve of g related to the smallest value corresponds to the cavity to be recovered.

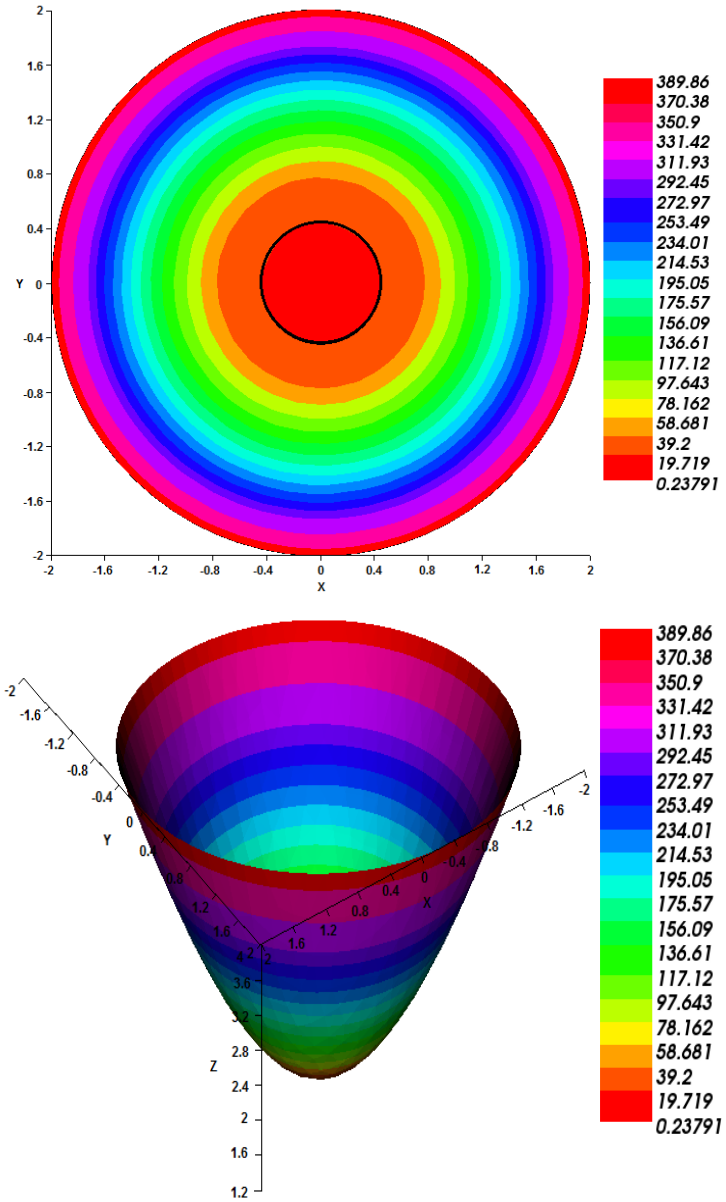

Figure 5.4: On the top: superposition of the actual cavity and the smallest isovalue of the topological gradient; on the bottom: the topological gradient g.

5.6.2.2 Second case

In the following cases, the measurements f and g are synthetic, i.e. generated by a numerical computation.
In this second case, we consider again a single cavity centered at $(-1.6; -0.3)$ with radius $R_{\text{exact}} = 0.3$. Figure 5.5 depicts the rough location of the cavity.

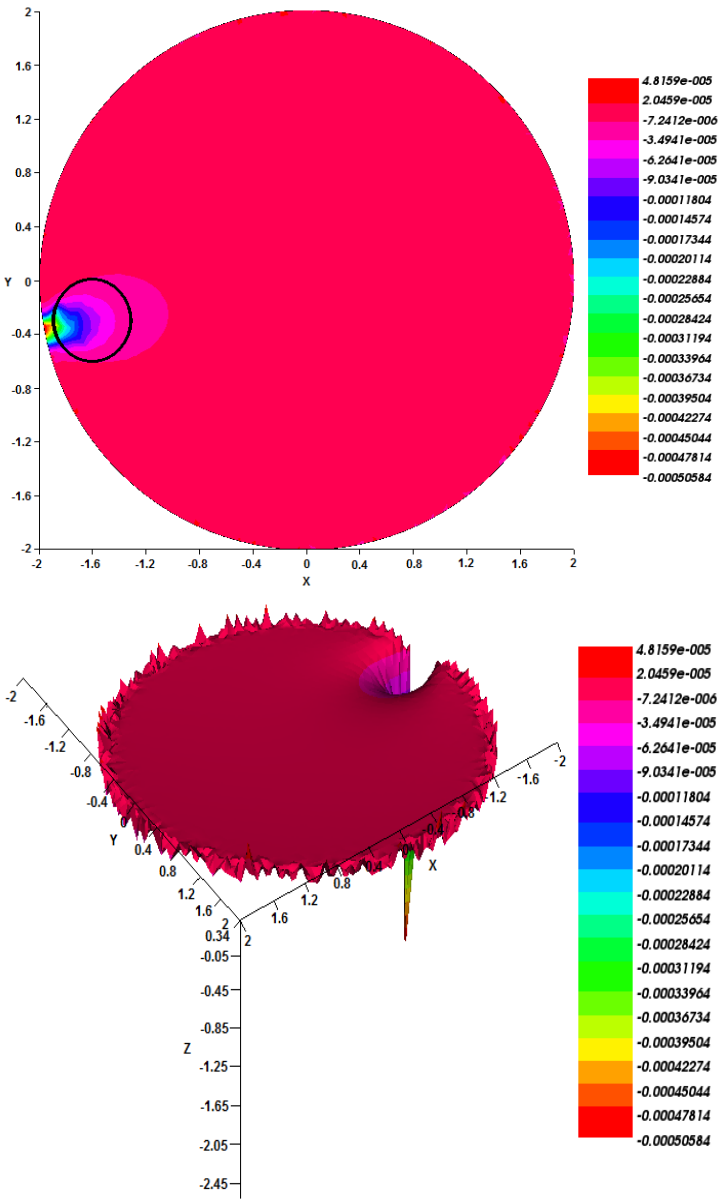

Figure 5.5: On the top: superposition of the actual cavity and negative level lines of the topological gradient; on the bottom: the topological gradient g.

In contrast to the first and second cases focusing on the identification of a single cavity, the issue discussed in the next cases deals with multiple cavities

detection insofar as the topological gradient does not depend on the number of cavities.

5.6.2.3 Third case

The aim of the third numerical experiment is to identify two cavities centered at $(-1.65; 0)$ and $(1.65; 0)$ with radius $R_{\text{exact}} = 0.3$. From Figure 5.6, it turns out that an accurate detection is achieved.

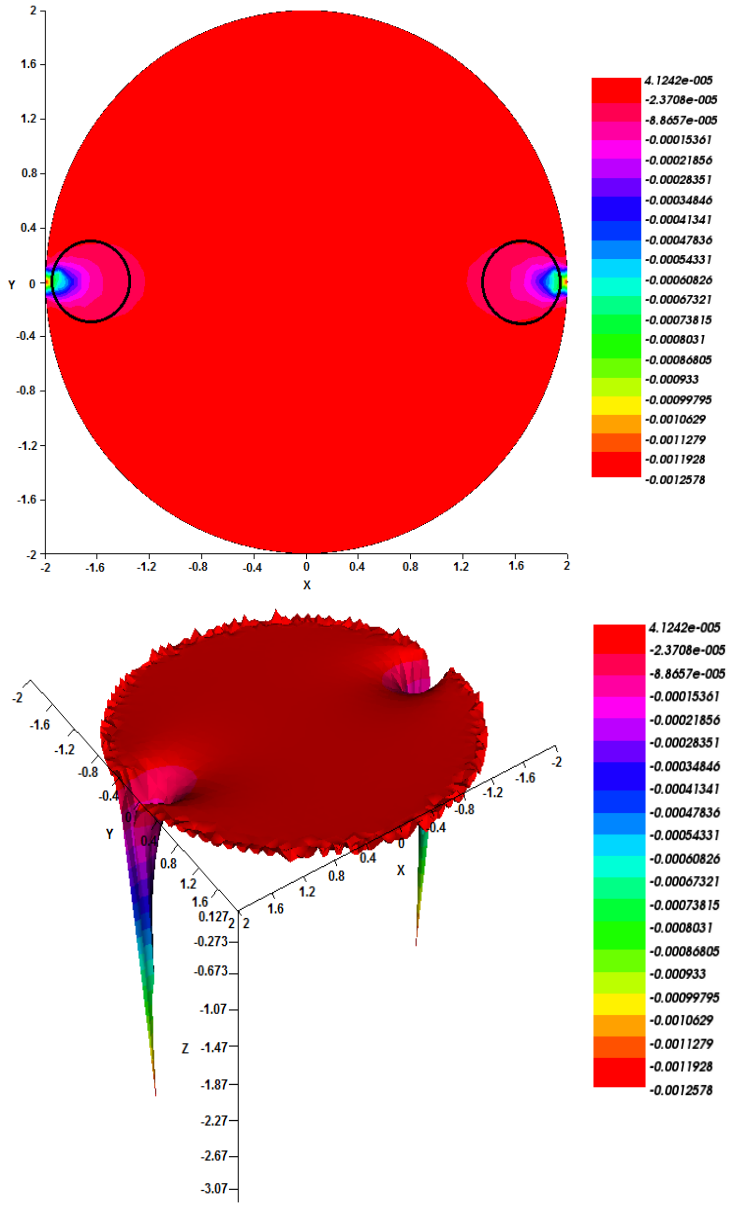

Figure 5.6: On the top: superposition of the actual cavities and negative level lines of the topological gradient; on the bottom: the topological gradient g.

5.6.2.4 Fourth case

For the numerical reconstruction in the last experiment, we focus on the case of a mechanical structure with four cavities, having the same radius $R_{\text{exact}} = 0.3$ and centered at $(-1.65; 0)$, $(1.65; 0)$, $(0; -1.65)$ and $(0; 1.65)$, to be recovered. The negative level lines of the topological gradient presented in Figure 5.7 coincide with the actual cavities.

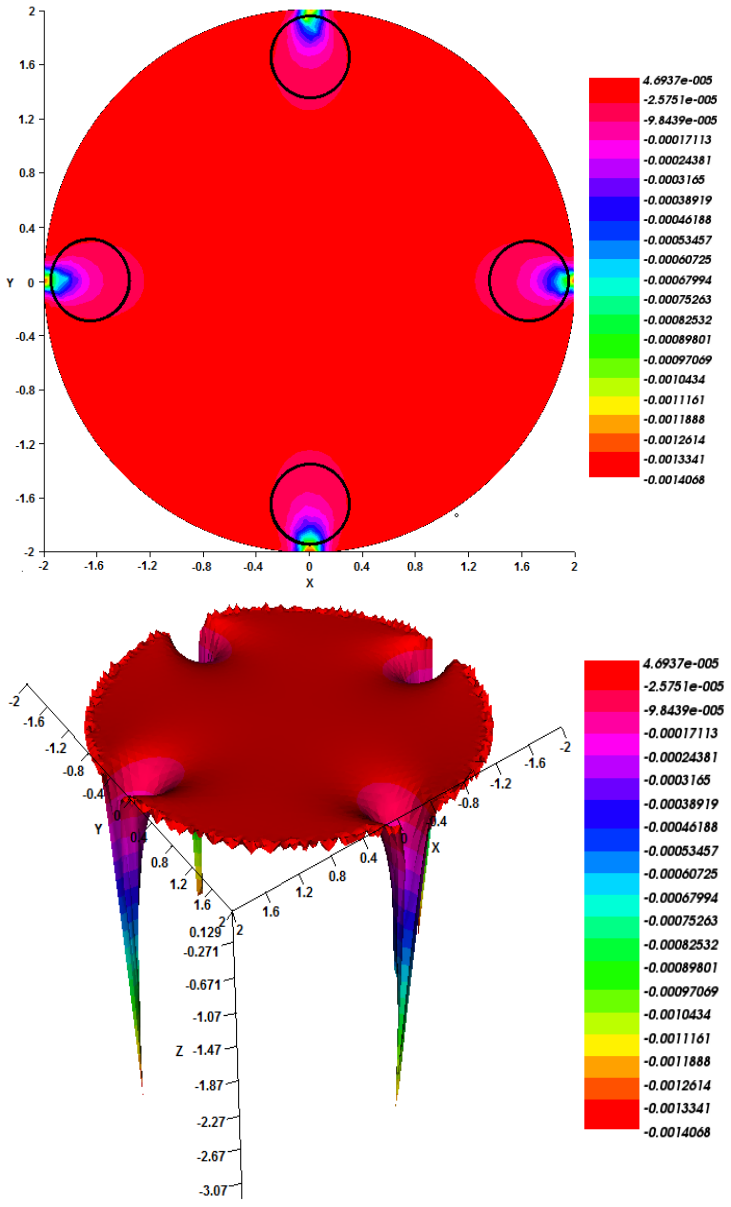

Figure 5.7: On the top: superposition of the actual cavities and negative level lines of the topological gradient; on the bottom: the topological gradient g.

Let us point that although the partially overdetermined boundary data

lead additional difficulties especially in the numerical part, the detection of the cavities is efficient. Thus, these numerical illustrations demonstrate that the approach, namely the topological gradient method combined with the Kohn-Vogelius functional, proposed herein, is a reliable tool to recover cavities in mechanical structures.

5.7 Comments

Among several techniques proposed to solve the problem of detection of geometrical faults arising in elasticity framework, we resort, in this work, to the topological gradient method which furnishes the sensitivity of a shape functional when modifying the topology of the domain with respect to the creation of a small hole.

We have proposed a one-shot approach based on the topological gradient method combined with the so-called Kohn-Vogelius gap cost functional. From the numerical results, the topological sensitivity method has been seen to be a powerful tool to be applied in topology optimization problems even in the case of partially overdetermined boundary data.

Moreover, the theoretical question related to the identifiability is still open since the uniqueness result was only derived for the case of monotonous cavities.

Although the process of the topological gradient method is not only cheap but also fast, it only allows to detect the rough location of faults. Hence, if one needs to determine a precise location, it should use some others approaches like level set method. A promising strategy [4] to be explored is so to combine the level set method with the topological gradient one from which a good initial guess can be obtained.

Chapter 6

Outlook: Voids identification from sub-Cauchy data

Contents

This chapter builds on the article entitled "**Voids identification from sub-Cauchy data**" in preparation. This work is done in collaboration with Amel Ben Abda and Sinda Khalfallah.

Abstract

An iterative method for solving a geometrical inverse problem in linear elasticity is proposed. The problem is to identify cavities in mechanical structure from the knowledge of partially overdetermined boundary data, namely the displacement field and the normal component of the normal stress. The approach proposed is based on the coupling of the data completion theory through the Steklov Poincaré operator to reconstruct the shear stress and of the shape gradient method combined with the level set method to identify cavities. Numerical simulations highlight the algorithm efficiency.

Keywords: Geometrical inverse problems, cavities identification, linear elasticity, partially overdetermined boundary data, shear stress reconstruction, optimization, shape derivative method, Steklov Poincaré operator, level set method.

Résumé

Ce travail développe une nouvelle stratégie pour la résolution d'un problème inverse géométrique relatif à l'identification de cavités à partir de données partiellement surdéterminées dans le cadre de l'élasticité linéaire. Plus précisément, la donnée accessible pour la reconstruction est le champ de déplacement et la composante normale de la contrainte normale. Aucune information n'est disponible pour la contrainte de cisaillement. La méthode proposée est itérative. Elle est basée sur un algorithme à deux étapes. En effet, en premieu lieu, nous nous intéressons à un problème de complétion de données relatif à la reconstruction de la contrainte de cisaillement par des données partiellement surdéterminées, en utilisant l'opérateur de Steklov Poincaré. Tandis qu'en deuxième lieu, la méthode de dérivation par rapport au domaine combinée avec la méthode level set est introduite dans le but d'identifier les cavités par des données surdéterminées. Pour mener à bien ces deux étapes, la même fonctionnelle d'écart énergétique est proposée pour la reformulation du problème inverse de reconstruction de la contrainte de cisaillement et celui de cavités en problèmes de minimisation. Les résultats numériques obtenus prouvent l'efficacité de notre méthodologie et sa capacité à identifier plusieurs cavités enfouies dans les structures mécaniques.

Mots clés: Problèmes inverses géométriques, identification de cavités, élasticité linéaire, données partiellement surdéterminées, reconstruction de la contrainte de cisaillement, optimisation, méthode de gradient de forme, opérateur de Steklov Poincaré, méthode level set.

6.1 Introduction

During the past few decades, special attention has been given to inverse problems in linear elasticity framework [32]. These problems can be classified as the detection of defaults (cavities, cracks or inclusions) or the reconstruction of inaccessible boundary conditions, among others.
On one hand, the identification of flaws in mechanical structures is extremely important in industry [70, 77] since it is crucial for engineers to assess the reliability of structures and to predict its remaining service life. On the other hand, overdetermined boundary data are crucial to such a geometrical inverse problem. To the best of our knowledge, all cavities identification problems in linear elasticity, investigated in the literature, are based on the essential assumption that overspecified boundary conditions are complete, i.e. both the displacement field and the normal stress are available for the reconstruction of flaws [24, 28, 29], expect of a recent work [25] where overdetermined boundary data are incomplete. Firstly, let us mention that while surfing the literature, one can remark that incomplete overdetermined boundary data in linear elasticity is related to Cauchy problem (see [30] and references therein). It is a question about the second class of inverse problems mentioned above. Such a problem can be formulated as follows: given the tractions and the displacement fields on the accessible part of the boundary of the domain of interest, one aims to evaluate the same information on the inaccessible part of the boundary.
Needless to say, this ill-posed Cauchy problem has already been strongly studied with a lot of methods which can be grouped as methods based on the minimization of an energy-like functional [7, 8] via the Steklov Poincaré operator, quasi reversibility method [34], iterative methods [45, 71, 72], iterative regularization methods (namely, relaxation procedures for alternating iterative algorithms) [73, 74], Tikhonov regularization [43]. We refer the reader to [30].
In some situations, no information about shear stress (namely the tangential component of the normal stress) is available and only the displacement field and the normal component of the normal stress are accessible. It is a question about sub-Cauchy data , that is partially overdetermined boundary data [25]

which consists the main motivation of this paper.
Such non standard situation derives for example from the devices used to compute measurements on the exterior boundary of the mechanical components. Motivated by the recent results of [27] obtained to recover lacking boundary conditions via sub-Cauchy data and results of [24] obtained to identify cavities from overdetermined boundary data; both results obtained in linear elasticity, we are concerned in this work with a geometrical inverse problem related to the identification of cavities in mechanical structures from sub-Cauchy data.
The problem under consideration might be formulated as follows: Let $B \subset \mathbb{R}^2$ denotes an open and bounded domain with boundary Υ occupied by a linear elastic material. We assume that there exists a cavity, namely a bounded domain $\overline{A} \subset B$ with boundary Γ and we denote by Ω the domain $B \backslash \overline{A}$. Given the normal component of the normal stress imposed $g \cdot n_\Upsilon$ and the displacement field f measured on the boundary Υ

$$\begin{cases} \sigma(u)\, n_\Upsilon \cdot n_\Upsilon & = g \cdot n_\Upsilon & \text{on } \Upsilon, \\ u & = f & \text{on } \Upsilon, \end{cases}$$

namely the exterior boundary measurements, the linear elasticity inverse problem consists so in recovering the cavity A, namely the unknown shape Γ and the displacement field u satisfying the following partially overdetermined boundary problem

$$\begin{cases} \operatorname{div} \sigma(u) & = 0 & \text{in } \Omega, \\ \sigma(u)\, n & = 0 & \text{on } \Gamma, \\ u & = f & \text{on } \Upsilon, \\ \sigma(u)\, n_\Upsilon \cdot n_\Upsilon & = g \cdot n_\Upsilon & \text{on } \Upsilon. \end{cases} \tag{6.1}$$

Above, n_Υ and n are the outward unit normals to the boundary of Ω. $\sigma(u)$ is the Cauchy stress tensor associated to the displacement field u and $\varepsilon(u)$ is the linearized strain tensor given by

$$\varepsilon(u) = \frac{1}{2}\left(\nabla u + \nabla u^T\right).$$

σ and ε are related by the Hooke constitutive law, the medium being assumed to be homogeneous and isotropic. Therefore,

$$\sigma\left(u\right) = \lambda \operatorname{tr} \varepsilon\left(u\right) \operatorname{Id} + 2\,\mu\, \varepsilon\left(u\right)$$

and conversely

$$\varepsilon\left(u\right) = \frac{1+\nu}{E}\, \sigma\left(u\right) - \frac{\nu}{E}\, \left(\operatorname{tr} \sigma\left(u\right)\right) \operatorname{Id}.$$

Above, tr denotes the trace of matrix and λ, μ are the Lamé coefficients related to Young's modulus E and Poisson's ratio ν via

$$\mu = \frac{E}{2\,(1+\nu)} \qquad \text{and} \qquad \lambda = \frac{E\,\nu}{(1-2\,\nu)\,(1+\nu)}\,.$$

The present research aims to develop an iterative method based on coupling the Steklov Poincaré operator and the shape gradient method combined with the level set method through the minimization of an energy-like functional [21, 24, 25, 27, 64] to numerically solve the problem (6.1). Up to our knowledge, such approach has never been carried out before.
However, it should be noted that some results related to the detection of cracks [26, 42] and obstacles [34] for the Laplace problem are achieved through iterative methods in the case of Cauchy data i.e. data known only on some part of the boundary of the domain. Indeed, a two-step recovery algorithm, based on least squares fit with an iterated Tikhonov regularization to extend the available data to the whole external boundary as a first step and on the reciprocity gap to retrieve the crack as a second step, was proposed in [42]. While, in [26], the recovery procedure was based firstly on building an extension of the available data to the whole boundary using constructive approximation techniques in classes of analytic and meromorphic functions and secondly on the reciprocity gap technique as it was the case in [42]. However, the approach proposed in [34] was based on an iterative procedure which consists in coupling the method of quasi-reversibility [69] and a simple level set method.
The overview of the paper is as follows: In the upcoming section, we are interested in the geometrical inverse problem related to cavities identification problem from complete overdetermined boundary data. The shape gradient is introduced. In the third section, we investigate the inverse problem of recovering the shear stress from the knowledge of sub-Cauchy data on the external boundary of the domain of interest. The first issue in the fourth section is to present the level set method whilst the second one is to outline the algorithm to be implemented. The fifth section is devoted to numerical results. Finally, some concluding remarks and possible future work are reported in section 6.

6.2 Voids identification

In this section, we aim to recover the cavity (void) A, that is to solve the geometrical inverse problem (6.1) provided the shear stress, namely $g \cdot \tau$ is known on Υ, where τ is the unit tangent vector to Υ. The problem under

consideration in this section is so to retrieve the cavity A and the displacement field u solution of the following problem

$$\begin{cases} \operatorname{div}\sigma(u) &= 0 & \text{in } \Omega, \\ \sigma(u)\,n &= 0 & \text{on } \Gamma, \\ u &= f & \text{on } \Upsilon, \\ \sigma(u)\,n_\Upsilon &= g & \text{on } \Upsilon. \end{cases} \tag{6.2}$$

The problem of the reconstruction of the shear stress $g \cdot \tau$ will be addressed in the next section.

We now present the same method investigated in [24] to solve this problem (6.2), namely the cavities identification problem from complete overdetermined boundary data. In this part, we only outline briefly the identification method. A comprehensive analysis is postponed in [24].

One approach to treat the problem (6.2) is to formulate it as a shape optimization one. To this end, we split the problem (6.2) into two sub-problems. Indeed, for a given Ω, let (σ_D, u_D) and (σ_N, u_N) be the solutions of the following Dirichlet (6.3), respectively Neumann (6.4) problems

$$\begin{cases} \operatorname{div}\sigma_D &= 0 & \text{in } \Omega, \\ \varepsilon_D &= \frac{1+\nu}{E}\,\sigma_D - \frac{\nu}{E}\,(\operatorname{tr}\,\sigma_D)\,\mathrm{Id} & \text{in } \Omega, \\ \sigma_D\,n &= 0 & \text{on } \Gamma, \\ u_D &= f & \text{on } \Upsilon, \end{cases} \tag{6.3}$$

respectively

$$\begin{cases} \operatorname{div}\sigma_N &= 0 & \text{in } \Omega, \\ \varepsilon_N &= \frac{1+\nu}{E}\,\sigma_N - \frac{\nu}{E}\,(\operatorname{tr}\,\sigma_N)\,\mathrm{Id} & \text{in } \Omega, \\ \sigma_N\,n &= 0 & \text{on } \Gamma, \\ \sigma_N\,n_\Upsilon &= g & \text{on } \Upsilon. \end{cases} \tag{6.4}$$

Writing both Dirichlet and Neumann problems in such a way is related to the use of the Hellinger-Reissner principle [93].

One can remark that the cavity to recover A^* is reached ($A = A^*$) when there is no misfit between both Dirichlet and Neumann solutions, that is, when $\sigma_D = \sigma_N$ and $u_D = u_N$. According to this observation, we propose an identification process based on the minimization of the following misfit functional J depending on the domain Ω

$$J(\Omega) := \frac{1}{2}\int_\Omega (\sigma_D - \sigma_N) : (\varepsilon(u_D) - \varepsilon(u_N)). \tag{6.5}$$

Hence, the cavities identification problem (6.2) can be formulated as a shape optimization one as follows

$$\begin{cases} \text{Find } \Omega \text{ such that} \\ J(\Omega) = \min\limits_{\tilde{\Omega} \subset B} J(\tilde{\Omega}). \end{cases} \tag{6.6}$$

The minimum has to be taken over all sufficiently smooth domains Ω such that $\Omega \subset B$.

6.2.1 Shape derivative method

In order to apply a gradient method to the minimization problem (6.6), we make use of the shape derivative method. To carry out the sensitivity analysis of the shape functional J, one needs to introduce a family of perturbations $\{\Omega_t\}$ of a given domain $\Omega \subset \mathbb{R}^2$. We make use of the transformations which are defined as the perturbations of the identity mapping id. Indeed, let us consider an open and bounded domain $U \supset \overline{\Omega}$ and construct a family of transformations F_t as follows [79]

$$F_t = id + th,$$

where h is a deformation field belonging to the space

$$Q = \{h \in \mathcal{C}^{1,1}(\overline{U})^2;\ h = 0 \text{ on } \Upsilon\},$$

and t is sufficiently small such that F_t is a diffeomorphism from Ω onto its image.
The family of domains $\{\Omega_t\}$ and $\{\Gamma_t\}$ are then defined by

$$\Omega_t := F_t(\Omega) \qquad \text{and} \qquad \Gamma_t := F_t(\Gamma).$$

The condition $h_{|\Upsilon} = 0$ means that the boundary Υ is clamped during the iterative process. Then, we shall consider the couples (σ_{Dt}, u_{Dt}) and (σ_{Nt}, u_{Nt}) as the respective solutions of the problems (6.3) and (6.4) defined on the perturbed domain Ω_t. More precisely, these couples (σ_{Dt}, u_{Dt}) and (σ_{Nt}, u_{Nt}) are solutions of the following problems

$$\begin{cases} \operatorname{div} \sigma_{Dt} &= 0 & \text{in } \Omega_t, \\ \varepsilon_{Dt} &= \frac{1+\nu}{E}\,\sigma_{Dt} - \frac{\nu}{E}\,(\operatorname{tr} \sigma_{Dt})\,\mathrm{Id} & \text{in } \Omega_t, \\ \sigma_{Dt}\, n_t &= 0 & \text{on } \Gamma_t, \\ u_{Dt} &= f & \text{on } \Upsilon, \end{cases}$$

and

$$\begin{cases} \operatorname{div}\sigma_{Nt} &= 0 & \text{in } \Omega_t, \\ \varepsilon_{Nt} &= \frac{1+\nu}{E}\,\sigma_{Nt} - \frac{\nu}{E}\,(\operatorname{tr}\,\sigma_{Nt})\,\mathrm{Id} & \text{in } \Omega_t, \\ \sigma_{Nt}\,n_t &= 0 & \text{on } \Gamma_t, \\ \sigma_{Nt}\,n_\Upsilon &= g & \text{on } \Upsilon. \end{cases}$$

where n_t is the outward unit normal to Ω_t on Γ_t.

Definition 4. *The Eulerian derivative of the functional J at Ω in the direction of an element $h \in Q$ is defined by the quantity, when it exists*

$$J'(\Omega, h) = \lim_{t \mapsto 0} \frac{J(\Omega_t) - J(\Omega)}{t}.$$

The Eulerian derivative is called shape derivative if $J'(\Omega, h)$ exists for all $h \in Q$ and the mapping $h \mapsto J'(\Omega, h)$ is linear and continuous with respect to the topology of $\mathcal{C}^{1,1}(\overline{\Omega})^2$.

Let us introduce the following spaces V and $L^2_s(\Omega)$

$$V = \left\{ v \in \left[H^1(\Omega)\right]^2 ; v = 0 \text{ on } \Upsilon \right\}.$$

$$L^2_s(\Omega) = \left\{ \tau = (\tau_{\alpha\,\beta}) \in \left[L^2(\Omega)\right]^4 ; \tau_{\alpha\,\beta} = \tau_{\beta\,\alpha} \right\}.$$

To derive the shape derivative of the error functional J (6.5), one needs the following theorems related to the asymptotic expansions of the Dirichlet and Neumann problems.

Theorem 11. (Related to the Dirichlet problem)
There exists $\eta_0 > 0$ such that, if $t < \eta_0$, we get

$$(\sigma^t_D, u^t_D) = (\sigma^0_D, u^0_D) + t\,(\sigma^1_D, u^1_D) + t\,o(t),$$

where $(\sigma^0_D, u^0_D), (\sigma^1_D, u^1_D)$ and $o(t)$ are elements of $L^2_s(\Omega) \times [H^1(\Omega)]^2$ satisfying

i) (σ^0_D, u^0_D) is the solution of the linear elasticity Dirichlet problem (6.3) hanging in Ω.

ii) $\lim\limits_{t \mapsto 0} ||o(t)||_{L^2_s(\Omega)\times V} = 0$.

iii) $(\sigma^1_D, u^1_D) \in L^2_s(\Omega) \times V$ is the unique solution of the following problem

$$\begin{cases} \forall \tau \in L^2_s(\Omega),\ a\left(\sigma^1_D, \tau\right) + b\left(\tau, u^1_D\right) = -\displaystyle\int_\Omega tr\left[\tau\left(\nabla u^0_D\,\nabla h\right)\right], \\ \qquad \forall v \in V,\ b\left(\sigma^1_D, v\right) = -\displaystyle\int_\Omega tr\left[\sigma^0_D\,(\nabla v\,\nabla h)\right] + \int_\Omega tr\left(\sigma^0_D\,\nabla v\right) div\ h. \end{cases}$$

Theorem 12. (Related to the Neumann problem)
There exists $\delta_0 > 0$ such that, if $t < \delta_0$, we get

$$(\sigma_N^t, u_N^t) = (\sigma_N^0, u_N^0) + t\,(\sigma_N^1, u_N^1) + t\,o(t),$$

where $(\sigma_N^0, u_N^0), (\sigma_N^1, u_N^1)$ and $o(t)$ are elements of $L_s^2(\Omega) \times [H^1(\Omega)]^2$ satisfying

i) (σ_N^0, u_N^0) is the solution of the linear elasticity Neumann problem (6.4) hanging in Ω.

ii) $\lim_{t\mapsto 0} ||o(t)||_{L_s^2(\Omega)\times[H^1(\Omega)]^2} = 0$.

iii) $(\sigma_N^1, u_N^1) \in L_s^2(\Omega) \times [H^1(\Omega)]^2$ is the unique solution of the following problem

$$\begin{cases} \forall \tau \in L_s^2(\Omega), & a\left(\sigma_N^1, \tau\right) + b\left(\tau, u_N^1\right) = -\displaystyle\int_\Omega tr\left[\tau\left(\nabla u_N^0\, \nabla h\right)\right], \\ \forall v \in \left[H^1(\Omega)\right]^2, & b\left(\sigma_N^1, v\right) = -\displaystyle\int_\Omega tr\left[\sigma_N^0\left(\nabla v\, \nabla h\right)\right] \\ & \qquad + \displaystyle\int_\Omega tr\left(\sigma_N^0\, \nabla v\right) div\ h. \end{cases}$$

Now, we can state the main result of this section which establishes the shape gradient of the functional J (6.5) under the knowledge of the shear stress.

Theorem 13. *The mapping $t \mapsto J(\Omega_t)$ is $\mathcal{C}^1$ in a neighborhood of 0 and its derivative at 0 is given by*

$$J'(\Omega, h) = \int_\Gamma G\,(h \cdot n),$$

with

$$G = \frac{1}{2}\left[\left(\sigma_D^0 : \varepsilon(u_D^0)\right) - \left(\sigma_N^0 : \varepsilon(u_N^0)\right)\right]. \tag{6.7}$$

6.3 Shear stress reconstruction

This part concerns the recovery of lacking boundary data, namely the shear stress $g \cdot \tau = (\sigma(u)\, n_\Upsilon) \cdot \tau$ on the exterior boundary of the domain of interest from the knowledge of sub-Cauchy data.
The problem is formulated mathematically as follows: Given the normal component of surface traction $g \cdot n_\Upsilon$ imposed and the displacement f measured on

Υ, the inverse problem is so to reconstruct $(\sigma(u)\, n_\Upsilon)\cdot\tau$ on Υ and both the displacement u and the traction $(\sigma(u)\, n)$ on Γ satisfying the following problem:

$$\begin{cases} \operatorname{div}\sigma(u) & = 0 & \text{in } \Omega, \\ (\sigma(u)\, n_\Upsilon)\cdot n_\Upsilon & = g\cdot n_\Upsilon & \text{on } \Upsilon, \\ u & = f & \text{on } \Upsilon. \end{cases} \tag{6.8}$$

Above, Ω, Υ, Γ and $\sigma(u)$ are as already defined in the first section. The important point to note here is that, to the best of our knowledge, there are no theoretical studies (existence and uniqueness) regarding this problem despite its great importance in applications. Hence, although the theoretical question is at present far from being answered, it is of interest to numerically reconstruct the shear stress. We resort to the same approach proposed in [27] that we briefly present herein. This part is concerned with the Steklov Poincaré operator carried out to solve the sub-Cauchy problem (6.8) which is nothing more than a data completion problem. One way to solve such a problem is to decompose the sub-Cauchy problem (6.8) through an unknown function η as follows:

$$(P_D)\begin{cases} \operatorname{div}\sigma(u_D) & = 0 & \text{in } \Omega, \\ u_D & = f & \text{on } \Upsilon, \\ u_D & = \eta & \text{on } \Gamma. \end{cases} \tag{6.9}$$

and

$$(P_N)\begin{cases} \operatorname{div}\sigma(u_N) & = 0 & \text{in } \Omega, \\ (\sigma(u_N)\, n_\Upsilon)\cdot n_\Upsilon & = g\cdot n_\Upsilon & \text{on } \Upsilon, \\ u_N\cdot\tau & = f\cdot\tau & \text{on } \Upsilon, \\ u_N & = \eta & \text{on } \Gamma, \end{cases} \tag{6.10}$$

where η is the virtual control. The solution u_D and u_N are functions of η ($u_D = u_D(\eta)$ and $u_N = u_N(\eta)$). The gap between these fields u_D and u_N is subsequently minimized with respect to the unknown boundary data η in order to produce the desired expanded elastic fields. The gap used herein is the same Kohn-Vogelius error functional investigated in the previous section but in this case depending on the virtual control η, that is:

$$J(\eta) = \frac{1}{2}\int_\Omega \sigma(u_D - u_N) : \varepsilon(u_D - u_N) \quad d\Omega \tag{6.11}$$

The inverse problem (6.8) is then formulated via the minimization of the energy error functional J (6.11) as

$$\inf_{\eta\in\left[H^{\frac{1}{2}}(\Gamma)\right]^2} J(\eta) \tag{6.12}$$

The solutions u_D and u_N can be written as:

$$u_D = \overline{u_D} + u_D^* \qquad \text{and} \qquad u_N = \overline{u_N} + u_N^* \tag{6.13}$$

where $\overline{u_D}$ and $\overline{u_N}$ depend on the sub-Cauchy data f and $g \cdot n_\Upsilon$ whilst u_D^* and u_N^* depend on η as follows:

$$(P_D^*) \begin{cases} \text{div } \sigma(u_D^*) & = 0 & \text{in } \Omega, \\ u_D^* & = 0 & \text{on } \Upsilon, \\ u_D^* & = \eta & \text{on } \Gamma. \end{cases}$$

$$(\overline{P_D}) \begin{cases} \text{div } \sigma(\overline{u_D}) & = 0 & \text{in } \Omega, \\ \overline{u_D} & = f & \text{on } \Upsilon, \\ \overline{u_D} & = 0 & \text{on } \Gamma. \end{cases}$$

Similarly, the decomposition of u_N is such that

$$(P_N^*) \begin{cases} \text{div } \sigma(u_N^*) & = 0 & \text{in } \Omega, \\ (\sigma(u_N^*)\, n_\Upsilon) \cdot n_\Upsilon & = 0 & \text{on } \Upsilon, \\ u_N^* \cdot \tau & = 0 & \text{on } \Upsilon, \\ u_N^* & = \eta & \text{on } \Gamma. \end{cases}$$

$$(\overline{P_N}) \begin{cases} \text{div } \sigma(\overline{u_N}) & = 0 & \text{in } \Omega, \\ (\sigma(\overline{u_N})\, n_\Upsilon) \cdot n_\Upsilon & = g \cdot n_\Upsilon & \text{on } \Upsilon, \\ \overline{u_N} \cdot \tau & = f \cdot \tau & \text{on } \Upsilon, \\ \overline{u_N} & = 0 & \text{on } \Gamma. \end{cases}$$

The solution of the problem (6.12) is recovered if:

$$\sigma(u_D)\, n = \sigma(u_N)\, n \qquad \text{on} \quad \Gamma. \tag{6.14}$$

According to (6.13), the condition (6.14) leads to the boundary equation

$$\sigma(u_D^*)\, n - \sigma(u_N^*)\, n = \sigma(\overline{u_N})\, n - \sigma(\overline{u_D})\, n \qquad \text{on} \quad \Gamma. \tag{6.15}$$

Let us introduce some notations useful in the sequel:

$$S_D\eta = \sigma(u_D^*)\, n, \qquad S_N\eta = \sigma(u_N^*)\, n \quad \text{and} \quad \xi = -(\sigma(\overline{u_D})\, n - \sigma(\overline{u_N})\, n).$$

Then, one can rewrite the equation (6.15) as

$$S\,\eta = (S_D - S_N)\eta = \xi \quad \text{on} \quad \Gamma, \tag{6.16}$$

where S is the Steklov Poincaré operator well known in the domain decomposition area [85].

6.4 Numerical analysis

6.4.1 Cavities identification

This part aims to develop an algorithm to numerically solve the shape optimization problem (6.6). Indeed, the theorem 13 suggests the implementation of a numerical minimization algorithm using the gradient method.
We consider for $t \geq 0$ and k^{th} iteration, the deformation of Γ, as in Section 6.2.1

$$\Gamma_t^k := F_t(\Gamma) = \{x + t\, h(x);\ x \in \Gamma\}, \tag{6.17}$$

where h is chosen as follows

$$h \in Q \quad \text{such that} \quad h_{|\Gamma} = -G\, n, \tag{6.18}$$

G being given by (6.7). This descent direction (6.18) guarantees the minimization of the shape functional J (6.5). To numerically implement this iterative procedure, we resort to the level set method.
Level set method: The level set method is a numerical technique for tracking shapes, developed in 1988 by Osher and Sethian [84]. During the past few decades, this method has been applied in various fields [82], since it provides a practical way to follow shapes that change topologies.
Let us consider the evolution of a boundary Γ_t (namely a domain $\Omega_t \subset U \subset \mathbb{R}^2$) under the velocity field h (6.18) related to the sensitivity of the energy error functional (6.5). The basic idea of the level set method is to construct a link between the boundary Γ_t (6.17) and a continuous function Φ defined on the whole domain U. More precisely, the boundary Γ_t can be implicitly represented using the level curve of a function Φ as follows

$$\Gamma_t = \{x \in U;\ \Phi(x,t) = 0\}.$$

During the process, the cavities to recover will be identified by change in level set functions values, with respect to fictitious time t. This change is related to the shape derivative of the functional (6.5).
Indeed, the derivation of the equation $\Phi(x,t) = 0$ with respect to t leads to the transport equation

$$\partial_t \Phi + h \cdot \nabla \Phi = 0.$$

Since the normal vector to Γ_t is given by $n = \frac{\nabla \Phi}{|\nabla \Phi|}$ [82], the evolution of Φ is then governed by the Hamilton-Jacobi equation

$$\partial_t \Phi + h_n\, |\nabla \Phi| = 0.$$

where h_n is the normal velocity. Or we has chosen $h = -G\,n = -G\,\frac{\nabla\Phi}{|\nabla\Phi|}$. As a consequence, the evolution of Γ_t (the evolution of Φ) is governed by the so-called level set equation

$$\left\{\begin{array}{lcll} \partial_t\Phi - G\,|\nabla\Phi| & = & 0 & \text{in } U\times\mathbb{R}_+, \\ \Phi(\cdot,0) & = & \Phi_0, & \end{array}\right. \tag{6.19}$$

where Φ_0 is the initial data chosen as the signed distance function to Γ_0.
Hence, moving the level-set lines along the descent gradient direction h (6.18) is equivalent to transporting the function Φ by solving the level set equation (6.19).

6.4.2 Shear stress reconstruction

Going back to the resolution of the linear system of equations (6.16), one can use an iterative preconditioned gradient algorithm which appears to be very efficient. Indeed, at k iteration, one can reinitialize η as

$$\eta^k = \eta^{k-1} + \rho\,M(S\,\eta^{k-1} - \xi)$$

and the key point, here, relies on choosing the preconditioner $M = S_D^{-1}$. Above, ρ is a relaxation coefficient.
Hence, each iteration of the algorithm, to be implemented in order to reconstruct the shear stress on Υ, involves the solution of both problems (6.9) and (6.10), to get $S\,\eta$ and the solution of the following problem

$$\left\{\begin{array}{lll} \operatorname{div}\sigma(w) & = 0 & \text{in } \Omega, \\ \sigma(w)\,n & = S\,\eta - \xi & \text{on } \Gamma, \\ w & = 0 & \text{on } \Upsilon, \end{array}\right. \tag{6.20}$$

needed to solve the system $S_D\chi = S\eta - \xi$ ($\chi = w$ on Γ).

6.4.3 Algorithm

Herein, we outline the algorithm to be implemented in order to solve the problem (6.1), that is to retrieve the void A from sub-Cauchy data $(f, g\cdot n_\Upsilon)$ on Υ.
Let Ω^{true} be a domain containing a cavity (or multiple cavities) whose location and shape are to be retrieved from boundary measurements. The sub-Cauchy data, namely the displacement f and the normal component of the normal stress $g\cdot n_\Upsilon$ are issued from a numerical computation of a direct problem

over the domain Ω^{true} containing the cavity (ies) to recover (synthetic data) as follows:
For given $\tilde{g} \in \left[H^{-\frac{1}{2}}(\Upsilon)\right]^2$, we solve the direct problem

$$\begin{cases} \operatorname{div}\sigma(u) &= 0 & \text{in } \Omega^{\text{true}}, \\ \sigma(u)\, n_\Upsilon &= \tilde{g} & \text{on } \Upsilon, \\ \sigma(u)\, n &= 0 & \text{on } \Gamma, \end{cases}$$

up to a constant. Then, we take $(f, g \cdot n_\Upsilon) = (u_{|\Upsilon}, (\tilde{g} \cdot n_\Upsilon)_{|\Upsilon})$.
Since the partially overdetermined boundary data $(f, g \cdot n_\Upsilon)$ are overspecified, the numerical procedure could be represented in the following algorithm stages. Let us assume that we know the interface $\Gamma^k := \Gamma$ and a level set function Φ^k associated to $\Gamma^k := \Gamma$.

1. **Shear stress reconstruction**
   (a) Choose an initial data η^0.
   (b) Solve problems (6.9) and (6.10) in the domain Ω_k.
   (c) Solve problem (6.20) and get w.
   (d) Let $\eta^{k+1} = \eta^k + \rho\, w$.
   (e) Go back to the first step (1 a) until the stopping condition: $||u_D - u_N||_{[L^2(\Omega))]^2} \leq \varepsilon$ is reached (ε is a given tolerance level; in the following section, we will choose $\varepsilon = 10^{-2}$).
2. **Cavities identification**
   (a) Compute the solutions (σ_D, u_D) and (σ_N, u_N) of the problems (6.3) and (6.4) in the domain Ω_k.
   (b) Compute the velocity function G on Γ, given by (6.7).
   (c) Update the level set function Φ by solving the level set equation (6.19) and get a new function Φ.
   (d) Go back to the first step (1) until the stopping criterion is fulfilled.

It should be noted that the stopping criterion of the algorithm exposed above is

$$d_H\left(\Gamma^k, \Gamma^{k-1}\right) < C\, \delta x^2,$$

where C is a constant independent of the grid parameter δx. d_H denotes the Hausdorff distance defined for two sets $A, B \subset \mathbb{R}^2$ by

$$d_H(A, B) = \max\left(\sup_{a \in A} d(a, B)\ ,\ \sup_{b \in B} d(b, A)\right)$$

where

$$d(a, B) = \inf_{b \in B} |a - b|.$$

6.5 Results

The purpose of this section is to present numerical results. The domain U is the square $[-1, 1] \times [-1, 1]$ and we consider the inverse problem of the identification of two cavities. Indeed, we consider disconnected cavities: the union of the two disjointed circles of radius 0.15 centered at $(-0.35, 0)$ and $(0.35, 0)$ and a connected initial guess: the circle of radius 0.65 centered at the origin. The initial guess is sufficiently big to include the unknown cavities. The results reported in Figure 6.1 are in good agreement with the exact ones and show the flexibility of the proposed methodology to recover multiple cavities even from sub-Cauchy data.

6.6 Conclusion

This paper introduces an iterative method for solving a geometrical inverse problem in linear elasticity. The problem consists in recovering voids from sub-Cauchy data. The approach proposed combines the resolution of a data completion problem and cavities identification one. While transforming these both problems into optimization ones, the same energy gap-cost functional is introduced. Numerical simulations have highlighted the efficiency of the method. Some open questions such as the existence and uniqueness of solution concerning the shear stress reconstruction problem deserve an answer. An extension to non-linear elasticity framework could be an interesting future direction of investigation.

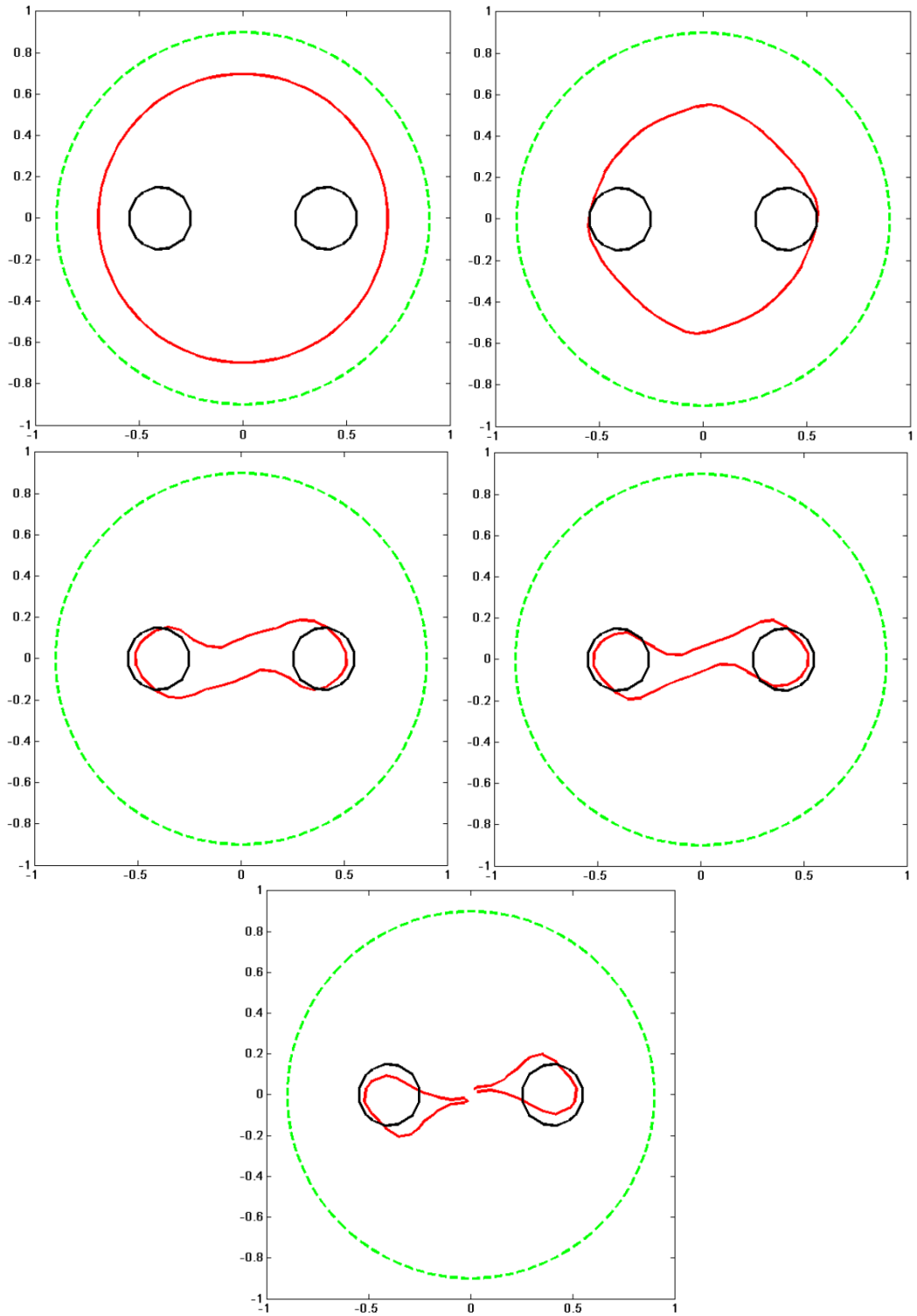

Figure 6.1: Υ_0 the exterior boundary (the dashed green line), Γ the exact solution (the black line), evolution of the boundary Γ^k (the red line) for $k = 1, 300, 434, 448, 449$ (left to right, top to bottom).

Conclusions and future works

Since finding defects (namely cavities) in mechanical structures is not a trivial task, the need of practical approaches was observed during the last few decades.

The purpose of this thesis was to adress this need. Indeed, as a first step, we had formulated our cavities identification problem into a shape optimization one by minimizing an energy gap cost functional $J(\Omega)$, the so-called Kohn Vogelius functional, reviewed in the second chapter. Then, we had considered different techniques that overcome the main numerical limitation of the classical shape optimization, that is the restriction on the topology of the domain.

The first technique is the level set method combined with the shape gradient one applied in both third and fourth chapters as well as the sixth chapter. Indeed, the problem investigated in the third chapter is modeled by the Laplace equation, while the problems studied in both fourth and sixth chapters are related to the linear elasticity framework. The main concern of these chapters was the study of the derivative of J with respect to the domain, carried out using the shape gradient method and needed to compute a descent direction for J (namely a velocity field V_Ω). As far as numerical simulations are concerned, the main difficulty encountered was to follow shapes that change topologies during the process. To deal with this issue, we had relied on the level set method as was originally suggested by Osher and Sethian [84]. Indeed, as expressed in terms of a boundary integral the shape derivative of the functional J was combined with the level set technique and an efficient numerical iterative scheme was constructed.

Although the numerical computation costs, it had been proved that the level set method is accurate and specially designed to identify the precise location of cavities. Indeed, the several numerical tests obtained have highlighted the ability of the level set method to follow shapes that split in two, develops holes or the inverse of these operations.

The second technique we are interested in is the topological gradient method

which aims to assess the behavior of a cost functional to be minimized (the Kohn Vogelius functional in our case) when a small hole is inserted inside the domain of interest. More precisely, the computation of its asymptotic expansion furnishes the topological gradient whose negative values give an insight where one should create holes to guarantee the minimization of the cost functional. An efficient, fast and cheap one-shot reconstruction algorithm had been developed in the fifth chapter for a new framework for a geometric inverse problem in linear elasticity concerning the recovery of cavities from the knowledge of partially overdetermined boundary data. An accurate detection of cavities was achieved.

The several numerical results obtained have indicated that all techniques investigated in this thesis come out to be effective recovery tools and can be applied to the engineering problem related to cavities identification for both case complete and partially overdetermined boundary data.

However, unless the detection of cavity(ies) by the level set method is accurate, it is computationally expansive and slow. On the other hand, the limitation of the one-shot reconstruction algorithm based on the topological gradient method proposed in the fifth chapter is related to the detection of the rough location of faults.

In contrast, this one-shot algorithm is not only cheap but also fast and is able to identify multiple cavities. Moreover, the strength of the level set method presented in the third, fourth and sixth chapters lies on the natural treatment of shapes that change topology as well as on the detection of the precise location of curves. Therefore, the numerical results obtained in this study could be improved in several ways. One possible extension is to combine these techniques: the topological gradient method from which one can obtain a good initial guess and the shape gradient method with the level set one in order to identify the precise location of cavities. In this case, the technique proposed by Allaire et al. in [4] could serve and the reconstruction method would certainly gain on speed.

Since the uniqueness question of the inverse problem, namely the identifiability of cavities in the case of partially overdetermined boundary data, was only proved for monotonous cavities, a second open question born from the fifth chapter is: How can we prove the identifiability for the general case. The main difficulty lies here on the fact that both displacement field and normal stress are required to apply Almansi's lemma [80]. A possible direction of investigations to answer such a question is to exploit a recent uniqueness result [60].

Moreover, thanks to the fast growing power of computers, the inverse problem related to cavities identification problem investigated in this dissertation can be extended to include more complex situations. Some potential extension of this study would concentrate on non linear elasticity framework, which poses a challenge. Indeed, it seems that all techniques explored in this work, that is the level set method combined with the shape gradient one and the topological gradient method can be exploited.

On the other hand, one can remark that the most of works investigated in literature and related to shape identification assume deterministic conditions for the input data. However, in most concrete situations, these data are affected by different sources of uncertainty. These uncertainties may be derived from the forcing terms, the boundary conditions, the Lamé coefficients when dealing with linear elasticity framework or even from the geometry. Such situations have gained much attention in the last few years. The question of influence of random uncertainties on the identification of defects in mechanical structures opens the door to new investigations. Indeed, one has to include uncertainty quantification to guarantee a reliable identification of faults. The techniques presented in [75] and in [3] offer a possible answer to this question cited herein and a starting point for future direction of investigations. On the other hand, when considering random uncetainties, a logic continuation of this work is to combine the techniques presented, namely the shape gradient method with the level set one and the topological gradient one with stochastic finite element method [14] which are designed for the numerical simulation of partial differential equations involving random coefficients.

Bibliography

[1] J.D. Achenbach, *Quantitative nondestructive evaluation*, (International Journal of Solids and Structures, 37, 13–27, 2000).

[2] L. Afraites, M. Dambrine, K. Eppler, D. Kateb, *Detecting perfectly insulated obstacles by shape optimization techniques of order two*, (Discrete Contin. Dyn. Syst. Ser. B, 8(2), 389–416, 2007).

[3] G. Allaire, C. Dapogny, *A deterministic approximation method in shape optimization under random uncertainties*, (hal-01160256, 2015).

[4] G. Allaire, F. Gournay, F. Jouve, A. M. Toader, *Structural optimization using topological and shape sensitivity via a level set method*, (Control and Cybernetics, 34(1), 2005).

[5] S. Amstutz, *Aspects théoriques et numériques en optimisation de forme topologique*, (Phd thesis, Institut National des Sciences Appliquées de Toulouse, 2003).

[6] S. Amstutz, I. Horchani, M. Masmoudi, *Crack detection by the topological gradient method*, (Control and Cybernetics, 34(1), 2005).

[7] S. Andrieux, T. N. Baranger, *An energy error-based method for the resolution of the Cauchy problem in 3D linear elasticity*, (Comput. Methods Appl. Mech. Engrg., 197, 902–920, 2008).

[8] S. Andrieux, T. N. Baranger, A. Ben Abda, *Solving Cauchy problems by minimizing an energy-like functional*, (Inverse Problems, 22, 115–134, 2006).

[9] S. Andrieux, A. Ben Abda, M. Jaoua, *On the inverse emergent plane crack problem*, (Math. Meth. Appl. Sci., 21, 895–906, 1998).

[10] D. Auroux, L. J. Belaid, B. Rjaibi, *Application of the topological gradient method to color image restoration*, (SIAM J. Imaging Sci., 3(2), 153–175, 2010).

[11] D. Auroux, L. J. Belaid, B. Rjaibi, *Application of the topological gradient method to tomography*, (ARIMA Proc. TamTam'09, 2010).

[12] D. Auroux, M. Masmoudi, *A one-shot inpainting algorithm based on the topological asymptotic analysis*, (Comput. Appl. Math., 25(2-3), Petrópolis, 2006).

[13] D. Auroux, M. Masmoudi, *Image processing by topological asymptotic analysis*, (ESAIM, Proc. Mathematical methods for imaging and inverse problems, 26, 24–44, 2009).

[14] I. Babuska, F. Nobile, R. Tempone *A Stochastic Collocation Method for Elliptic Partial Differential Equations with Random Input Data*, (SIAM J. Numer. Anal., 45(3), 1005–1034, 2007)

[15] J. B. Bacani, G. Peichl, *The second-order Eulerian derivative of a shape functional of a free Bernoulli problem* (J. Korean Math. Soc., submitted for publication, 2014)

[16] J. B. Bacani, G. Peichl, *Solving the exterior Bernoulli problem using the shape derivative approach*, (In Mathematics and Computing : Springer Proceedings in Mathematics and Statistics, Vol. 91; Mohapatra, R., Giri, D., Saxena, P.K., Srivastava, P.D., Eds.; Springer India: New Delhi, India; Volume XXV, 251–269, 2013).

[17] J. B. Bacani, G. Peichl, *On the first-order shape derivative of Kohn-Vogelius cost functional of the Bernoulli problem*, (Hindawi Publishing Corporation, Abstract and Applied Analysis Article ID 384320, 19 pages, 2013).

[18] J. B. Bacani, G. Peichl, *The second-order shape derivative of Kohn-Vogelius-type cost functional using the boundary differentiation approach*, (Mathematics, 12, 196–217, 2014).

[19] M. Badra, F. Caubet, M. Dambrine, *Detecting an obstacle immersed in a fluid by shape optimization methods*, (Math. Models Methods Appl. Sci., 21(10), 2069–2101, 2011).

[20] L. J. Belaid, M. Jaoua, M. Masmoudi, L. Siala, *Application of the topological gradient to image restoration and edge detection*, (Engineering Analysis with boundary Elements, 32(11), 891–899, 2008).

[21] A. Ben Abda, F. Bouchon, G. H. Peichl, M. Sayeh, R. Touzani, *A Dirichlet-Neumann cost functional approach for the Bernoulli problem*, (Journal of Engineering Mathematics 81(1), 157–176, 2013).

[22] A. Ben Abda, S. Chaabane, F. El Dabaghi, M. Jaoua, *On a non-linear geometrical inverse problem of Signorini type: Identifiability and stability*, (Math. Meth. Appl. Sci., 21, 1379–1398, 1998).

[23] A. Ben Abda, M. Hassine, M. Jaoua, M. Masmoudi, *Topological sensitivity analysis for the location of small cavities in Stokes flow*, (SIAM J. Control Optim 48(5), 2871–2900, 2009).

[24] A. Ben Abda, E. Jaïem, S. Khalfallah, A. Zine, *An energy gap functional: Cavities identification in linear elasticity*, (Submitted, 2016).

[25] A. Ben Abda, E. Jaïem, B. Rjaibi, *Cavities identification from partially overdetermined boundary data in linear elasticity*, (Journal of Applied and Computational Mathematics, 5:295. doi:10.4172/2168-9679.1000295, 2016).

[26] A. Ben Abda, M. Kallel, J. Leblond, J. P. Marmorat, *Line segment crack recovery from incomplete boundary data*, (Inverse Problems, 18, 1057–1077, 2002).

[27] A. Ben Abda, S. Khalfallah, *Lacking data recovery via partially overdetermined boundary conditions in linear elasticity* (Accepted for publication in J. Appl. Mech. Eng., 2016).

[28] H. Ben Ameur, M. Burger, B. Hackl, *Cavity identification in linear elasticity and thermoelasticity*, (Inverse Problems 30, 625–647, 2007).

[29] H. Ben Ameur, M. Burger, B. Hackl, *Level set methods for geometric inverse problems in linear elasticity*, (Inverse Problems 12, 673–696, 2004).

[30] A. Bilotta, E. Turco, *A numerical study on the solution of Cauchy problem in elasticity*, (International Journal of Solids and Structures, 46, 4451–4477, 2009).

[31] M. Bonnet, *Fast identification of cracks using higher-order topological sensitivity for 2-D potential problems* (Engineering Analysis with Boundary Elements, 35(2), 223–235, 2011).

[32] M. Bonnet, A. Constantinescu, *Inverse problems in elasticity*, (Inverse Problems 21(2), 1–50, 2005).

[33] L. Borcea 2002, *Electrical impedance tomography* (Inverse Problems, 18, R99–R136, 2002).

[34] L. Bourgeois, J. Dardé, *A quasi-reversibility approach to solve the inverse obstacle problem*, (Inverse Problems and Imaging 4(3), 351–377, 2010).

[35] A. Carpio, M.L. Rapún, *Hybrid topological derivative and gradient-based methods for electrical impedance tomography*, (Inverse Problems, 28(9), Article 095010, 22 pages, 2012).

[36] F. Caubet, M. Dambrine, *Localization of small obstacles in Stokes flow*, (Inverse Problems, 28(10), 2012).

[37] F. Caubet, M. Dambrine, D. Kateb, *Shape optimization methods for the inverse obstacle problem with generalized impedance boundary conditions*, (Inverse Problems, 29, 115011 (26pp), 2013).

[38] D.J. Cedio-Fengya, S. Moskov, M.S. Vogelius, *Identification of conductivity imperfections of small diameter by boundary measurements. Continuous dependence and computational reconstruction*, (Inverse Problems, 14(3), 553–595, 1998).

[39] S. Chaabane, C. Elhechmi, M. Jaoua, *A stable recovery algorithm for the Robin inverse problem*, (Math. Comput. Simulation, 66, 367–383, 2004).

[40] S. Chaabane, M. Jaoua, *Un algorithme d'identification de frontières soumises à des conditions aux limites de Signorini*, (M2AN, 34(3), 707–722, 2000).

[41] S. Chaabane, M. Masmoudi, H. Meftahi, *Topological and shape gradient strategy for solving geometrical inverse problems*, (J. Math. Anal. Appl., 400, 724–742, 2013).

[42] A. Cimetière, F. Delvare, M. Jaoua, M. Kallel, F. Pons, *Recovery of Cracks from Incomplete Boundary Data*, (Inverse Problems in Engineering, 10(4), 377–392, 2002).

[43] A. Cimetière, F. Delvare, M. Jaoua, F. Pons, *Solution of the Cauchy problem using iterated Tikhonov regularization*, (Inverse Problems, 17(3), 553–570, 2001).

[44] MC. Delfour, J-P. Zolesio, *Shapes and Geometries*, (SIAM, 2001).

[45] F. Delvare, A. Cimetière, J. L. Hanus, P. Bailly, *An iterative method for the Cauchy problem in linear elasticity with fading regularization effect*, (Computer Methods in Applied Mechanics and Engineering, 199(49-52), 3336–3344, 2010).

[46] P. Destuynder, M. Djaoua, *Sur une Interprétation Mathématique de l'Intégrale de Rice en Théorie de la Rupture Fragile*, (Math. Meth. in the Appl. Sci. 3, 70–87, 1981).

[47] N.P.van Dijk, K. Maute, M. Langelaar, F.van Keulen, *Level-set methods for structural topology optimization: a review*, (Structural and Multidisciplinary Optimization, 48(3), 437–472, 2013)

[48] K. Eppler, H. Harbrecht *A regularized Newton method in electrical impedance tomography using Hessian information*, (Control Cybernet, 34, 203–225, 2005).

[49] K. Eppler, H. Harbrecht, *On a Kohn-Vogelius like formulation of free boundary problems*, (Comput. Optim. Appl., 52, 69–85, 2012).

[50] H.A. Eschenauer, V.V. Kobolev, A. Schumacher, *Bubble method for topology and shape optimization of structures*, (Journal of Structural Optimization, 8, 42–51, 1994).

[51] I. Faye, M. Ndiaye, I. Ly, D. Seck, *Problem of detecting inclusions by topological optimization*, (Opuscula Math, 34(1), 81–96, 2014).

[52] S. Garreau, P. Guillaume, M. Masmoudi, *The topological asymptotic for PDE systems: The elasticity case*, (SIAM J. Control Optim., 39(6), 1756–1778, 2001).

[53] R. Gong, X. Cheng, W. Han, *A fast solver for an inverse problem arising in bioluminescence tomography*, (Journal of Computational and Applied Mathematics, 267, 228–243, 2014).

[54] S. Gottlieb, C-W. Shu, E. Tadmor, *Strong stability-preserving high-order time discretization methods*, (SIAM Review, 43(1), 89–112, 2001).

[55] S. Gutman, *Alternating directions method for impedance computed tomography* (Inverse Problems, 5, 1027–1047, 1989).

[56] B.B. Guzina, M. Bonnet, *Small-inclusion asymptotic of misfit functional for inverse problems in acoustics* (Inverse problems, 22, 1761–1785, 2006).

[57] J. Hadamard, *Le problème de Cauchy et les équations aux dérivées partielles linéaires hyperboliques*, (Hermann: Paris, 1932).

[58] J. Hadamard, *Mémoire sur le problème d'analyse relatif à l'équilibre des plaques élastiques encastrées.*, (Paris : Imprimerie nationale, 1909).

[59] J. Haslinger, T. Kozubek, K. Kunish, G. Peichl, *Shape optimization and fictitious domain approach for solving free-boundary value problems of Bernoulli type*, (Comput. Optim. Appl., 26, 231–251, 2003).

[60] H. Hedenmalm, *On the uniqueness theorem of Holmgren*, (Mathematische Zeitschrift, 281(1), 357–378, 2015).

[61] A. Henrot, M. Pierre, *Variation et optimisation de forme, Une analyse géométrique*, (Springer, Paris, 2005).

[62] K. Ito, K. Kunisch, Z. Li, *Level-set function approach to an inverse interface problem*, (Inverse Problems 17, 1225–1242, 2001).

[63] K. Ito, K. Kunisch, G. Peichl, *Variational approach to shape derivative for a class of Bernoulli problem*, (J. Math. Anal. App., 314, 126–149, 2006).

[64] E. Jaïem, S. Khalfallah, *An energy-gap cost functional for cavities identification*, (To appear in Nonlinear Studies, 2016).

[65] G-S. Jiang, D. Peng, *Weighted ENO schemes for Hamilton-Jacobi equations*, (SIAM Journal of Scientific Computation 21(6), 2126–2143, 2000).

[66] RV. Kohn, A. McKenney, *Numerical implementation of a variational method for electrical impedance tomography*, (Inverse Problems, 6(3), :389, 1990).

[67] R. V. Kohn, M. Vogelius, *Relaxation of a variational method for impedance computed tomography*, (Communications on Pure and Applied Mathematics, 40, 745–777, 1987).

[68] S. Larnier, J. Fehrenbach, M. Masmoudi, *The topological gradient method: From optimal design to image processing*, (Milan Journal of Mathematics, 80(2), 411–441, 2012).

[69] R. Lattès, J-L. Lions, *Méthode de quasi-réversibilité et applications*, (Dunod, Paris, 1967).

[70] J. Lemaitre, *A course on damage mechanics*, (Springer-Verlag Berlin Heidelberg, 1996).

[71] L. Marin, *The minimal error method for the Cauchy problem in linear elasticity. Numerical implementation for two-dimensional homogeneous isotropic linear elasticity*, (International Journal of Solids and Structures, 46, 957–974, 2009).

[72] L. Marin, F. Delvare, A. Cimetière, *Fading regularization MFS algorithm for inverse boundary value problems in two-dimensional linear elasticity*, (International Journal of Solids and Structures, 78-79, 9–20, 2016).

[73] L. Marin, B. T. Johansson, *A relaxation method of an alternating iterative algorithm for the Cauchy problem in linear isotropic elasticity*, (Computer Methods in Applied Mechanics and Engineering, 199, 3179–3196, 2010).

[74] L. Marin, B. T. Johansson, *Relaxation procedures for an iterative MFS algorithm for the stable reconstruction of elastic fields from Cauchy data in two-dimensional isotropic linear elasticity*, (International Journal of Solids and Structures, 47, 3462–3479, 2010).

[75] J. Martínez-Frutosa, D. Herrero-Péreza, M. Kesslerb, F. Periagob, *Robust shape optimization of continuous structures via the level set method*, (Computer Methods in Applied Mechanics and Engineering, 305, 271–291, 2016).

[76] H. Meftahi, J-P. Zolésio, *Sensitivity analysis for some inverse problems in linear elasticity via minimax differentiability*, (Applied Mathematical Modelling, 2014).

[77] JR. L. Mishnaevsky, *Computational Mesomechanics of Composites: Numerical analysis of the effect of microstructures of composites on their strength and damage resistance*, (John Wiley & Sons, Ltd, England, 2007).

[78] J. L. Mueller, S. Siltanen, D. Isaacson, *A direct reconstruction algorithm for electrical impedance tomography*, (IEEE Transactions on Medical Imaging, 2(6), 2002).

[79] F. Murat, J. Simon, *Sur le contrôle par un domaine géométrique*, (Thèse d'état, Université Pierre et Marie Curie, Paris, 1976).

[80] NI. Muskhelishvili, *Some basic problems of mathematical theory of elasticity*, (North International Publishing: The Netherlands, 1975).

[81] A.A. Novotny, J. Sokolowski, *Topological Derivatives in Shape Optimization*, (Springer, 2013).

[82] S. Osher, R. Fedkiw, *Level Set Methods and Dynamic Implicit Surfaces*, (Springer-Verlag, New York, 2003).

[83] S. Osher, F. Santosa, *Level Set Methods for Optimization Problems Involving Geometry and Constraints : I. Frequencies of a Two-Density Inhomogeneous Drum*, (Journal of Computational Physics, 171(1), 272–288, 2001).

[84] S. Osher, J. Sethian, *Fronts propagating with curvature dependent speed: Algorithms based on Hamilton-Jacobi formulations*, (J. Comp. Phys. 12(56), 12–49, 1988).

[85] A. Quarteroni, A.Valli, *Domain decomposition methods for partial differential equations*, (Oxford ; New York, Clarendon press, XV-360 p. 24 cm, Numerical mathematics and scientific computation, 1999.

[86] B. Samet, S. Amstutz, M. Masmoudi, *The Topological Asymptotic for the Helmholtz Equation*, (SIAM J. Control Optim., 42(5), 1523–1544, 2003).

[87] T. Sato, K. Shirota, *Coefficient identification of the wave equation using the alternating directions method*, (Inverse problems in Engineering mechanics III M. Tanaka, G.S. Dulikravich (Eds.), 1985).

[88] J.A. Sethian, *Level Set Methods and Fast Marching Methods (Evolving Interfaces in Computational Geometry, Fluid Mechanics, Computer Vision, and Materials Science)* (Part of Cambridge Monographs on Applied and Computational Mathematics, 2nd Edition, 1999).

[89] A. Schumacher, *Topologieoptimierung von Bauteilstrukturen unter Verwendung von Lopchpositionierungkrieterien*, (Thesis, Universität-Gesamthochschule Siegen, Siegen, Germany, 1995).

[90] J. Sokolowski, A. Żochowski, *On the topological derivative in shape optimization*, (SIAM, J. Control Optim., 37, 1251–1272, 1999).

[91] J. Sokolowski, JP. Zolesio *Introduction to shape optimization: Shape Sensitivity Analysis*, (Springer, 1992).

[92] M. Sussman, P. Smereka, S. Osher, *A Level Set Approach for Computing Solutions to Incompressible Two-Phase Flow*, (Journal of Computational Physics, 114(1), 146–159, 1994).

[93] R. Valid, *La mécanique des milieux continus et le calcul des structures*, (Eyrolles, Paris, 1977).

[94] A. Wexler, B. Fry, M. R. Neuman *Impedance-computed tomography algorithm and system*, (Applied Optics 24(23), 1985).

[95] T. J. Yorkey, J. G. Webster, W. J. Tomkins, *Comparing reconstruction algorithms for electrical impedance tomography*, (IEEE Transactions on Biomedical Engineering BME-34(11), 1987).